Use of water isotope tracers to elucidate hydrological conditions of lakes in the Peace-Athabasca Delta over space and time: A foundation for lake ecosystem monitoring

by

Casey Rose Remmer

A thesis
presented to the University of Waterloo
in fulfilment of the
thesis requirement for the degree of
Doctor of Philosophy
in
Biology

Waterloo, Ontario, Canada, 2021

Examining Committee Membership

The following served on the Examining Committee for this thesis. The decision of the Examining Committee is by majority vote.

External Examiner	**Dr. Renee Brooks** *Environmental Protection Agency, USA*
Supervisor(s)	**Roland I. Hall** *Professor* *Department of Biology* **Brent B. Wolfe** *Adjunct Professor* *Department of Biology* *Professor, Department of Geography & Environmental Studies, Wilfrid Laurier University*
Internal Member	**Rebecca Rooney** *Professor* *Department of Biology* **Garry Scrimgeour** *Adjunct Professor* *Department of Biology* *Executive Director, Office of the Chief Scientist, Alberta Environment and Parks Government of Alberta*
Internal-external Member	**Merrin Macrae** *Professor* *Department of Geography & Environmental Management*

Author's Declaration

This thesis consists of material all of which I authored or co-authored: see Statement of Contributions included in the thesis. This is a true copy of the thesis, including any required final revisions, as accepted by my examiners.

I understand that my thesis may be made electronically available to the public.

Statement of Contributions

Casey Remmer was the sole author for Chapters 1 and 5 which were written under the supervision of Dr. Roland Hall and Dr. Brent Wolfe and were not written for publication.

Dr. Roland Hall and Dr. Brent Wolfe were the primary co-investigators on a NSERC Collaborative Research and Development grant that included contributions from partner organizations (Alberta Environment and Parks, BC Hydro, Canadian Natural Resources Limited, Suncor Energy, Wood Buffalo National Park). Research was also funded by Northern Water Futures of the Global Water Futures program, as well as NSERC Discovery and Northern Research Supplement grants to Hall and Wolfe. Supplemental funding from the Polar Continental Shelf Program and the Northern Scientific Training Program supported fieldwork.

This thesis consists in part of three manuscripts written for publication as peer-reviewed scientific journal papers. Exceptions to sole authorship of material are as follows:

Research presented in Chapter 2:

Casey Remmer, Roland Hall and Brent Wolfe contributed to study design. Casey Remmer, Roland Hall, Brent Wolfe and Wynona Klemt conducted fieldwork and laboratory analyses. Data analysis was primarily conducted by Casey Remmer, with participation by Wynona Klemt. Casey Remmer drafted the manuscript, which was reviewed and refined in collaboration with co-authors.

Citation: Remmer, CR, Klemt, WH, Wolfe, BB, Hall, RI. 2018. Inconsequential effects of flooding in 2014 on lakes in the Peace-Athabasca Delta (Canada) due to long-term drying. *Limnology and Oceanography* 63: 1502-1518. https://doi.org/10.1002/lno.10787

Research presented in Chapter 3:

Field work for this research was conducted by Casey Remmer, Laura Neary and Tanner Owca with assistance from Roland Hall and Brent Wolfe. The study design was primarily developed by Casey Remmer and Brent Wolfe, with input from Roland Hall and Laura Neary. Analysis was conducted by Casey Remmer. Casey Remmer drafted the manuscript, which was reviewed and refined in collaboration with co-authors.

Citation: Remmer, CR**,** Owca, T, Neary, LN, Wiklund, JA, Kay, ML, Wolfe, BB, Hall, RI. 2020. Delineating extent and magnitude of river flooding to lakes across a northern delta using water isotope tracers. *Hydrological Processes* 34: 303-320.DOI:10.1002/hyp.13585

Research presented in Chapter 4:

Casey Remmer conducted a majority of the fieldwork for this research, with assistance from many others, primarily Laura Neary and Mitchell Kay. Initial study design by Casey Remmer evolved in collaboration with co-authors. Analysis was conducted by Casey Remmer, with the assistance of Laura Neary and Mitchell Kay, and the guidance of Roland Hall and Brent Wolfe. Casey Remmer drafted the manuscript, which was reviewed and refined in collaboration with co-authors.

Citation: Remmer CR, Neary, LK, Kay, ML, Wolfe, BB, Hall, RI. 2020. Multi-year isoscapes of lake water balances across a dynamic northern freshwater delta. *Environmental Research Letters* 15: 104066. DOI:10.1088/1748-9326/abb267

Abstract

Hydrological monitoring in complex, dynamic northern floodplain landscapes is challenging but increasingly important as these ecosystems come under threat from multiple stressors, including climate-driven decline in freshwater supplied by rivers draining the hydrographic apex of western North America. Sustainable approaches capable of tracking status, trends and drivers of lake water balances in complex, remote landscapes are needed to inform ecosystem stewardship and water-security actions. The Peace-Athabasca Delta (PAD) in northern Alberta, Canada, is a Ramsar Wetland of International Importance reliant on episodic river ice-jam flood events to recharge abundant perched lakes and wetlands. However, the frequency of these floods has been in decline for decades over much of its area. Compounding concerns about water-level drawdown have prompted the need to improve knowledge of lake water balances and establish a lake monitoring program. Yet, the delta's remoteness and dynamic nature present challenges to these goals. In this thesis, I address hydrological knowledge gaps essential to understanding spatial and temporal patterns of hydrological processes and their influence on lakes in the PAD.

First, we assess the legacy influence of a large-scale ice-jam flood in 2014 on hydrological and limnological status of lakes in the PAD by integrating spatial and temporal data. Analysis of water isotope compositions and water chemistry measured at numerous lakes across the delta shows that hydro-limnological effects of the flood event of 2014 failed to persist beyond the early ice-free season of 2015. Isotope-inferred paleohydrological records from five hydrologically representative lakes in the PAD indicate that periodic desiccation during the Little Ice Age occurred at the most elevated basin in response to locally arid climatic conditions and reduced flood frequency, yet other lower elevation sites were influenced by high water level on Lake Athabasca owing to increased snowmelt- and glacier-derived river discharge. In contrast, water isotope data during the past 15 years at all five lakes consistently document the strong role of evaporation, a trend which began in the early to mid-20th century according to sediment records and is indicative of widespread aridity unprecedented during the past 400 yr. We suggest that integration of hydrological and limnological approaches over space and time is needed to inform assessment of contemporary lake conditions in large, complex floodplain landscapes.

Next, we use water isotope compositions, supplemented by measurements of specific conductivity and field observations, from 68 lakes and 9 river sites in May 2018 to delineate the extent and magnitude of spring ice-jam induced flooding along the Peace and Athabasca rivers. Lake-specific estimates of input water isotope composition (δ_I) using a coupled-isotope tracer approach were modelled after accounting for the influence of evaporative isotopic enrichment. Then, using the distinct isotopic signature of input water sources, we develop a set of binary mixing models and estimate the proportion of input to flooded lakes attributable to river floodwater and precipitation (snow or rain). This approach allowed identification of areas and magnitude of flooding that were not captured by other methods, including direct observations from flyovers, and to demarcate flow pathways in the delta. We demonstrate water isotope tracers as an efficient and effective monitoring tool for delineating spatial extent and magnitude of an important hydrological process and elucidating connectivity in the PAD, an approach that can be readily adopted at other floodplain landscapes.

Finally, we use over 1000 measurements of water isotope composition at ~60 lakes and 9 river sites during the spring, summer and fall of five consecutive years (2015–2019) to identify patterns in lake water balance over time and space, the influential roles of evaporation and river floodwaters, and relations with meteorological conditions and river water levels. Calculation of evaporation-to-inflow ratios using a coupled-isotope tracer approach, displayed via generalized additive models and geospatial 'isoscapes', reveal strongly varying lake water balances. Results identify distinct areas vulnerable to lake-level drawdown, given the likelihood of continued decline in ice-jam flood frequency, longer ice-free season duration and reduced snowmelt runoff. Results also demarcate areas of the delta where lakes are more resilient to factors that cause drawdown. The former defines the Peace sector, which is influenced by floodwaters from the Peace River during episodic ice-jam flood events, whereas the latter describes portions of the active floodplain environment of the Athabasca sector which receives more frequent contributions of Athabasca River floodwaters during both spring ice-jam and open-water seasons. Efficiency of water isotope tracers to capture the marked temporal and spatial heterogeneity in lake water balances during this 5-year time span, and their diagnostic responses to key hydrological processes, serves as a foundation for ongoing lake monitoring, an approach readily transferable to other remote and dynamic lake-rich landscapes.

Acknowledgements

I owe thanks to many who have supported me through this journey. Roland and Brent, thank-you for believing in me and seeing the possibilities, 5 years ago I could not have imagined being here today. The opportunities you have given me have been life-changing, and your support has expanded my horizons. Dr. Rebecca Rooney, thank-you for being a role model and a mentor, I have learned so much from you. Dr. Garry Scrimgeour, thank-you for your guidance through these projects and for your thought-provoking questions. I am also grateful for the friendship and adventures shared with members of the Hall and Wolfe lab, especially Wynona Klemt, Eva Meher, Laura Neary, Jelle Faber, Tanner Owca and Mitchell Kay, you have been such a fantastic group to work and I have such wonderful and unique memories.

Thank-you to Robert and Barbara Grandjambe, who always welcomed us into Fort Chipewyan and showed an unparalleled kindness and generosity. I would also like to thank Queenie Gray, for support in the field and for her valuable perspectives.

To Courtney Robichaud, I would not be finishing this Thesis if it weren't for you, and I am so glad we can be Dr. CR^2 forever. I am a better scientist and a better person for our (many) conversations, and I continue to be inspired by how you move through the world. To Meghan Mechler, thank-you for sharing my particular sense of humor and for your endless support, for being there during so many of the most important moments of my life. To Jennie Egerdie, thank-you for being one of my forever people, and the coolest, funniest aunt to my kids.

I am deeply grateful to my parents, Dorothy and Richard, who have believed in me and supported me from the very beginning until the very end of this journey. The countless hours of puzzles, crafts and kids' activities you have done so I can work made this Thesis possible, and you surely deserve a best grandparents award. To my brother Vinnie and sister Annie, you may not understand what it is I have been doing all these years, but it has never stopped you from being there when I needed you.

To my husband Andy, you dropped everything to move to a place you had never been so I could finish this degree, and you have made my life so much bigger and better. You are such an amazing father and partner, thank-you for keeping a bustling household running when I am busy and for the endless ways you take care of us every day. To my daughters Lilia and River, thank-you for the joy you bring and all the ways you make me grow.

Dedication

To Lilia, my guiding light.

To grow with you has been the greatest adventure, and though you are currently unimpressed by this dedication I hope that one day you will understand what we have achieved together.

TABLE OF CONTENTS

List of Figures

List of Tables

1.0 Introduction

1.1 Northern Freshwater Landscapes

Globally, freshwater ecosystems are reliant on the security of water supply to maintain their biodiversity and essential role in biogeochemical and hydrologic cycling. Culminating stressors, including climate change, industrial development and land use, challenge effective stewardship (e.g., Gleick, 2003; Hassan, 2005; Woodward et al., 2010; Dudgeon et al., 2006). More than 50% of global wetlands have been lost since the 1900s, with inland wetlands lost at a rate almost twice as fast as coastal sites and up to 75% lost in the 20th century (Davidson, 2014). Freshwater ecosystems contain up to 12% of known species despite occupying less than 1% of the Earth's surface (Juffe-Bignoli et al., 2016). Consequently, these ecosystems have the highest rate of biodiversity loss (Diaz et al., 2019; Southee et al., 2021), yet remain under-studied and poorly understood. At northern latitudes, where many shallow freshwater ecosystems are found, inadequate knowledge is often due to remote locations and the associated difficulties in collecting adequate scientific and monitoring data. In northwestern North America, the abundant small, shallow, freshwater lakes and wetlands are particularly sensitive to environmental changes, as even small hydrologic shifts can result in cascading ecological changes (e.g., Smol et al., 2005; Prowse et al., 2006; Schindler and Donahue, 2006; Schindler and Smol, 2006). Threats to remaining inland wetland complexes are continually increasing, as rising human water use converges with declining supply from upstream glaciers and high elevation snowpacks, increasing temperature, and longer ice-free seasons, which promote evaporative water loss coincident with reduced input (e.g., Schindler and Smol, 2006; Dery and Wood, 2005; Rood et al., 2005; Schindler and Donahue, 2006; Barnett et al., 2008; Burn et al., 2010; Sauchyn et al., 2015; Scalzitti et al., 2016). As knowledge of the ecological and biophysical importance of

inland freshwater systems and their vulnerability develops, it is increasingly recognized that understanding the hydrological processes driving landscape scale responses is needed to predict future conditions. Appropriate temporal and spatial scale are required for hydrological research to succeed in capturing the effects of climate and related hydrological change on important landscape scale connectivity among freshwater ecosystems (rivers, channels, wetlands, lakes; Fausch et al., 2002).

1.2 The Peace-Athabasca Delta

The Peace-Athabasca Delta (PAD), northern Alberta, is threatened by climate-driven decline of river discharge and upstream industrial development (e.g., PADPG, 1973; Prowse and Conly, 1998; Beltaos, 2014; WHC/IUCN, 2017; Figure 1.1). Located primarily within Wood Buffalo National Park, the PAD is a dynamic, productive northern floodplain. It is the world's largest inland boreal freshwater delta, spanning 6,000 km^2, and receives input from two major rivers – the Peace and Athabasca. The hundreds of shallow lakes and wetlands that characterize the delta provide important natural resources for Indigenous communities and habitat for a variety of biota, whose populations are influenced by water availability (Straka et al., 2018; Vannini and Vannini, 2019; Ward et al., 2018, 2020).

The PAD contains mainly two hydro-ecologically distinct sectors. The northern Peace sector is a relic delta with numerous inliers of Precambrian Shield protruding above the fluviodeltaic plain. Lakes in this sector receive Peace River floodwater during episodic ice-jam events that result in widespread flooding, but is otherwise primarily influenced by snowmelt, rainfall and evaporation (PADPG, 1973, Peters et al., 2006). The southern Athabasca sector has less topographic relief and is an active delta. It is fed by frequent flooding of the Athabasca River, which divides into numerous distributaries as it flows towards Lake Athabasca or

Mamawi Lake (PADPG, 1973). Spatial variability in physical, chemical and biological conditions of lakes in the PAD is driven primarily by the relative roles of hydrological processes (river floodwater, snowmelt, rainfall, evaporation) that influence lake water balances (PADPG, 1973; Pietroniro et al., 1999; Wolfe et al., 2007b; Prowse et al., 2002; Wiklund et al., 2012). In recognition of its ecological, historical and cultural significance, the PAD is listed as a Ramsar Wetland of International Importance and contributed importantly to the listing of Wood Buffalo National Park (WBNP) as a UNESCO World Heritage Site. Water quality and quantity in this hydrologically-driven landscape is threatened by multiple stressors including hydroelectric regulation of Peace River flow, water withdrawals and the potential for contaminant loading by upstream oilsands development on the Athabasca River, and climate-driven decline of river discharge. These concerns have led to a reactive monitoring mission by the World Heritage Committee (WHC) in response to a petition submitted by the Mikisew Cree First Nation to place WBNP on the List of World Heritage Sites in Danger (MCFN, 2014; WHO/IUCN, 2017).

A wealth of literature has been written about hydrology in the PAD, in recognition of the central role hydrological processes play in shaping the landscape. Low water levels in Lake Athabasca during the filling of the WAC Bennett Dam reservoir upstream on the Peace River in 1968-1971 sparked concern and prompted an environmental impact assessment of Peace River regulation on the Peace-Athabasca Delta (PADPG 1972, 1973). As a result, a Peace-Athabasca Delta Implementation Committee installed two rockfill weirs in the 1980s (PADIC, 1987). This was followed in the mid-90s by the Peace–Athabasca Delta Technical Studies, which aimed to guide restoration in the delta (PADTS, 1996) and the Northern River Basin study, which focused on flow regulation impacts (Prowse and Conley, 2002). These early studies examined primarily the Peace sector of the delta and identified the importance of spring ice-jam floods for recharging

the perched basins that characterise this sector. Subsequent work based largely on the water balance of a singular perched basin identified the strong role of evaporation in water level drawdown (Prowse and Conly, 2002). Studies focused on understanding hydrological conditions in the context of longer records emerged, with the focus again on ice-jam floods along the Peace River and their role in the water balance of lakes in the Peace delta (Timoney, 1997; summarized in Wolfe et al., 2012). Paleolimnological investigations of a set of representative lakes highlighted marked spatial and temporal variability and the strong influence of climate on lake water balances (Wolfe et al., 2012). Categorization of a broader set of lakes across both sectors of the delta was achieved by Wolfe et al. (2007b), using water isotope compositions and water chemistry. Subsequent isotope-based studies focused more closely on a few lakes and established the connections between hydrological processes (flooding, precipitation, evaporation) and lake conditions (Yi et al., 2008; Wiklund et al., 2012). With the exception of Wolfe et al. (2007b) and Yi et al. (2008), these investigations have relied either on river hydrometric records or a handful of representative lake sites, and findings are extrapolated to the many other lakes of the delta. More recently, work using satellite imagery and remote sensing (Peters et al., 2021) has contributed to understanding landscape level hydrological events and change, but is sensitive to timing, focused on spatial extent and cannot quantify influence of the various hydrological processes on lake water level variation and water balance.

Among several recommendations made by the WHC/IUCN (2017) are to "*establish adequate baseline hydrological information of the Peace and Athabasca River Basins to enhance the reference for monitoring and assessing current and future hydrological conditions*" (p. 4) and "*expand the scope of monitoring and project assessments to encompass possible individual and cumulative impacts on the Outstanding Universal Value of the property* [i.e., WBNP] *and in*

particular the PAD" (p. 4). WHC/IUCN (2017) also recognized the effects of climate change on the Outstanding Universal Value of WBNP and the PAD and identified a "*need to invest in better understanding the interactions between this naturally dynamic high latitude ecosystem and climate* (p. 16)". Data of sufficient spatial and temporal scales are required to address these needs. Recently, an Action Plan for WBNP released by the Canadian government (WBNP, 2019) reiterated the importance of comprehensive hydrological understanding to guide conservation efforts and maintain the value of the Peace-Athabasca Delta. Research presented in this Thesis will address this need and advances our understanding of hydrological processes by generating multiple datasets of hydrological conditions across space and time for the freshwater basins of the PAD. The knowledge generated is grounded in the repeated sampling of a large representative set of lakes, capturing the range of potential water balance responses to various hydrological processes.

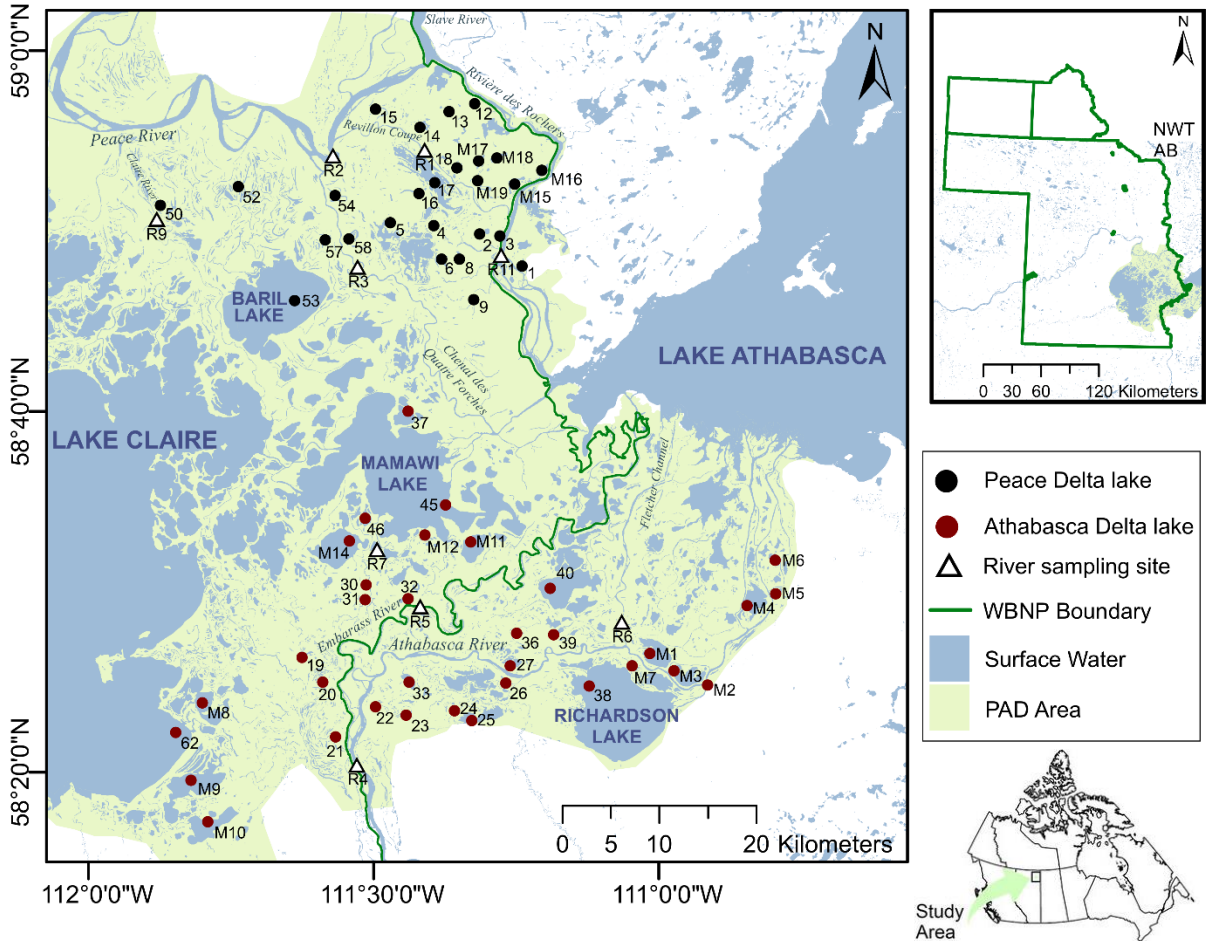

Figure 1.1. Map showing the location of the Peace-Athabasca Delta, Alberta Canada. The boundary of Wood Buffalo National Park (WBNP) is outlined in dark green and the area of the entire Peace-Athabasca Delta is light green. Primary sampling sites are indicated by circles (lakes) and triangles (rivers). Lake sites in the Athabasca Delta are solid red circles and lake sites in the Peace Delta are solid black circles.

1.3 Water Isotopes and Isoscapes

As analytical instrumentation and understanding has rapidly improved over recent decades, water isotope tracers are increasingly recognized for their unique value in understanding hydrological processes. Focused initially on the systematic variation of isotopic compositions in global precipitation (Craig, 1961; Dansgaard, 1964) and isotopic fractionation during evaporation (Craig and Gordon, 1965), current work covers a wide array of locations and conditions including many applications in Canada's freshwater systems (reviewed in Gibson et al., 2005). Systematic mass-dependent isotope fractionation in the hydrological cycle (Rozanski et al., 1993; Gat, 1996; Gibson and Edwards, 2002) results in key relationships that form the foundation of water isotope analysis. The Global Meteoric Water line (GMWL) represents the relationship between $\delta^{18}O$ and $\delta^{2}H$ in precipitation derived from atmospheric moisture originating from the subtropic ocean and undergoing progressive distillation as air masses move poleward (Craig, 1965). The slope of the GMWL reflects the temperature-dependent equilibrium fractionation occurring between atmospheric vapour and precipitation. At a local scale, a Local Meteoric Water Line (LMWL) may be used to represent local precipitation, which may diverge from the GMWL due to kinetic fractionation of snow formation and raindrop re-evaporation (Rozanski et al., 1993). A Local Evaporation Line (LEL) is often a key component of a water isotope analysis, and this line represents the mass-dependent fractionation that occurs when surface water undergoes evaporation. The slope of the LEL usually ranges between 4 to 6, and depends on local atmospheric conditions (Gibson and Edwards, 2002). Surface water bodies fed by the same mean annual isotope composition of precipitation (δ_P) will cluster along a LEL anchored to the GMWL/LMWL by δ_P with their position along the line dependant on the degree of evaporative isotope enrichment. The theoretical maximum isotopic enrichment, represented

by δ*, anchors the terminal end of the LEL. Additionally, the isotope composition of a terminal basin at steady-state (δ_{SSL}) will lie approximately midway along the LEL.

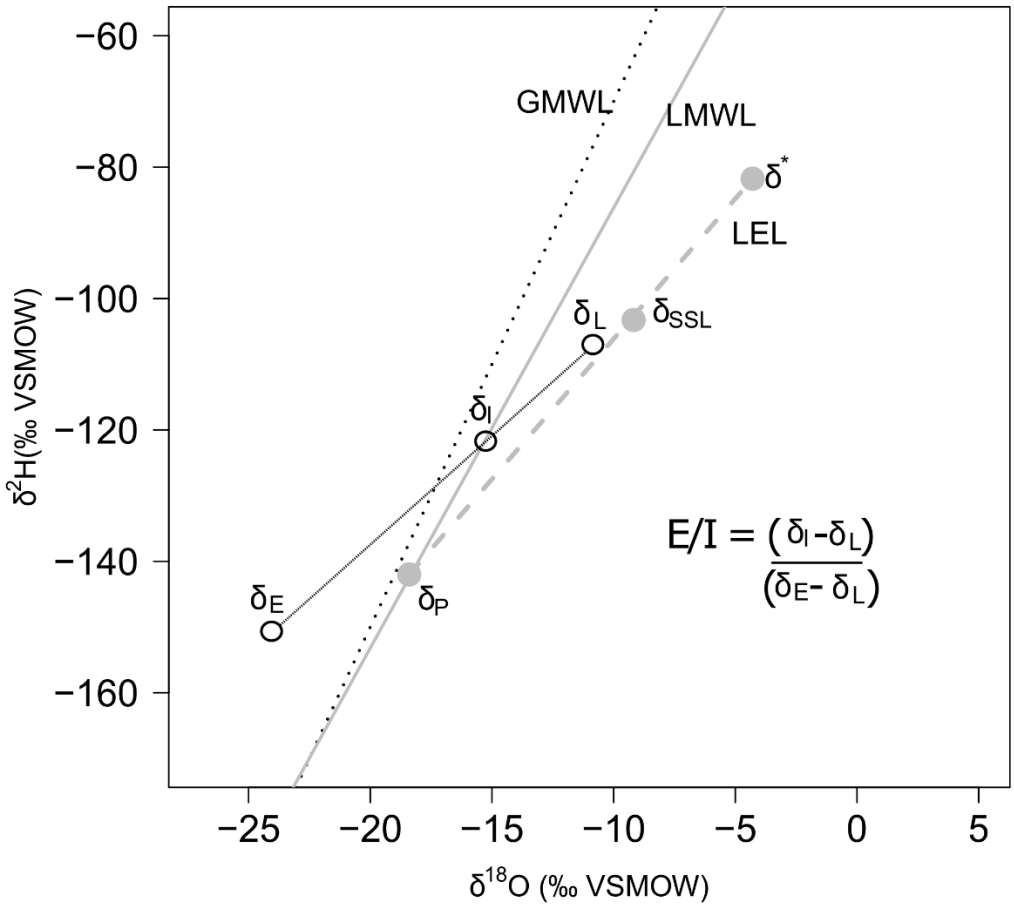

Figure 1.2 Schematic $\delta^{18}O$-$\delta^{2}H$ diagram illustrating water isotope compositions of a hypothetical lake (δ_L) that plots along a lake-specific evaporation line (solid black line). The intersection of lake-specific evaporation line with the Local Meteoric Water Line (LMWL) provides an estimate of input water isotope composition (δ_I). Important features of the Local Evaporation Line (LEL) include the steady-state isotope composition for a terminal basin (δ_{SSL}), which represents the special case of a lake at hydrological and isotopic steady state in which evaporation exactly equals inflow, and the limiting non-steady-state isotope composition (δ*), which indicates the maximum potential isotopic enrichment of a lake as it approaches complete desiccation. The LEL is anchored at the mean annual isotope composition of precipitation (δ_P). Parameters used in the isotope mass-balance model to derive δ_I include the lake water isotope composition (δ_L) and the isotope composition of evaporated vapor from the lake (δ_E).

In this Thesis I apply the isotopic mass balance approaches developed in Yi et al. (2008) to generate quantitative estimates of lake water balances. This includes utilizing 13 years of data collection from an index lake to infer $\delta_{SSL,}$ and to calculate the isotopic composition of atmospheric moisture (δ_A). We were then able to calculate a predicted LEL, in contrast to the more commonly used regression-based LEL. For each lake water isotopic composition, assumed to experience the same atmospheric conditions, we can then calculate a lake-specific evaporation line that terminates at δ^*. The isotopic composition of evaporative flux (δ_E) should lie on an extension of the lake evaporation line to the left of the GMWL/LMWL (except under conditions of non-steady-state evaporation) and can be estimated using the isotopic composition of atmospheric moisture (δ_A), the isotopic composition of lake water (δ_L), relative humidity (h) and temperature (T; Gonfiantini, 1986). Since the lake specific isotopic composition of input water is primarily considered to be meteoric water (or isotopically-equivalent), it can be constrained to the LMWL, directly coupling the oxygen and hydrogen isotopic signatures (referred to as the coupled isotope tracer method in Yi et al., 2008). These parameters can then be used to calculate equivalent $\delta^{18}O$ and $\delta^{2}H$ derived evaporation-to-inflow ratios (E/I), an index of lake-water balance (Gibson and Edwards, 2002; Yi et al., 2008). Lake water balance has been compared among basins at numerous scales, including watersheds (Cui et al., 2017; Kang et al., 2017; MacKinnon et al., 2016), regions (MacDonald et al., 2017; Narancic et al., 2017; Turner et al., 2014; Gibson et al., 2002, 2016, 2017) and continents (Brooks et al., 2014). Regional scale studies have been developed with great success in the vast, generally unmonitored and difficult to access lake rich landscapes of northern Canada (Brock et al., 2007; Gibson, 2001, 2002; Gibson and Edwards, 2002; Turner et al., 2014; Wolfe et al., 2007b; Yi et al., 2008).

The importance of understanding spatial patterns of variation in hydrological processes and water balance has long been recognized in the field of isotope hydrology (e.g., Rozanski et al., 1993; Gibson and Edwards, 2002; Bowen and Revenaugh, 2003). Evolving statistical approaches and rapid improvement in computing power have advanced the combination of isotopes with geostatistics into the field of isoscapes (isotopic landscapes). A majority of the research using isoscapes have relied on large, distributed collection networks operating at global or continental scales, and such analyses have occurred for precipitation (Allen et al., 2018; Bowen and Revenaugh, 2003; Hatvani et al., 2020; Terzer et al., 2013), groundwater (Scheliga et al., 2017; Wassenaar et al., 2009; Wright and Novakowski, 2020) and surface water (Birkel et al., 2018; Brooks et al., 2012; Mountain et al., 2015). More recently, regional- and catchment-scale collection campaigns have demonstrated the utility of isoscapes in understanding finer-scale patterns and their ecosystem effects (i.e., Brooks et al., 2012; Scheliga et al., 2017; Birkel et al., 2020). Isoscapes of surface water provide one of the few observational methods for understanding water balance and climate change at catchment to continental scales, and can be used to estimate isotopic values at unmonitored sites, expanding the ability of investigators to understand patterns and processes (Bowen, 2010). For example, Gibson and Edwards (2002) used isoscapes of northern Canadian lakes to identify variations in evaporative water loss across the forest to tundra transition. Turner et al. (2014) used isoscapes to identify seasonal patterns of input water sources to thermokarst lakes in the Arctic and the variability of these patterns between years. Identification of spatial relationships can be used to elucidate the underlying processes driving lake water balances, and to validate or test prevailing understanding of landscape patterns.

1.4 Research Approach and Objectives

Informed decision making and stewardship of the PAD requires spatially and temporally comprehensive understanding of the complex and dynamic hydrological processes that regulate ecosystems in this landscape. The aim of this thesis is to determine the primary drivers of water availability in the lakes of the Peace-Athabasca Delta and to generate new, comprehensive understanding of the patterns of hydrological conditions in the landscape over space and time. The thesis consists of three data chapters where specific objectives are provided. Throughout my thesis, I generate isoscapes whose interpretation is strengthened by combination with other datasets. Water isotopes form the foundation of the analyses, and I demonstrate repeatedly their utility as a sensitive, informative and accessible approach to capturing hydrological processes in remote, dynamic landscapes. In my final chapter, I integrate findings from all three chapters, and summarize the management implications.

Chapter 2. Inconsequential effects of flooding in 2014 on lakes in the Peace-Athabasca Delta (Canada) due to long-term drying

Citation: Remmer, CR, Klemt, WH, Wolfe, BB, Hall, RI. 2018. Inconsequential effects of flooding in 2014 on lakes in the Peace-Athabasca Delta (Canada) due to long-term drying. *Limnology and Oceanography* 63: 1502-1518. https://doi.org/10.1002/lno.10787

2.1 Introduction

Climate-driven reductions in mid- to high-elevation snowpack and headwater glacier volume have resulted in declining flow of rivers draining the hydrographic apex of western North America during the past century (e.g., Dery and Wood, 2005; Rood et al., 2005; Schindler and Donahue, 2006; Barnett et al., 2008; Burn et al., 2010; Sauchyn et al., 2015; Scalzitti et al., 2016). Diminishing river discharge threatens downstream ecosystems and societies, where freshwater resources have traditionally been managed under the assumption of hydrological stationarity (Schindler and Donahue, 2006; Milly et al., 2008). This assumption may, however, lead to misguided water resource planning and decision-making (Milly et al., 2008), as best exemplified by numerous paleohydrological reconstructions which show there have been extended periods (decades to centuries) in the past when river discharge has been well below that experienced during the instrumental period (Watson and Luckman, 2004; Wolfe et al., 2008a; Wolfe et al., 2011; Sauchyn et al., 2015; Coulthard et al., 2016). Furthermore, evidence suggests that time since European settlement has been an era of relatively abundant freshwater supply, enhanced by glacial meltwater contributions to river discharge in response to glacier expansion during the Little Ice Age (Wolfe et al., 2011). Long-term perspectives identify that this era of abundant freshwater is ending, with significant and imminent consequences for downstream ecosystems and societies (Rood et al., 2005; Schindler and Donahue, 2006; Wolfe et al., 2008a; Rasouli et al., 2013).

The Peace-Athabasca Delta (PAD), northern Alberta, is one such downstream landscape that is responsive to, and heavily reliant upon, eastward-flowing river discharge originating in the Rocky Mountains to support its rich biological diversity (e.g., PADPG, 1973; Prowse and Conly, 1998). The PAD is recognized as a Ramsar Wetland of International Importance and contributed to the listing of Wood Buffalo National Park (WBNP), which contains 80% of the PAD, as a UNESCO World Heritage Site. River water that recharges the abundant shallow lakes and wetlands during periodic spring ice-jam floods is a crucial hydrological process for sustaining the ecological integrity of the delta (Prowse and Conly, 1998), but the frequency of such events has been in decline for decades (Timoney et al., 1997; Timoney et al., 2002; Wolfe et al., 2006; Wolfe et al., 2008a). For example, 2014 marked the first time in nearly 20 years (since 1997) that widespread ice-jam flooding has occurred. The cause for declining ice-jam flood frequency has long been the subject of analysis, which has centered on identifying relative contributions of climate change and regulation of the Peace River by the WAC Bennett Dam (e.g., Prowse and Conly, 1998; Wolfe et al., 2012; Beltaos, 2014). Reduction of flooding has resulted in a decline of open water habitat and encroachment of willows as wetlands dry out (Timoney, 2013). Concerns over lower lake and wetland water levels in the PAD have been heightened with the recent approval and onset of construction of the Site C hydroelectric dam on the Peace River, and water withdrawals from the Athabasca River to support the oil sands industry. These concerns have led to a petition submitted to UNESCO by the Mikisew Cree First Nation to place WBNP on the List of World Heritage Sites in Danger, in recognition of the multiple stressors that threaten the PAD (MCFN, 2014).

A key challenge to contextualizing the effects of declining river discharge and frequency of flood events on lakes in the hydrologically-dynamic PAD is that hydrometric data only span

the past few decades and are sparse in spatial extent, which inhibit ability to clearly identify the causes of declining lake water levels and flood frequency within the delta. This impedes resource management decision-making and stewardship. To address this pressing knowledge gap, a series of paleolimnological investigations were conducted at several lakes in the PAD during the early 2000s, which provided new insights into the evolution, variability and drivers of lake hydrological conditions within the delta (reviewed in Wolfe et al., 2012). A central finding was the identification of complex relations among climate change, river discharge and flood frequency, and lake hydrology, which are expressed at varying spatial and temporal scales. For instance, during the Little Ice Age (~1600-1900 CE), high summer river discharge raised Lake Athabasca water levels and inundated low-lying central portions of the delta (Wolfe et al., 2008a; Johnston et al., 2010; Sinnatamby et al., 2010). Concurrently, lakes in elevated areas of the delta underwent water-level drawdown in response to local climate aridity and low frequency of ice-jam floods because of delayed and protracted upstream, high-elevation snowmelt runoff. In contrast, during the 20th century, evaporation-driven water-level drawdown has occurred at both high and low elevation areas of the PAD due to climate change and declining spring and summer river discharge. With expected continued declines in high-elevation snowpack and headwater glacier volume, Wolfe et al. (2008a) predicted that increasingly low river discharge would lead to further drying of the delta.

In the PAD, river floodwaters exert strong influence on limnological conditions of the floodplain lakes. As illustrated by Wiklund et al. (2012), floodwaters raise concentrations of suspended sediment, total phosphorus (TP), sulfate and dissolved silica (DSi) of receiving lakes, and reduce concentrations of total nitrogen (TN), dissolved organic carbon (DOC) and most major ions. After flooding, limnological conditions respond at two timescales (Wiklund et al.,

2012). One occurs over a few weeks to months as suspended sediments settle out of the water column of lakes, which increases water clarity and reduces TP concentration but without substantial change in concentration of DOC, sulfate, TN or ions. The other timescale occurs over several years to decades, as evaporation raises concentrations of most nutrients, DOC and ions. Thus, alteration of flood regimes has potential to alter physical and chemical characteristics of lakes in the PAD.

In light of widespread ice-jam flooding in 2014 and subsequent arid conditions in 2015, we integrate spatial and temporal data to assess current hydrological and limnological conditions in lakes of the PAD. First, we use a map produced by WBNP that marks the extent of 2014 floodwaters, supplemented by lake and river water isotope data, and water isotope and limnological data from across the delta in 2015 to show that the 2014 floodwaters had largely short-term (within-year) effects. Second, we demonstrate strong, uniform influence of evaporation during the past 15 years on water balance at five representative lakes, a trend that began in the early to mid-20th century and is unprecedented in the context of the past ~400 years. Findings strongly suggest that the delta has entered a new climate-driven regime of low water availability during the past few decades, which threatens aquatic habitat and ecological integrity.

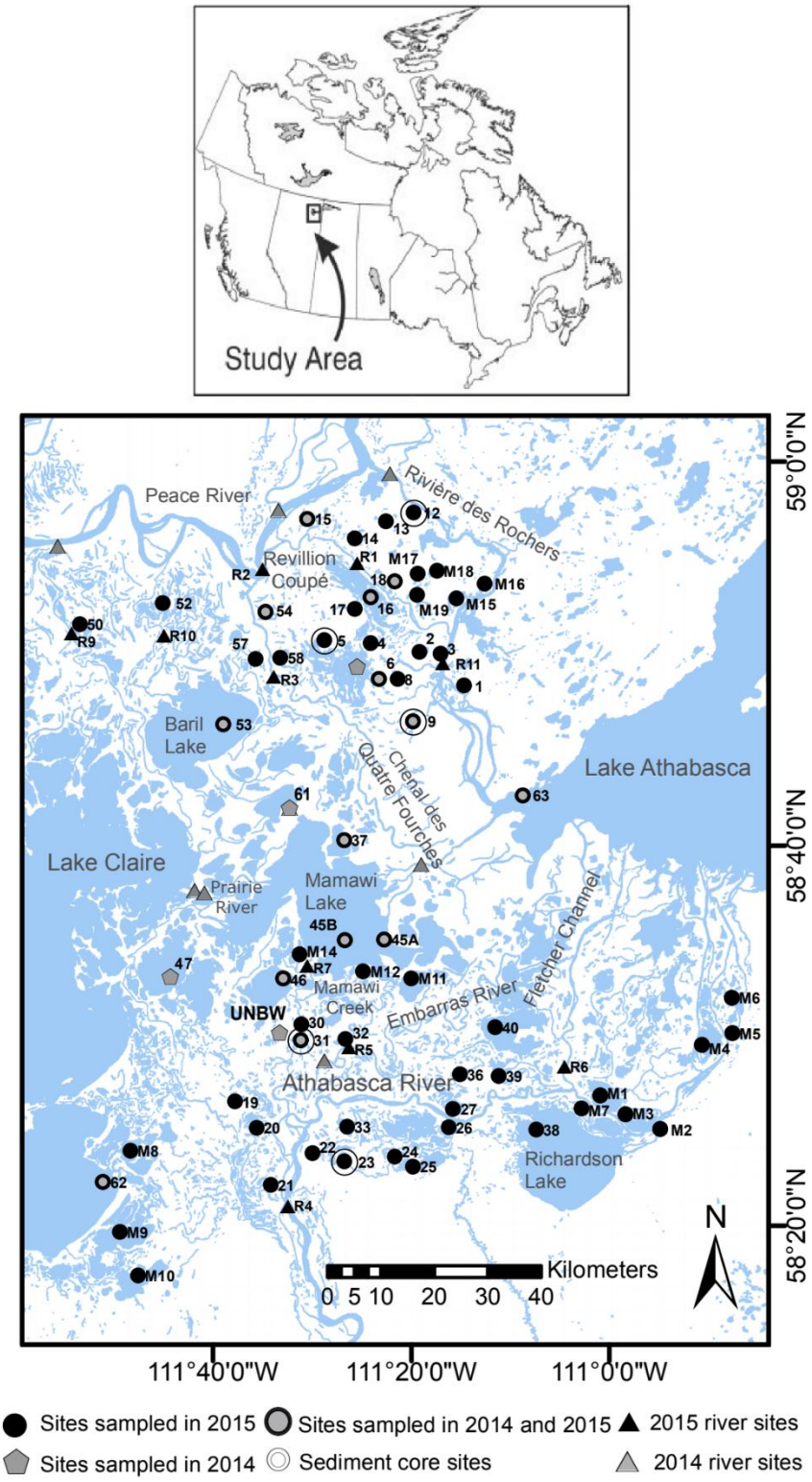

Figure 2.1. Map showing location of the Peace-Athabasca Delta, Alberta, and the location of 61 lake (black circles) and 9 river (black triangles) sites within the delta sampled in 2015. Sites additionally sampled in 2014 (grey samples) and the five sediment core collection sites (circles) are noted.

2.2 Methods

2.2.1 Study area and sampling locations

The Peace-Athabasca Delta spans 6,000 km^2 and contains three distinct sectors, differentiated by the relative roles of hydrological processes that influence lake water balances (Figure 2.1) (PADPG, 1973; Pietroniro et al., 1999; Wolfe et al., 2007b). The northern Peace sector is a relic delta, which receives Peace River floodwater during infrequent high-elevation ice-jam flood events. These events can result in widespread flooding of the delta. Consequently, lakes in this region of the delta are strongly influenced by evaporation (except on occasions when they are flooded) and have been termed closed-drainage, isolated or perched basins. The southern Athabasca sector contains both relic and active delta regions. Lakes in the relic portion of the Athabasca sector tend to be closed drainage, whereas lakes in the active portion are mainly restricted drainage, which capture a broad gradient of influence from river floodwaters. The central, low-lying portion of the delta contains broad, shallow lakes that continuously receive discharge from many rivers and creeks and are classified as open drainage. A subset of closed-drainage lakes in the central interior of the delta are termed shallow rainfall-influenced lakes, as recognized by Wolfe et al. (2007b), and tend to be ephemeral.

The extent of the 2014 spring ice-jam flood was determined from flight surveys by staff of WBNP and confirmed by measurement of water isotope compositions from 16 lakes and eight river locations on 30 May – 3 June 2014 (Figure 2.2). This information was used to categorize 61 lakes as flooded or not flooded in 2014. One large, open-drainage basin, Mamawi Lake, was sampled in two locations, one near the outlet (Chenal des Quatre Fourches; PAD 45A) and one near the inflow (Mamawi Creek; PAD 45B). These lakes (and nine river sites) were used to evaluate hydrological and limnological conditions one year after the 2014 flood event based on

measurements of water isotope composition and water chemistry (on 26-31 May, 26-28 June [only water isotope composition], 27-28 July and 15-16 September 2015; Figure 2.1).

To place recent water isotope data into a longer temporal perspective, sediment core records of cellulose-inferred lake water oxygen isotope composition previously published from a subset of five lakes (Wolfe et al., 2008a; Wolfe et al., 2008b; Sinnatamby et al., 2010; Figure 2.1) were assembled and combined with water isotope compositions measured periodically in the same lakes between 2000-2006. Three of these lakes are located in the northern Peace sector (PAD 5 [informally called 'Spruce Island Lake'; Wolfe et al., 2005], PAD 9 and PAD 12) and are closed-drainage basins that, presently, receive river floodwaters infrequently. The other two lakes are located in the southern Athabasca sector (PAD 23 and PAD 31 [local name: 'Johnny Cabin Pond'; Wolfe et al., 2008b]), and their hydrological conditions have been recently influenced by geomorphic changes in the flow path of the Athabasca River and its distributaries. PAD 23 is a closed-drainage basin and has infrequently received river floodwaters since engineered excavation of the Athabasca River Cut-Off in 1972. PAD 31 is a restricted-drainage basin that has frequently received river floodwater from Mamawi Creek since the Embarras Breakthrough in 1982. Further site details may be found in the original publications (Wolfe et al., 2005; Wolfe et al., 2008a; Wolfe et al., 2008b; Sinnatamby et al., 2010).

2.2.2 Isotope hydrology of lakes

Water samples for oxygen and hydrogen isotope analysis were collected mid-lake (or mid-channel) from a depth of ~10 cm and stored in sealed 30 ml high-density polyethylene bottles. Lake water isotope compositions pre-2014 were measured by conventional Continuous Flow Isotope Ratio Mass Spectrometry (CF-IRMS), whereas 2014 and 2015 samples were measured by Off-Axis Integrated Cavity Output Spectroscopy (O-AICOS). For the samples

measured by CF-IRMS, $\delta^{18}O$ was analyzed by 2% CO_2 headspace equilibration on a multi-flow coupled with GV instruments Isoprime (MF-GVI-Isoprime) and $\delta^{2}H$ was analyzed by hot chromium reduction on a High Temperature Euro Vector EA coupled with GV Instruments Isoprime (HT-EA-Isoprime). For the samples measured by O-AICOS, a Los Gatos Research Triple Liquid Water Isotope Analyzer (LGR T-LWIA 45-EP) was used. All samples were analyzed at the University of Waterloo – Environmental Isotope Laboratory (UW-EIL). Isotope compositions are expressed as δ-values, representing deviations in per mil (‰) from Vienna Standard Mean Ocean Water (VSMOW) such that $\delta_{sample} = [(R_{sample}/R_{VSMOW}) - 1] \times 10^3$, where R is the $^{18}O/^{16}O$ or $^{2}H/^{1}H$ ratio in the sample and VSMOW. Results of $\delta^{18}O$ and $\delta^{2}H$ analyses are normalized to -55.5‰ and -428‰, respectively, for Standard Light Antarctic Precipitation (Coplen, 1996). Analytical uncertainties are ±0.2‰ for $\delta^{18}O$ and ±2.0‰ for $\delta^{2}H$ for samples analyzed by CF-IRMS, and ±0.2‰ for $\delta^{18}O$ and ±0.8‰ for $\delta^{2}H$ for those analyzed by O-AICOS.

To identify the hydrological processes controlling lake-water balances at the individual lake and landscape scale, a coupled-isotope tracer approach was used (Yi et al., 2008) based on the classic linear resistance model (Craig and Gordon, 1965). Initially, an isotope framework representing average conditions from 2000-2015 was developed using techniques similar to those described in Wolfe et al. (2007b) and Yi et al. (2008) for the PAD. The isotope framework provides a semi-quantitative method of assessing the water balance of rivers and lakes during the ice-free season.

The isotope framework consists of two linear trends in $\delta^{18}O$-$\delta^{2}H$ space, which are the result of mass-dependent partitioning of stable isotopes $^{1}H_2{}^{16}O$, $^{1}H^{2}H^{16}O$ and $^{1}H_2{}^{18}O$ within the hydrological cycle (Edwards et al., 2004). The isotope composition of precipitation at a site will cluster along a Local Meteoric Water Line (LMWL), which often lies close to the Global

Meteoric Water Line (GMWL). The GMWL represents the observed relation between $\delta^{18}O$ and $\delta^{2}H$ in amount-weighted annual precipitation worldwide, described by $\delta^{2}H = 8\ \delta^{18}O + 10$ (Craig, 1961). For the PAD, the LMWL is approximated by $\delta^{2}H = 6.7\ \delta^{18}O - 19.2$, based on precipitation collected at Fort Smith, NWT (Wolfe et al., 2007b).

The isotope composition of local surface water fed by mean annual isotope composition of precipitation (δ_P) undergoing evaporation will plot in a linear cluster offset from the LMWL, forming a linear trend called the Local Evaporation Line (LEL) (Gibson and Edwards, 2002). Movement of lake and river water samples up the LEL occurs due to isotopic enrichment and indicates increasing influence of evaporation and the resulting heavy isotope build-up in remaining surface water. Enrichment of ^{18}O and ^{2}H in evaporating water bodies is described by the linear resistance model of Craig and Gordon (1965), which can be combined with local hydroclimate data (temperature and relative humidity, isotope composition of ambient atmospheric moisture) to predict the trajectory of the LEL (Gibson and Edwards, 2002; Edwards et al., 2004; Wolfe et al., 2007b; Gibson et al., 2016). This is advantageous to the more common technique of applying linear regression through measured lake water isotope compositions, because lake water isotope compositions can be interpreted independently based on their position along (degree of evaporation) and about (i.e., above/below; relative influence of different input waters such as snowmelt and rainfall) the LEL.

For the PAD, average ice-free season flux-weighted relative humidity and temperature were calculated for the period of 2000-2015 using Thornthwaite (1948) and climate data from Environment Canada (station number 71305; www.climate.weather.gc.ca) and the National Research Council of Canada (http://www.nrc-cnrc.gc.ca/eng/services/sunrise/). Important features of the LEL include the mean annual isotope composition of precipitation (δ_P), the

steady-state isotope composition for a terminal basin (δ_{SSL}), which represents the special case of a lake at hydrologic and isotopic steady state in which evaporation exactly equals inflow, and the limiting non-steady-state isotope composition (δ*), which indicates the maximum potential isotopic enrichment of a lake as it approaches complete desiccation. A well-suited index lake known to be in isotopic steady-state was used to determine δ_{SSL} and atmospheric moisture for the ice-free season (δ_{AS}) (Yi et al., 2008), while δ* was calculated using Gonfiantini (1986). See Appendix 1 for calculations to determine the LEL.

The 2000-2015 PAD isotope framework was then used to calculate evaporation to inflow (E/I) ratios, an index of lake-water balance described by Gibson and Edwards (2002) and others. As in many regional studies that have used this approach (e.g., Brooks et al., 2014; Gibson et al., 2017; MacDonald et al., 2017), we compare E/I ratios across a large number of lakes to differentiate regions of the delta. E/I ratios were calculated as:

$$\frac{E}{I} = \frac{(\delta_I - \delta_L)}{(\delta_E - \delta_L)}$$

where δ_E is the isotope composition of evaporative flux (Craig and Gordon, 1965), δ_L is the lake water isotope composition and δ_I is the isotope composition of input waters to the lake (see Appendix 1). E/I ratios determined from 2015 lake water isotope data were interpolated across the delta surface by ordinary kriging using ArcMap 10.3 software. Because the model becomes increasingly unrealistic when E/I ratios exceed 1.5, we set this as a maximum value to differentiate the lakes experiencing strong non-steady state conditions.

2.2.3 *Limnology*

In-situ measurements of limnological parameters (pH, specific conductivity) were measured using YSI ProDSS sondes and water depths were measured using a plumb-bomb. At

each site, 5 L of water were collected from ~10 cm depth for water chemistry analysis. Samples were refrigerated until filtration later that day or the following day. Coarse-filtered (80-μm mesh) lake water was used for analysis of total nitrogen (TN) and total phosphorus (TP), while sub-samples for analysis of total dissolved nitrogen (TDN), total dissolved phosphorus (TDP), dissolved silica (DSi), dissolved inorganic carbon (DIC), dissolved organic carbon (DOC) and major ions were passed through Sartorius cellulose acetate filters (0.45 μm). Major cations were preserved using nitric acid. For analysis of chlorophyll *a* (Chl *a*), water samples were passed through Whatman GF/F filters, which were kept frozen until analysis. Samples were analyzed at the University of Alberta's Biogeochemical Analysis Services Laboratory (TN, TP, TDN, TDP, DSi, DIC, DOC, major ions) or the University of Waterloo (Chl *a*).

Principal Components Analysis (PCA) was used to determine whether limnological effects of floodwaters to lakes during spring 2014 persisted into the 2015 ice-free season, as expected based on Wiklund et al. (2012). The PCA was performed on limnological data from 56 lakes that did not flood during 2015, determined primarily on water isotope data. Six of the 62 lake sites were removed from the analysis because their 2014 flood status was uncertain (PAD M1, PAD M2, PAD M3, PAD M4, PAD M5, PAD M6). All nine river sites and four of the lake sites with continuous or near-continuous river channel connections (PAD 45A, PAD 45B, PAD 62, PAD 63) were included passively in the PCA to provide a reference for limnological conditions of lakes receiving floodwaters, without influencing the relative positions of the sample scores for the lakes that were not flooded in 2015. PAD 54 was also included as a passive sample, because it flooded again in spring 2015 based on isotopic and limnological overlap with river sites, a feature which confounds the ability to detect if limnological effects of the 2014 flood persisted through 2015. In this way, PAD 54 also serves as a useful reference for expected

river floodwater-influenced limnological conditions in the absence of 2014 limnological data. Thus, PCAs were run with 51 lake sites as active samples. Limnological variables were natural-log transformed. In the PCAs, scaling focused on inter-sample distances, variable scores were divided by their standard deviation, and variables were centered and standardized. Sample scores for lakes were coded in PCA plots according to whether or not they flooded during the ice-jam flood of 2014. All water chemistry variables listed above were included as active variables in the PCAs, except for $\delta^{18}O$ which was included passively to assess influence of floodwaters and evaporation on water chemistry of lakes. ANOSIM tests were conducted on the 51-lake dataset to determine if water chemistry in May, July and September 2015 differs significantly between lakes that flooded in spring of 2014 and those that did not flood. The PCA was performed using CANOCO version 4.5 (ter Braak and Smilauer, 2002) and the ANOSIM tests were run using R (R Core Team, 2017), RStudio (Rstudio Team, 2016) and the vegan package (Oksanen et al., 2017).

2.2.4 Isotope paleohydrology

Cellulose-inferred lake water oxygen isotope reconstructions, spanning the past 200-400 years, were derived from sediment cores collected at lakes PAD 5, PAD 9, PAD 12, PAD 23 and PAD 31 and have been reported previously (Wolfe et al., 2008a; Wolfe et al., 2008b; Sinnatamby et al., 2010). Briefly, cellulose was isolated on most 0.5-cm sediment core intervals using standard methods and analyzed for oxygen isotope composition at the UW-EIL (Wolfe et al., 2001; Wolfe et al., 2007a). Results were converted to lake water oxygen isotope composition using a cellulose-water oxygen isotope fractionation factor of 1.028 (Wolfe et al., 2001) and expressed as δ-values relative to the VSMOW standard. Analytical uncertainty is approximately ±0.5‰. Sediment core chronologies were determined from ^{210}Pb activity measured by alpha

spectrometry and using the Constant Rate of Supply model (Appleby, 2001), extrapolated downcore. For the longer records available from PAD 5, PAD 9 and PAD 12, sediment core chronologies were additionally constrained by radiocarbon dates (Wolfe et al., 2008a).

2.3 Results

2.3.1 The 2014 ice-jam flood event

Extensive overland flooding of the PAD occurred for about a week between May 3-10, 2014, when ice-jams formed on the Peace and Athabasca rivers (Straka and Gray, 2014; Figure 2.2a). Maximum water level rise (an estimated 6 m) on the Peace River occurred around May 5-6, which inundated substantial low-lying portions of the Peace sector of the delta. The north and south banks of the Peace River were breached in several areas and major channels south of the Peace River carried floodwater into the delta. An ice-jam on the Quatre Fourches channel was reported to form and persist during May 7-10, which resulted in flooding in this area. In the Athabasca sector, much of the area between the Athabasca and Embarras rivers, as well as south of the Athabasca River, were inundated with floodwater. Water levels rose as much as 4 m on the Embarras River and Mamawi Creek, causing some overbank flooding in this region.

The river and lake water isotope compositions measured at 16 lakes and 8 river sites in May 2014 were plotted on a $\delta^{18}O$-$\delta^{2}H$ graph to determine whether the lakes received river floodwaters, and were then compared with the aerial extent of flooding mapped by WBNP staff (Figure 2.2a,b). The Peace River is isotopically depleted and plots below the LEL in both sampling locations, as expected given the influence of snowmelt on the spring river water isotope composition. The Rivière des Rochers also plots below the LEL, suggesting flow reversal may have occurred in this channel causing floodwater from the Peace River to be carried south. Similarly, the Embarras River in the Athabasca sector plots below the LEL, likely as a

result of receiving floodwater from the isotopically depleted Athabasca River. Prairie River, which flows between Mamawi Lake and Lake Claire, was sampled in two locations, both of which plot along the LEL, indicating some influence of evaporation. This is likely due to the inflow of evaporatively enriched lake water from Lake Claire and Mamawi Lake to this channel.

For most lakes sampled in spring (May) 2014, water isotope compositions plot at the lower, isotopically-depleted end of the LEL, in the range of values for the Peace River, Rivière des Rochers and Embarras River, indicating that these lakes received river floodwaters. Exceptions include PAD 18, PAD 47 (Hilda Lake) and PAD 61 (Sonny's Lake), which were isotopically-enriched due to greater influence of evaporation in the absence of river flooding (Figure 2.2b). Observations indicated that all three of these lakes were not turbid at the time of sampling, also consistent with having not received river floodwaters (Yusuf, 2015). The isotope-inferred flood status of the lakes are in agreement with the flood extent mapped by WBNP staff, except for PAD 9. This lake, located in the southern portion of the Peace sector, lies outside of the mapped flood extent (Figure 2.2a) but is strongly isotopically depleted suggesting it likely received river floodwater (Figure 2.2b). Observations of nearby overland flooding and high water levels made by the sampling crew during the aerial survey and water isotope sample collection on June 1st, 2014, suggest that floodwaters entered this lake.

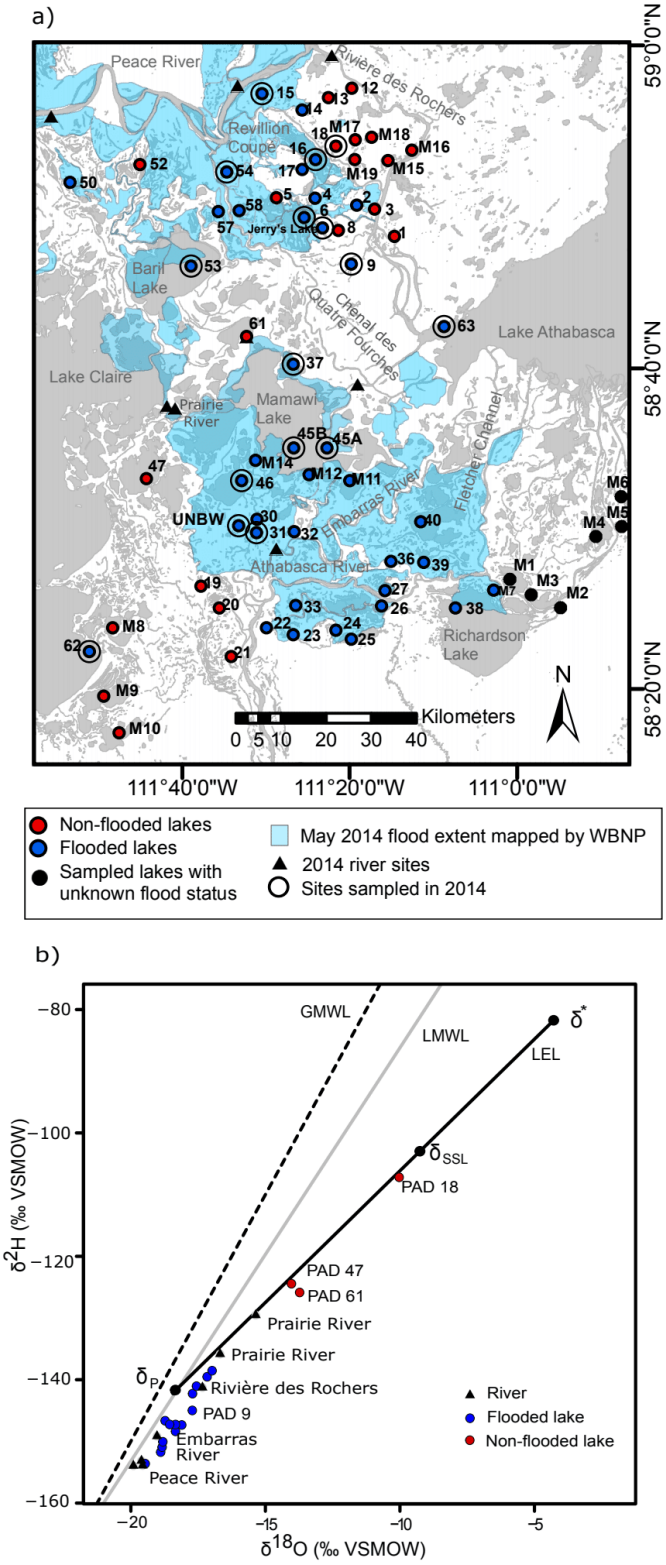

Figure 2.2. a) The extent of 2014 spring flooding as mapped by WBNP staff is shown in light blue (Straka and Gray, 2014). Note that the extent of floodwaters east of the WBNP boundary (east of Fletcher Channel) was not mapped. Sites sampled in 2015 are coded according to whether they were flooded in spring of 2014 (dark blue), not-flooded (red) or flood status unknown (black). Hydrological coding is based on location primarily, as well as isotope data where available. b) $\delta^{18}O$-$\delta^{2}H$ graph showing the water isotope values from lakes and rivers sampled in May 2014, colour-coded as flooded (blue) or not flooded (red) in spring of 2014.

2.3.2 Hydrological conditions during 2015

In May 2015, lakes that flooded and lakes that did not flood in 2014 show separation of isotope compositions along the LEL (Figure 2.3a). Isotope compositions of most of the lakes that flooded in 2014 are more isotopically depleted, plotting lower on the LEL. Four lake sites (PAD 45B, PAD 54, PAD M5, PAD M6) plot below the LEL, in the range of the river sites, indicating contribution of river water into these basins. The lakes that were not flooded in 2014 typically plot higher along the LEL, closer to δ_{SSL}, suggesting greater influence of evaporation in the absence of river flooding. By June 2015, the separation between flooded and non-flooded lakes diminishes as evaporation caused isotope composition of most of the lakes that were flooded in 2014 to move up the LEL and overlap with the non-flooded lakes. The most isotopically enriched lakes (PAD 19, PAD 20, PAD 21) were not flooded in 2014. As the ice-free season progresses and lakes experience increasing evaporation, the isotope compositions of 2014 flooded and non-flooded lakes become increasingly tightly clustered and continue to move up the LEL due to greater influence of atmospheric parameters (isotope composition of atmospheric moisture, temperature, relative humidity) on the lake-water isotope compositions with increasing influence of evaporation. Exceptions are the few lakes in the low-lying central portion of the delta that receive near-continuous river input and, thus, remain isotopically depleted throughout the ice-free season. By September 2015, lakes are clustered along the LEL and many lakes from both 2014 non-flooded and flooded categories plot between δ_{SSL} and δ^* indicting strong influence of evaporation on lake water balance.

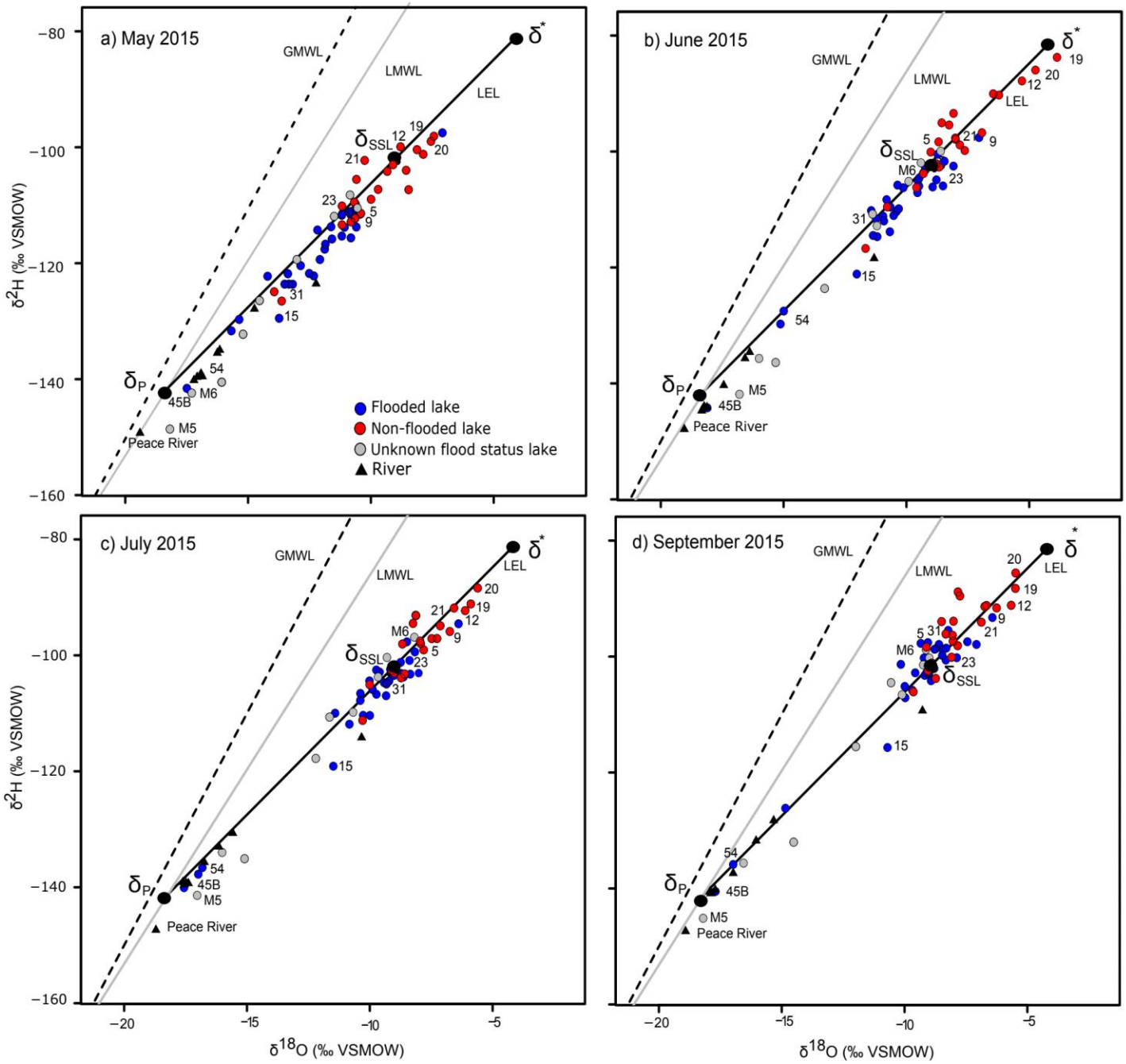

Figure 2.3. $\delta^{18}O$-$\delta^{2}H$ graph showing the water isotope compositions of the 61 lake and 9 river sites sampled in the Peace-Athabasca Delta during a) May, b) June, c) July and d) September 2015. Flood status refers to lake hydrological conditions during May 2014. The sites are coded according to whether they are rivers (black triangles), lakes flooded in 2014 (blue circles), lakes not flooded in 2014 (red circles), or lakes with unknown flood status in 2014 (grey circles).

To compare the extent of flooding in 2014 to the spatial patterns of isotopic enrichment in 2015, calculated E/I ratios were interpolated across the PAD (Figure 2.4). Moran's I coefficient calculated for the E/I ratios during sampling periods show moderate spatial association (May: *Moran's I* = 0.305, $p < 0.001$; June: *Moran's I* = 0.344, $p < 0.001$; July: *Moran's I* = 0.442, $p < 0.001$; September: *Moran's I* = 0.350, $p < 0.001$). In May 2015, lakes in the central area of the Peace sector around the Chenal des Quatre Fourches, which was extensively flooded in 2014, had relatively low E/I ratios (0.3 to 0.5). The northwestern portion of the Peace sector, which experienced some flooding in 2014, and the northeastern portion of the Peace sector, which was not flooded in 2014, had higher E/I ratios (0.7 to 1.1). Lower E/I ratios in the central portion of the Peace sector compared to the northwestern and northeastern portions in May 2015 could be a result of lasting effects of the 2014 flooding in this area or river water input into the low-lying central area during May 2015, although we have no field observations to support the latter. As early as June 2015, E/I ratios in the areas of the Peace sector that were flooded in 2014 were comparable to those areas that were not flooded. By July and continuing in September, E/I ratios were >1.0 across most of the Peace sector. Only some lakes in the northern reaches of the Chenal des Quatre Fourches, closest to the Peace River, possessed E/I ratios <1.0 in September 2015.

In the Athabasca sector, lakes in the southeastern and central portions that were extensively flooded in 2014 had low E/I ratios (0.3 to 0.6) in May 2015. The non-flooded southwestern area had higher E/I ratios in May (0.7 to 1.2). E/I ratios in the flooded (2014) areas of the Athabasca sector increased by June (0.7 to 0.9) and remained high for the rest of the ice-free season. By June 2015, the non-flooded southwestern area also experienced an increase in E/I ratios to >1.0. Low-lying areas in the central and southeastern portions of the Athabasca sector

may be displaying lasting effects of the 2014 flood, although this is difficult to distinguish from 'normal' hydrological conditions in the delta as this area generally receives continuous river inflow under both flood and non-flood conditions. Notably, the highest E/I ratios were in the elevated northeastern portion of the Peace sector and the southwestern portion of the Athabasca sector, which were outside of the extent of the spring flood of 2014 and likely have not received river floodwater for many decades, implying that the high E/I ratios in 2015 are a continuation of long-term seasonal evaporative water loss.

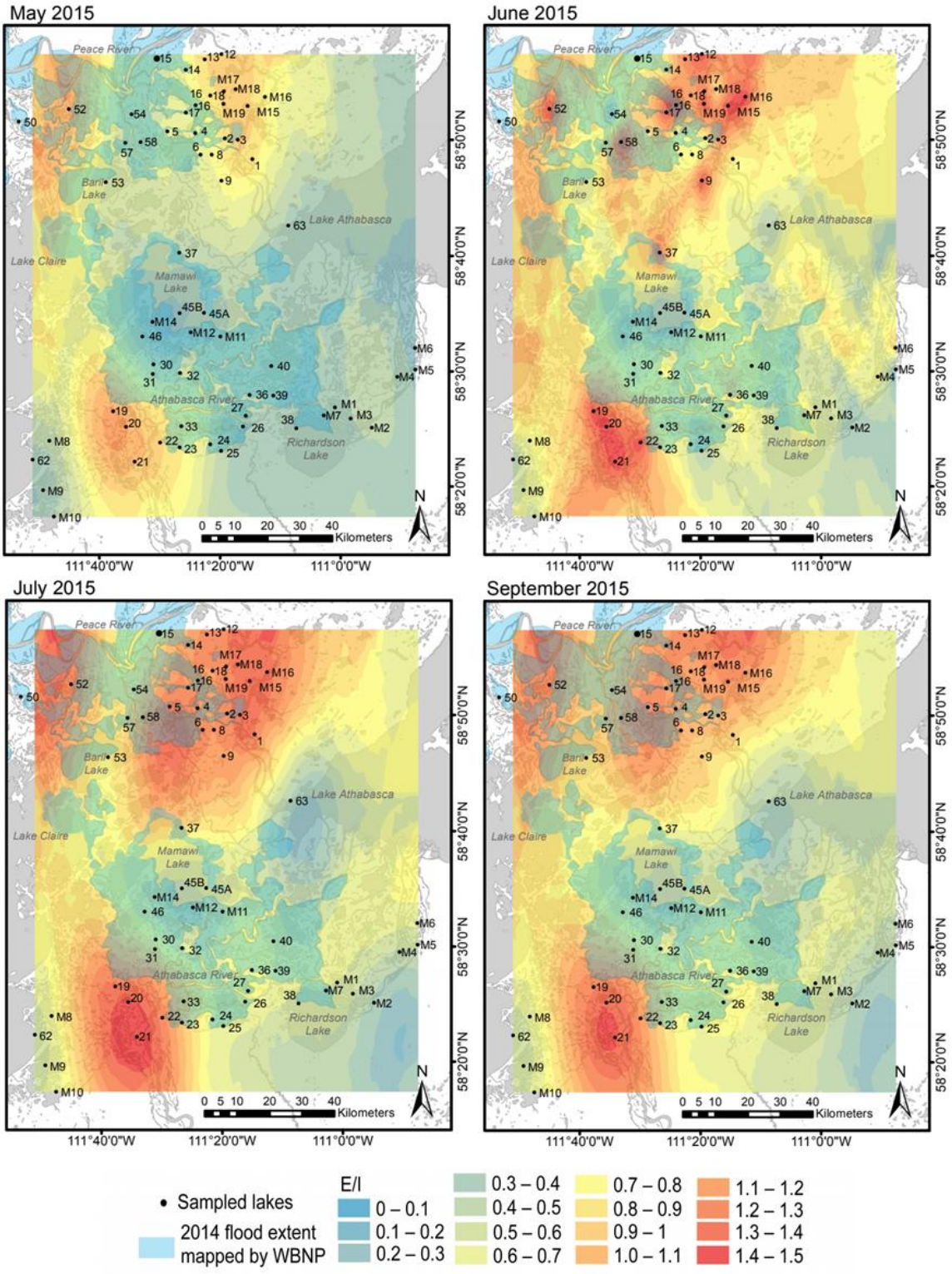

Figure 2.4. Maps showing spatial interpolation (by ordinary kriging) of evaporation-to-inflow (E/I) ratios for 61 lakes across the Peace-Athabasca Delta in May, June, July and September 2015, the year after an extensive ice-jam flood event. Overlain is the 2014 flood extent map from Figure 2.2a.

2.3.3 Limnological conditions during 2015

For all three limnological sampling episodes in 2015 (May, July, September), PCAs capture similar amounts of variation along the first two axes (May: AX1 = 36.5%, AX2 = 17.6%, Total = 54.1%; July: AX1 = 32.5%, AX2 = 18.5%, Total = 51.0%; September: AX1 = 37.8%, AX2 = 16.2%, Total = 54.0%), and vectors of the water chemistry variables show consistent associations with the first two axes (Figure 2.5). PCA axis 1 captures mainly a gradient of ionic content, whereas axis 2 captures mainly gradients of pH and concentrations of nutrients, DOC and sulfate. Sample scores for the river sites (black triangles in Figure 2.5), included passively in the PCAs, are positioned to the right along PCA axis 1 and high on PCA axis 2, indicating relatively high turbidity and high concentrations of SiO_2, Na, SO_4 and Cl, and relatively low concentrations of K, DOC and nutrients (TP, TDP, TN, TDN) and low $\delta^{18}O$. Passive sample scores for the three open-drainage lakes (blue squares; Lake Clair (PAD 62), Lake Athabasca (PAD 63), and Mamawi Lake (PAD 45A/B)) cluster near the river sites, indicating that continuous to near-continuous river inflow strongly influences their water chemistry. PAD 54, also included passively, is consistently positioned with the river sites for all three sampling episodes, because it was flooded in May 2015. Sample scores for the lakes that flooded in 2014 and the non-flooded lakes are positioned lower on the second axis than the rivers, indicating relatively lower turbidity and lower concentrations of Na, SO_4 and Cl, but higher concentrations of DOC, nutrients (TP, TDP, TN, TDN) and higher $\delta^{18}O$. Both flooded (2014) and non-flooded lakes are also scattered along axis 1, indicating a range of conductivity, DIC and ionic content. The high degree of overlap of sample scores throughout the 2015 season for lakes that flooded and did not flood in 2014 suggests that limnological effects of the 2014 flood did not persist to 2015. The one exception may be PAD 15, which was flooded in 2014 and has similar

limnological characteristics as the river sites during 2015. However, dilute water chemistry at PAD 15 may also have been influenced by snowmelt given that its isotope composition plots well below the LEL (Figure 2.5). ANOSIM tests confirm that water chemistry conditions do not differ significantly ($P > 0.05$) during any of the months sampled in 2015 between lakes that flooded and those that did not flood in 2014 (May: $R = 0.095$; July: $R = 0.058$; September: $R = 0.057$).

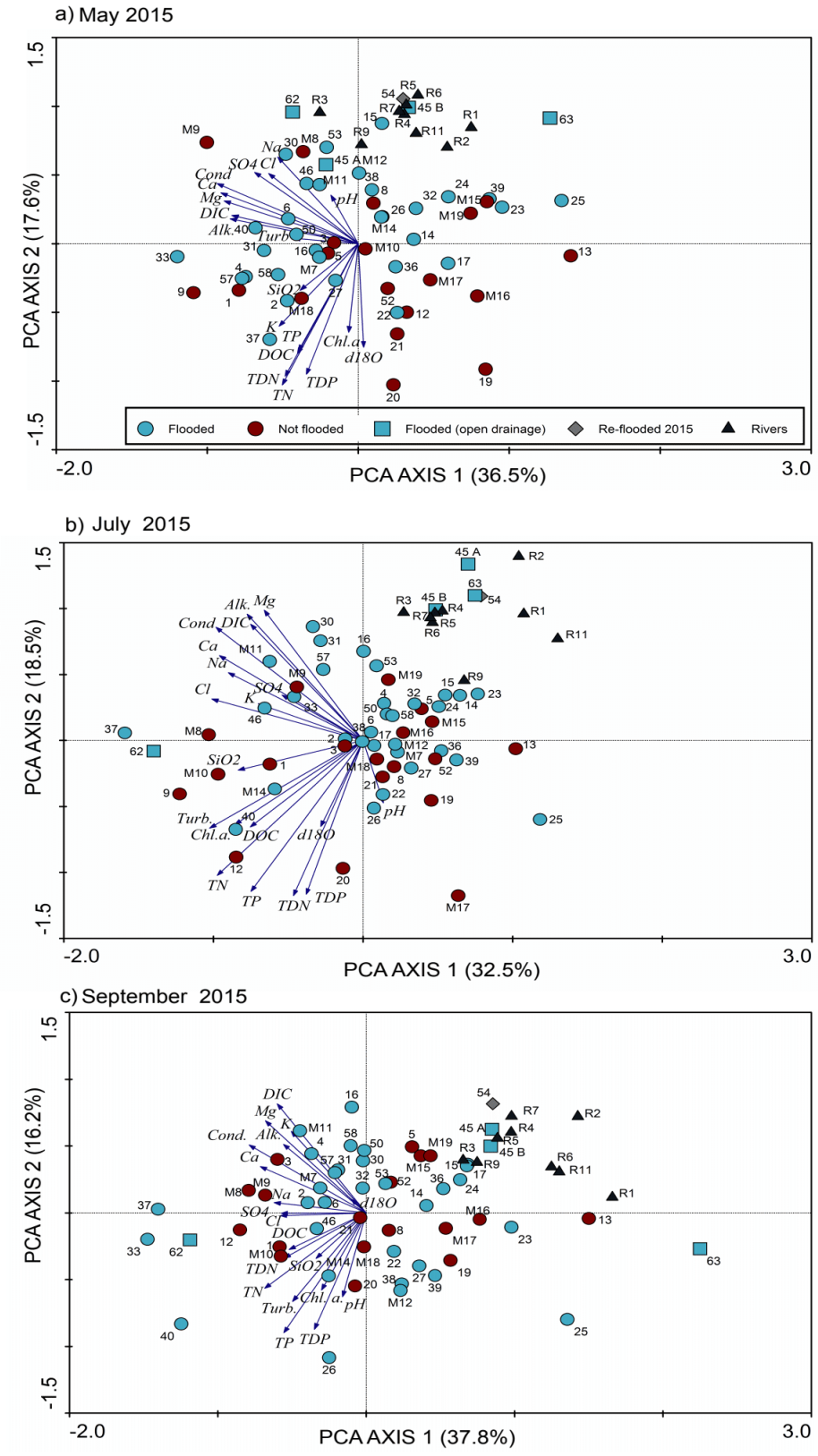

Figure 2.5. Principal component analysis ordination diagram from analysis of water chemistry variables obtained from 51 lake sites and 9 river sites in the Peace-Athabasca Delta sampled in May, July and September 2015. The sites (sample scores) are coded according to whether they are rivers (black triangles), lakes flooded in 2014 (blue circles), open-drainage lakes that flood near-continuously (blue squares), and lakes not flooded in 2014 (red circles).

2.3.4 Paleohydrological records

To provide temporal context for contemporary lake hydrological conditions, cellulose-inferred lake water $\delta^{18}O$ ($\delta^{18}O_{lw}$) records spanning the past ~200-400 years were assembled from five lakes along with directly measured mean ice-free season lake water $\delta^{18}O$ values from 2000-2006 and 2014-2015 (Figure 2.6).

During the Little Ice Age (LIA; 1600-1900), the $\delta^{18}O_{lw}$ records of the five lakes reflect different hydrological conditions depending on their physiographic settings (Figure 2.6). The most elevated basin, PAD 5, displays varying but isotopically-enriched values (~-13 to -3 ‰) that occasionally exceed δ_{SSL}, consistent with evidence for periodic desiccation due to locally arid climate (Wolfe et al., 2005; Wolfe et al., 2008a). In contrast, low-lying basins (PAD 9, PAD 12, PAD 31) possess low $\delta^{18}O_{lw}$ values (~-20 to -14 ‰) because they were all varyingly flooded by isotopically depleted water from Lake Athabasca (modern $\delta^{18}O$ = -17 to -15 ‰) and the Rivière des Rochers, which rose by as much as 2.3 m due to increased supply of glacial meltwater to the Peace and Athabasca rivers during summer (Wolfe et al., 2008a; Johnston et al., 2010; Sinnatamby et al., 2010). Although PAD 23 was likely south of the margin of the Lake Athabasca LIA highstand, low $\delta^{18}O_{lw}$ values (~-20 to -15 ‰) suggest it was strongly influenced by Athabasca River floodwaters.

Gradual increase in $\delta^{18}O_{lw}$ values in the Peace sector lakes (PAD 5, PAD 9, PAD 12) suggests an increasing role of evaporation post-LIA (i.e., after 1900). These trends reflect decline in ice-jam flood frequency and Lake Athabasca water level due to reduction in high-elevation snow and glacial contributions to river discharge (Wolfe et al., 2006; Wolfe et al., 2008a; Wolfe et al., 2011), which is also evident in shorter hydrometric records of rivers draining the hydrographic apex of North America (e.g., Dery and Wood, 2005; Rood et al., 2005; Schindler

and Donahue, 2006; Barnett et al., 2008; Burn et al., 2010; Sauchyn et al., 2015; Scalzitti et al., 2016). Locally decreasing relative humidity (Wolfe et al., 2008b) and possibly a longer-ice free season also contribute to these trends. For the Athabasca sector lakes, anthropogenic and natural changes in the flow of the Athabasca River and distributaries are responsible for the contrasting late 20th century $\delta^{18}O_{lw}$ trends at PAD 23 and PAD 31 (Wolfe et al., 2008b). Sharply increasing $\delta^{18}O_{lw}$ at PAD 23 after 1970 is due to the engineered Athabasca River Cut-Off, which reduced the propensity of ice-jam flooding in the vicinity of PAD 23. In contrast, the decline and more variable $\delta^{18}O_{lw}$ at PAD 31 after 1980 is due to the Embarras Breakthrough, which re-directed substantial flow from the Embarras River to Cree and Mamawi creeks leading to increased flooding in this area.

During the past 15 years when we have direct measurements of lake water $\delta^{18}O$, all lakes with the exception of PAD 5 possess values higher than at any time during the paleohydrological records. PAD 9, PAD 12 and PAD 23 lake water $\delta^{18}O$ values approach, and occasionally exceed, the critical threshold of δ_{SSL}. Likewise, PAD 5 lake water $\delta^{18}O$ values hover near δ_{SSL}, having only been higher during the LIA. Based on our field observations, an increasing and persistent role of evaporation has led to marked declines in water level at PAD 5 and PAD 9 during the past decade, despite apparent floodwaters reaching PAD 9 in 2014 (Figure 2.7). Even recent (i.e., post-1982 Embarras Breakthrough) river floodwater 'buffering' of PAD 31, including during 2014, appears to be waning given the evidence of generally higher lake water $\delta^{18}O$ values at this lake (Figure 2.6)

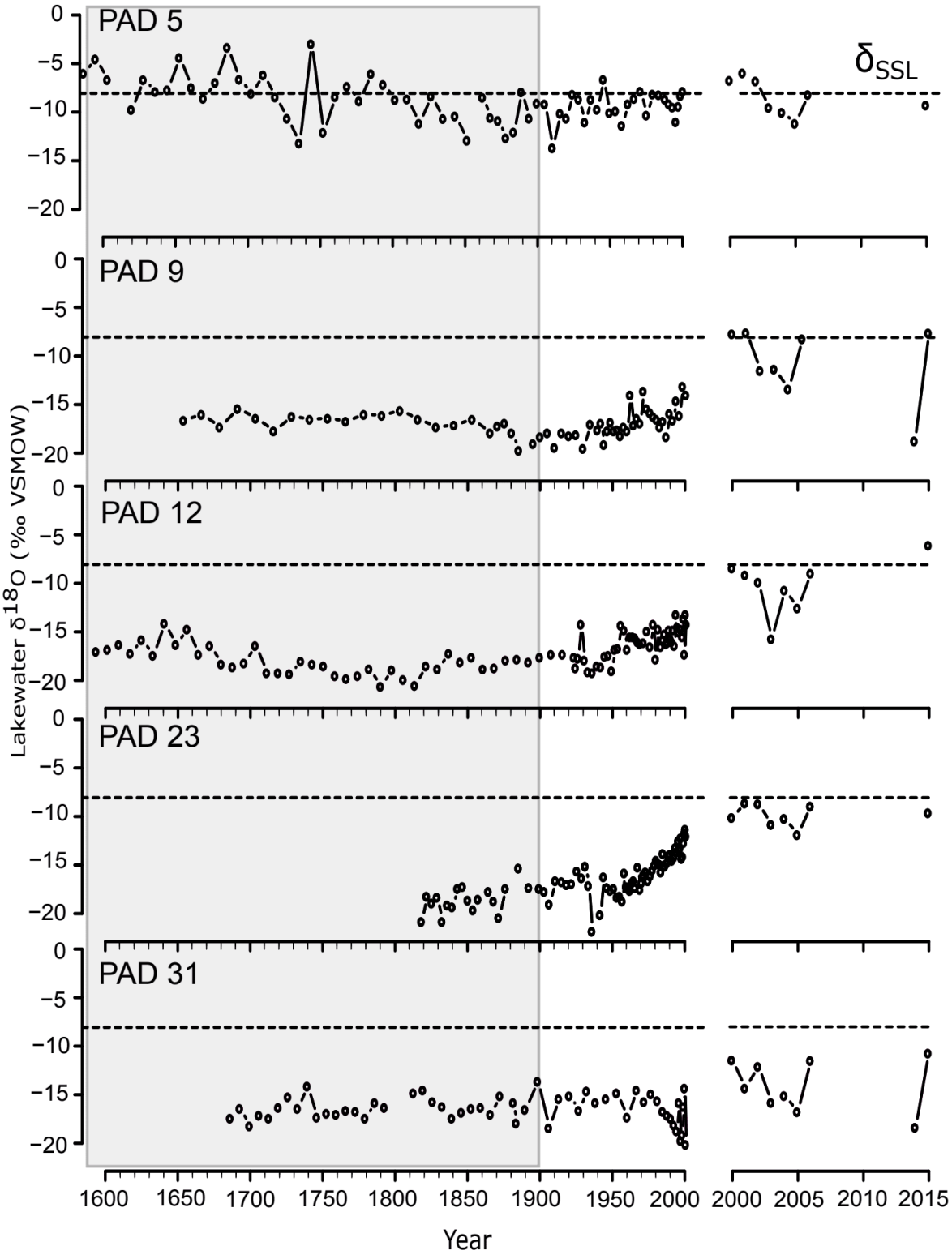

Figure 2.6. Temporal patterns of variation in cellulose-inferred lake water δ18O values (pre-2000) and directly measured lake water $\delta^{18}O$ values (average of ice-free season) for five lakes in the Peace-Athabasca Delta. Paleohydrological records are from Wolfe et al. (2008a; PAD 5, 12), Wolfe et al. (2008b; PAD 23, 31) and Sinnatamby et al. (2010; PAD 9). Reconstructions are plotted relative to contemporary δ_{SSL}, which represents isotopic steady-state for a terminal basin. The Little Ice Age interval, as used in Wolfe et al. (2008a), is shaded.

2.4 Discussion

Despite extensive flooding of the Peace-Athabasca Delta in May 2014, analysis of water isotope compositions and limnological variables in 2015 indicated only short-lived, mostly within-year effects of the 2014 flood. By as early as June 2015, lakes that were both flooded and not flooded in 2014 were isotopically enriched to a similar extent due to evaporation, and little hydrological distinction existed between these two groups. Although the central portion of the Peace sector and southeastern portion of the Athabasca sector were most strongly influenced by flooding in 2014, E/I ratios during June 2015 were already greater than 0.5 indicating strong evaporative influence.

Limnological data support the short-lived isotope-inferred hydrological effects of the 2014 flood. By May 2015, water chemistry conditions did not differ significantly between lakes that flooded and lakes that did not flood in 2014 (with the exception of PAD 15). Although we do not have water chemistry from 2014 to verify the effects of flooding on limnological conditions in spring 2014, previous research by Wiklund et al. (2012) has shown that flooded lakes have similar water chemistry characteristics as river water. This effect is evident in PAD 15 (which flooded in May 2014 but not 2015) and PAD 54 (flooded in May of 2014 and 2015), and thus both lakes possess water chemistry characteristics that overlap with river sites throughout the 2015 ice-free season (Figure 2.5). The short-lived effects of flooding on limnological conditions on the other lakes that flooded in 2014 was surprising, because Wiklund et al. (2012) observed that infrequently flooded lakes in the Peace and Athabasca sectors of the delta took multiple years after a flood to return to typical closed-drainage limnological conditions characterized by high concentrations of DOC, TKN, bio-available nutrients and ions, and low concentrations of suspended sediments and SO_4. In contrast, we found that the magnitude of

evaporative water loss during the remainder of the 2014 post-flood ice-free season and early 2015 ice-free season leading up to our sampling in May 2015 resulted in a more rapid than predicted return to limnological conditions typical of those found during long periods (many years to decades) without flooding.

The flood-pulse concept, as applied to river floodplain lakes, postulates that river flooding acts to homogenize limnological conditions, followed by increasing heterogeneity during the post-flood period (Junk et al., 1989; Tockner et al., 2000; Junk and Wantzen, 2004). Here, we find a situation where the post-flood period appears to have been truncated by the strong influence of evaporation. This agrees with model predictions that lakes in the Mackenzie Delta, downstream of the PAD, will become increasingly sensitive to local climate conditions as frequency and magnitude of flooding decreases (Marsh and Lesack, 1996). We suspect that cumulative effects of long-term and ongoing declines in frequency and magnitude of river flooding, and arid conditions, are the dominant influence on the hydrological and limnological trajectory of lakes in the PAD, which, apparently is now unlikely to be altered by a single and isolated large flood event.

Isotope paleohydrological records provide coherent evidence of multi-decadal drying of lakes in the PAD. In the northern Peace sector, this began after the conclusion of the Little Ice Age during the early to mid-20th century. In the southern Athabasca sector, engineered and natural changes in flow of the Athabasca River and distributaries have had profound influence on hydrological conditions of lakes but trends towards drier conditions (i.e., higher measured lake-water $\delta^{18}O$ values) are now evident even along a re-directed river flow path as observed at low-lying PAD 31. Indeed, in four of the five paleohydrological records, the highest lake water $\delta^{18}O$ values (i.e., greatest evaporative isotopic enrichment) during the past 200-400 years has occurred

during the recent monitoring period. We acknowledge that direct comparison of time-integrated cellulose-inferred lake water $\delta^{18}O$ and annual averages of directly measured lake water $\delta^{18}O$ may be affected by seasonal offsets due to algal growth during the early ice-free season when lake water $\delta^{18}O$ tends to be lower, or small uncertainties in the cellulose-water oxygen isotope fractionation factor. However, neither are likely explanations for the recent observed trends in lake water $\delta^{18}O$. For example, unequivocal evidence of lake-level lowering at PAD 5 and PAD 9 (Figure 2.7) is consistent with trends depicting strong influence of evaporation during recent decades.

In the PAD, some have attributed long-term drying mainly to river regulation by the WAC Bennett Dam in 1968, which has clearly altered the flow regime of the Peace River (Peters and Prowse, 2001). As recently as in the past year, such statements were made by the UNESCO reactive monitoring mission (WHC/IUCN, 2017) in response to the MCFN (2014) petition. However, in the northern Peace sector of the delta, most proximal to the Peace River (PAD 5, PAD 12), increasing influence of lake evaporation, evident in Figure 2.6 and other proxy indicators from these lakes (Wolfe et al., 2005; Wolfe et al., 2008a), began soon after the end of the LIA, well before the dam became operational. Sediment records from other lakes in the PAD also indicate that flood frequency and magnitude began to decline in the late 1800s (Wolfe et al., 2006). While PAD 5 desiccated during the LIA, water has persisted in PAD 9 for at least the past 1000 years (Wolfe et al., 2008a). Substantial lake-level drawdown (~0.5 to 1.0 m) since the early 2000s is now visible at PAD 5 and PAD 9 (Figure 2.7). Although lake-level changes in low-lying riverine environments can be extremely heterogeneous, our spatial assessment of lake water balances across the delta suggests that conditions at PAD 5 and PAD 9 are reflective of a landscape-wide trend of rapidly declining water availability during the past decade. Increasing

evaporation during the past few decades recorded by the PAD 23 sediment record is unlikely to be caused by construction of the WAC Bennett Dam. PAD 23 is the most distal site from the Peace River on our transect and dredging of the nearby Athabasca River Cut-Off in 1972, which straightened the course of the river and reduced the likelihood of ice-jams developing at this location, is a primary cause for drying at this location (Wolfe et al., 2008b).

Climate-driven drying of northern shallow lakes is not unique to the PAD. Smith et al. (2005) identified widespread late 20th century decline in lake abundance and area in Siberia. Smol and Douglas (2007) observed drying of shallow lakes in the Canadian High Arctic, previously permanent water bodies for millennia. In Alaska, studies have revealed that there has been a reduction in area and number of ponds during the late 20th century (Riordan et al., 2006). Carroll et al. (2011) utilized satellite data to show that a net reduction in lake surface area of more than 6,700 km^2 occurred in the Canadian Arctic from 2000-2009. Bouchard et al. (2013) determined that lakes in low-relief, open tundra catchments are particularly vulnerable to drying when snowmelt runoff is low and identified that recent desiccation of a shallow lake in the Hudson Bay Lowlands (Canada) may be unprecedented during at least the past 200 years. While mechanisms leading to drying of shallow northern lakes may vary across these landscapes (e.g., permafrost thaw and lake drainage, decline in snowmelt runoff, increase in evaporation, decline in river discharge), and these need to be evaluated with due consideration of the regional context, this does appear to be a widespread consequence of climate change in northern regions.

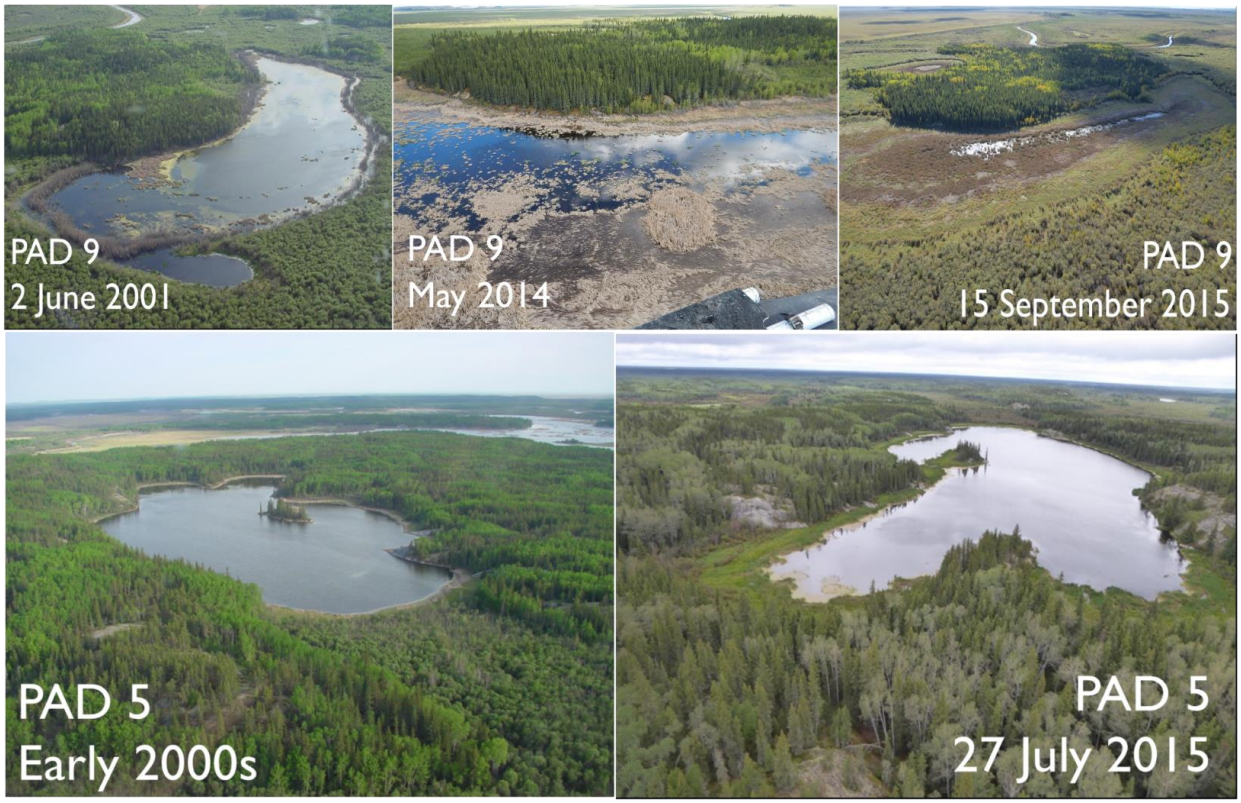

Figure 2.7. Aerial photographs of PAD 5 and PAD 9 in 2000 and 2015 showing marked water-level declines in both basins. For PAD 5, note the island visible in 2000 is connected to the shoreline in 2015.

2.5 Concluding Comments

Here we integrate spatial and temporal data to determine that widespread ice-jam flooding in May 2014 had largely within-year effects on hydrological and limnological conditions in lakes of the PAD, which we attribute to a multi-decadal trend of increasing evaporative influence across the landscape. Climate change since the end of the Little Ice Age has led to reduction in mid- to high-elevation snowpack and headwater glacier volume, and thus lower river discharge. These factors have conspired to produce clear evidence of rapidly declining freshwater availability in the delta, perhaps unprecedented in scale during the past 400 years, and this firmly entrenched trajectory of change is such that a single ice-jam flood event is insufficient to mitigate these effects.

Despite their global importance, inland freshwater ecosystems may be among the most threatened, as they are particularly vulnerable to the combination of climate change and increasing impairment by human development and upstream activities (e.g., Gleick, 2003; Woodward et al., 2010; Dudgeon et al., 2015). High-latitude freshwater landscapes, which are experiencing some of the fastest rates of warming (Hassan, 2005) and are often downstream of human activity (Gleick, 2003; Schindler and Smol, 2006), have unique ability to act as 'sentinel systems' (Woodward et al., 2010) and provide an early warning signal of hydroecological change. Hydrologists and ecologists increasingly recognize the need to understand connectivity in ecosystems, especially for 'riverscapes' (Tetzlaff et al., 2007). However, the spatial and temporal scales of hydroecological research have often been too short and too narrowly defined to adequately capture landscape-scale connectivity among freshwater ecosystems (rivers, channels, wetlands, lakes), such that the importance of these connections has been poorly characterized (Fausch et al., 2002). To understand how variability in climate and hydrological conditions affect the ecological integrity and connectivity of freshwater landscapes, research needs to encompass appropriate spatial and temporal scales (Fausch et al., 2002). Here we used hydrological, limnological and paleolimnological approaches to generate multiple datasets across space and time, which served to comprehensively assess the current status of hydroecological conditions in a large floodplain landscape. These results have important implications for management of the delta, as they highlight widespread long-term drying is reducing the hydrological and limnological heterogeneity of the landscape. Furthermore, they address recommendations for the PAD listed in the recent WHC/IUCN (2017) report, which include to 1) establish adequate baseline information to enhance the reference for monitoring [as demonstrated by our paleohydrological records], 2) expand the scope of monitoring [which we suggest should

include continued use of water isotope tracers, along with strategic sampling for water chemistry, to track rapidly shifting lake water balances over space and time], and 3) recognize the interaction of the ecosystem and climate [demonstrated here via assembling multiple records and observations over sufficient spatial and temporal scales]. Despite the challenges of generating these datasets, especially in remote northern landscapes, the value of such approaches cannot be understated as science attempts to address increasingly complex water-related problems.

2.6 References

Barnett, T. P., and others. 2008. Human-induced changes in the hydrology of the western United States. Science 319: 1080–1083, doi:10.1126/science.1152538

Beltaos, S. 2014. Comparing the impacts of regulation and climate on ice-jam flooding of the Peace-Athabasca Delta. Cold Reg. Sci. Technol. 108: 49-58, doi:10.1016/j.coldregions.2014.08.006

Bouchard, F. and others. 2013. Vulnerability of shallow subarctic lakes to evaporate and desiccate when snowmelt runoff is low. Geophys. Res. Lett. 40: 6112-6117, doi:10.1002/2013GL058635

Brooks, J. R., Gibson, J. J., Birks, S. J., Weber, M. H., Rodecap, K. D., and Stoddard, J. L. 2014. Stable isotope estimates of evaporation: Inflow and water residence time for lakes across the United States as a tool for national lake water quality assessments. Limnol. Oceanogr. 59: 2150-2165, doi:10.4319/lo.2014.59.6.2150

Burn D. H., S. Mohammed, and K. Zhang. 2010. Detection of trends in hydrological extremes for Canadian watersheds. Hydrol. Process. 24: 1781–1790, doi:10.1002/hyp.7625

Carroll, M. L., J. R. G. Townshend, C. M. DiMiceli, T. Loboda, and R. A. Sohlberg. 2011. Shrinking lakes of the Arctic: Spatial relationships and trajectory of change. Geophys. Res. Lett. 38: L20406, doi:10.1029/2011GL049427

Coplen T. B. 1996. New guidelines for reporting stable hydrogen, carbon, and oxygen isotope-ratio data. Geochim. Cosmochim. Acta 60: 3359–3360.

Coulthard B, D. J. Smith, and D. M. Meko. 2016. Is worst-case scenario streamflow drought underestimated in British Columbia? A multi-century perspective for the south coast, derived from tree-rings. J. Hydrol. 534: 205-18, doi:10.1016/j.jhydrol.2015.12.030

Dery, S. J., and E. F. Wood. 2005. Decreasing river discharge in northern Canada. Geophys. Res. Lett. 32: 10401, doi:10.1029/2005GL022845

Dudgeon, D. and others. 2006. Freshwater Biodiversity: Importance, Threats, Status and Conservation Challenges. Biol. Rev. Camb. Philos. Soc. 81: 163-82, doi:10.1017/S1464793105006950

Fausch K. D., C. E. Torgersen, C. V. Baxter, and H. W. Li. 2002. Landscapes to riverscapes: bridging the gap between research and conservation of stream fishes. Bioscience 52: 483–498, doi:10.1641/0006-3568(2002)052[0483:LTRBTG]2.0.CO;2

Finlayson C. M., S. J. Clarke, N.C. Davidson and P. Gell. 2015. Role of palaeoecology in describing the ecological character of wetlands. Mar. Freshwater Res. 67: 687-694, doi:10.1071/MF15293

Gibson, J. J., Birks, S. J., and Yi, Y. 2016. Stable isotope mass balance of lakes: A contemporary perspective. Quat. Sci. Rev. 131: 316-328, doi:10.1016/j.quascirev.2015.04.013

Gibson, J. J., Birks, S. J., Jeffries, D., and Yi, Y. 2017. Regional trends in evaporation loss and water yield based on stable isotope mass balance of lakes: The Ontario Precambrian Shield surveys. J. Hydrol. 544: 500-510, doi:10.1016/j.jhydrol.2016.11.016

Gibson, J. J., and T. W. D. Edwards. 2002. Regional water balance trends and evaporative transpiration partitioning from a stable isotope survey of lakes in northern Canada. Glob. Biogeochem. Cycles 16: 1–9, doi:10.1029/2001GB001839

Gleick, P. 2003. Global freshwater resources: soft-path solutions for the 21st century. Science 302: 1524-1528, doi:10.1126/science.1089967

Hassan, R., R. Scholes, and N. Ash. 2005. Millenium Ecosystem Assessment. Ecosystems and Human Well-being: Current State and Trends, vol. 1. Washington, DC: Island Press.

Johnston, J. W., and others. 2010. Quantifying Lake Athabasca (Canada) water level during the Little Ice Age highstand from paleolimnological and geophysical analyses of a transgressive barrier- beach complex. The Holocene 20: 801–811, doi:10.1177/0959683610362816

Junk, W. J., P. B. Bayley, and R. E. Sparks. 1989. The flood pulse concept in river–floodplain systems. Can. Spec. Publ. Fish. Aquat. Sci. 106: 110–127.

Junk, W. J., and K. M. Wantzen. 2004. The flood pulse concept: New aspects, approaches, and applications - an update, p. 117-149. In R. Welcomme and T. Petr [eds.], Proceedings of the 2nd Large River Symposium (LARS). Bangkok: RAP Publication.

MacDonald, L. A., and others. 2017. A synthesis of thermokarst lake water balance in high-latitude regions of North America from isotope tracers. Arctic Science. 3: 118-149, doi:10.1139/as-2016-0019

Marsh P., and L. F. W. Lesack. 1996. The hydrologic regime of perched lakes in the Mackenzie Delta: Potential responses to climate change. Limnol. Oceanogr. 41: 849-856, doi:10.4319/lo.1996.41.5.0849

MCFN. 2014. Petition to The World Heritage Committee Requesting Inclusion of Wood Buffalo National Park on the List of World Heritage in Danger. Mikisew Cree First Nation.

Milly, P. C. D., J. Betancourt, M. Falkenmark, R. M. Hirsch, Z. W. Kundzewicz, D. P. Lettenmaier, and R. J. Stouffer. 2008. Stationarity is dead: Whither water management? Science 319: 573–574, doi:10.1126/science.1151915

Oksanen, J., and others. 2017. Vegan: Community Ecology Package. R package version 2.4-3. available at https://CRAN.R-project.org/package=vegan.

PADPG. 1973. Peace–Athabasca Delta Project, technical report and appendices, volume 1: hydrological investigations, volume 2: ecological investigations. Peace–Athabasca Delta Project Group, Delta Implementation Committee, Governments of Alberta, Saskatchewan and Canada.

Peters D. L, and T. D. Prowse. 2001. Effects of flow regulation on the lower Peace River, Canada. Hydrol. Process. 15: 3181–3194, doi:10.1002/hyp.321

Pietroniro, A., T. D. Prowse, and D. L. Peters. 1999. Hydrologic assessment of an inland freshwater delta using multi-temporal satellite remote sensing. Hydrol. Process. 13: 2483–2498, doi:10.1002/(SICI)1099-1085(199911)13:16<2483::AID-HYP934>3.0.CO;2-9

Prowse, T. D., and F. M. Conly. 1998. Impacts of climatic variability and flow regulation on ice-jam flooding of a northern delta. Hydrol. Process. 12: 1589–1610, doi:10.1002/(SICI)1099-1085(199808/09)12:10/11<1589::AID-HYP683>3.0.CO;2-G

Rasouli K., M. A Hernandez-Henriquez, and S. J. Dery. 2013. Streamflow input to lake Athabasca, Canada. Hydrol. Earth Syst. Sci. 17: 1681-91, doi:10.5194/hess-17-1681-2013

Riordan, B., D. Verbyla, and A. D. McGuire. 2006. Shrinking ponds in subarctic Alaska based on 1950–2002 remotely sensed images. J. Geophys. Res. 111: G04002, doi:10.1029/2005JG000150

Rood, S. B., G. M. Samuelson, J. K. Weber, and K. A. Wywrot. 2005. Twentieth-century decline in streamflows from the hydrographic apex of North America. J. Hydrol. 306: 215–233, doi:10.1016/j.jhydrol.2004.09.010

RStudio Team. 2016. RStudio: Integrated Development for R. RStudio, Inc., Boston, MA. available at www.rstudio.com.

R Core Team. 2017. R: A language and environment for statistical computing. R Foundation for Statistical Computing, Vienna, Austria. available at https://www.R-project.org/.

ter Braak C. J. F., and P. Smilauer. 2002. Canoco reference manual and Canodraw for Windows user's guide. Software for canonical community ordination (ver 4.5). Microcomputer Power, Ithaca New York, USA.

Tockner K., F. Malard, and J. V. Ward. 2000. An extension of the flood pulse concept. Hydrol. Process. 14: 2861–2883, doi:10.1002/1099-1085(200011/12)14:16/17<2861::AID-HYP124>3.0.CO;2-F

Sauchyn, D. J., J. St-Jacques, and B. H. Luckman. 2015. Long-term reliability of the Athabasca River (Alberta, Canada) as the water source for oil sands mining. Proc. Natl. Acad. Sci. U.S.A. 112: 12621-6, doi: 10.1073/pnas.1509726112

Scalzitti, J., C. Strong, and A. Kochanski. 2016. Climate change impact on the roles of temperature and precipitation in western U.S. snowpack variability. Geophys. Res. Lett. 43: 5361–5369, doi:10.1002/2016GL068798.

Schindler, D. W., and W. F. Donahue. 2006. An impending water crisis in Canada's western prairie provinces. Proc. Natl. Acad. Sci. U.S.A. 103: 7210-7216. doi:10.1073/pnas.0601568103

Schindler D. W., and J. P. Smol. 2006. Cumulative effects of climate warming and other human activities on freshwaters of arctic and subarctic North America. Ambio 35: 160–168, doi:10.1579/0044-7447(2006)35[160:CEOCWA]2.0.CO;2

Sinnatamby, R. N., and others. 2010. Historical and paleolimnological evidence for expansion of Lake Athabasca (Canada) during the Little Ice Age. J. Paleolimnol. 43: 705–717, doi:10.1007/s10933-009-9361-4

Smith, L., Y. Sheng, G. MacDonald, and L. Hinzman. 2005. Disappearing arctic lakes. Science 308: 1429-1429, doi:10.1126/science.1108142

Smol J. P., and M. S. V Douglas. 2007. Crossing the final ecological threshold in high Arctic ponds. Proc. Natl. Acad. Sci. U.S.A. 104:12395-12397, doi:10.1073/pnas.0702777104

Straka, J and Q. Gray. 2014. Wood Buffalo National Park Flood Report, Spring 2014. Parks Canada.

Tetzlaff, D., C. Soulsby, P. J. Bacon, A. F. Youngson, C. Gibbins, and I. A. Malcolm. 2007. Connectivity between landscapes and riverscapes—a unifying theme in integrating hydrology and ecology in catchment science? Hydrol. Process. 21: 1385–1389, doi:10.1002/hyp.6701

Timoney, K., G. Peterson, and P. Fargey. 1997. Spring ice-jam flooding of the Peace-Athabasca Delta: evidence of a climatic oscillation. Clim. Change 35: 463, doi:10.1023/A:1005394031390

Timoney, K. 2002. A dying delta? a case study of a wetland paradigm. Wetlands 22: 282–300, doi:10.1672/0277-5212(2002)022[0282:ADDACS]2.0.CO;2

Timoney, K. P. 2013. The Peace-Athabasca Delta – Portrait of a dynamic ecosystem. Edmonton: The University of Alberta Press.

Watson, E., and B. Luckman. 2004. Tree-ring based reconstructions of precipitation for the southern Canadian cordillera. Clim. Change 65: 209-41, doi:10.1023/B:CLIM.0000037487.83308.02

WHC/IUCN. 2017. Reactive monitoring mission to Wood Buffalo National Park, Canada; mission report, March 2017. United Nations Educational, Scientific and Cultural Organization. available at http://whc.unesco.org/en/documents/156893.

Wiklund, J. A., R. I. Hall, and B. B. Wolfe. 2012. Timescales of hydrolimnological change in floodplain lakes of the Peace–Athabasca Delta, northern Alberta, Canada. Ecohydrology 5: 351–367, doi:10.1002/eco.226

Woodward, G., D. Perkins, and L. Brown. 2010. Climate change and freshwater ecosystems: Impacts across multiple levels of organization. Philos. Trans.: Biol. Sci. 365: 2093-2106, doi: 10.1098/rstb.2010.0055

Wolfe, B. B., T. W. D. Edwards, R. J. Elgood, and K. R. M. Beuning. 2001. Carbon and oxygen isotope analysis of lake sediment cellulose: Methods and applications, p. 373-400. In W. M. Last and J. P. Smol [eds.], Tracking Environmental Change Using Lake Sediments,Vol. 2. Kluwer Academic Publishers.

Wolfe, B. B., T. L. Karst-Riddoch, S. R.Vardy, M. D. Falcone, R. I. Hall, and T. W. D. Edwards. 2005. Impacts of climate and river flooding on the hydroecology of a floodplain basin, Peace–Athabasca Delta, Canada: A.D. 1700–present. Quat. Res. 64: 147–162, doi: 10.1016/j.yqres.2005.05.001

Wolfe, B. B., R. I. Hall, W. M. Last, T. W. D. Edwards, M. C. English, T. L. Karst-Riddoch, A. Paterson, and R. Palmini. 2006. Reconstruction of multi-century flood histories from oxbow lake sediments, Peace-Athabasca Delta, Canada. Hydrol. Process. 20: 4131-4153, doi:10.1002/hyp.6423

Wolfe B. B., and others. 2007a. Progress in isotope paleohydrology using lake sediment cellulose. J. Paleolimnol. 37: 221–231, doi:10.1007/s10933-006-9015-8

Wolfe, B. B., and others. 2007b. Classification of hydrologic regimes of northern floodplain basins (Peace-Athabasca Delta, Canada) from analysis of stable isotopes ($\delta^{18}O$, $\delta^{2}H$) and water chemistry. Hydrol. Process. 21: 151–168, doi:10.1002/hyp.6229

Wolfe B. B., R. I. Hall, T. W. D. Edwards, S. R Jarvis, R. Sinnatamby, Y. Yi, and J. W. Johnston. 2008a. Climate-driven shifts in quantity and seasonality of river discharge over the past 1000 years from the hydrographic apex of North America. Geophys. Res. Lett. 35: L24402, doi:10.1029/2008GL036125

Wolfe, B. B., and others. 2008b. Hydroecological responses of the Athabasca Delta, Canada, to changes in river flow and climate during the 20th century. Ecohydrology 1: 131–148, doi:10.1002/eco.13

Wolfe, B. B., T. W. D. Edwards, R. I. Hall, and J. W. Johnston. 2011. A 5200-year record of freshwater availability for regions in western North America fed by high-elevation runoff. Geophys. Res. Lett. 38: 11404, doi:10.1029/2011GL047599

Wolfe, B. B., T. W. D. Edwards, R. I. Hall, and J. Johnston. 2012. Developing temporal hydroecological perspectives to inform stewardship of a northern floodplain landscape subject to multiple stressors: Paleolimnological investigations of the Peace-Athabasca Delta. Environ. Rev. 20: 191–210, doi:10.1139/a2012-008

Yi, Y., B. E. Brock, M. D. Falcone, B. B. Wolfe, and T. W. D. Edwards. 2008. A coupled isotope tracer method to characterize input water to lakes. J. Hydrol. 350: 1–13, doi:10.1016/j.jhydrol.2007.11.008

Yusuf, F. 2015. Peace-Athabasca Delta Peace River 2014 ice jam field work report. BC Hydro report to Parks Canada.

Chapter 3: Delineating extent and magnitude of river flooding to lakes across a northern delta using water isotope tracers

Citation: Remmer, CR**,** Owca, T, Neary, LN, Wiklund, JA, Kay, M, Wolfe, BB, Hall, RI. 2020. Delineating extent and magnitude of river flooding to lakes across a northern delta using water isotope tracers. *Hydrological Processes* 34: 303-320.DOI:10.1002/hyp.13585

3.1 Introduction

Hydrological monitoring in complex, dynamic, water-rich floodplain landscapes is logistically challenging, especially in vast, remote areas at northern latitudes. Overcoming these barriers is essential as these inland freshwaters are globally important yet threatened by climate change and upstream human developments (Dudgeon et al., 2015; Gleick, 2003; Woodward, Perkins & Brown, 2010). In western North America, climate-driven reductions in mid- to high-elevation snowpack and headwater glacier volumes are reducing river flow and altering hydrological processes at downstream connected freshwater ecosystems (Barnett et al., 2008; Sauchyn, St-Jacques, & Luckman, 2015; Schindler & Donahue, 2006). Small shifts in hydrological conditions can result in cascading ecological changes in small, shallow, freshwater lakes and wetlands (Prowse et al., 2006; Schindler & Donahue, 2006; Schindler & Smol, 2006; Smol et al., 2005). These changes are generally poorly understood at the landscape scale, because data provided by research projects and monitoring programs are typically of insufficient spatial and temporal scales to adequately capture episodes of hydrological connectivity (Fausch, Torgersen, Baxter, & Li, 2002). To address this, comprehensive and systematic hydrological monitoring of complex, northern freshwater landscapes requires innovative approaches to ensure they are effective and sustainable.

Challenges to landscape-scale monitoring of key hydrological events have long prevailed in the Peace-Athabasca Delta (PAD), a complex floodplain landscape in northern Alberta, Canada.

Spanning ~6,000 km^2, the PAD is one of the world's largest inland boreal freshwater deltas and receives input from two major rivers, the Peace River and the Athabasca River, as well as the smaller Birch River (Timoney, 2013). The hundreds of shallow lakes and wetlands that characterize the PAD provide important habitat for a variety of biota and natural resources for indigenous communities. In recognition of its ecological, historical and cultural significance, the PAD is a Ramsar Wetland of International Importance and contributed to the listing of Wood Buffalo National Park (WBNP) as a UNESCO World Heritage Site. Lakes and wetlands of the PAD are influenced to varying degrees by river floodwater, snowmelt, rainfall and evaporation, resulting in a broad spectrum of spatially varying hydrological regimes (PADPG, 1973; Pietroniro, Prowse, & Peters, 1999; Prowse & Conly, 2002; Wolfe et al., 2007). The PAD is a low-relief system where small changes in water levels can alter hydrological connectivity and set forth temporal patterns of change in limnology, habitat availability, biodiversity and ecosystem productivity (Monk, Peters, & Baird, 2012; Wiklund, Hall, & Wolfe, 2012).

Freshwater availability has declined over large portions of the PAD, stimulating research that has long focused on deciphering effects of upstream industrial development, including the WAC Bennett Dam on the Peace River, and climate change on the frequency of ice-jam flood events because of the importance of this hydrological process as a recharge mechanism for lakes and wetlands in the delta (Beltaos, 2014; Hall, Wolfe, & Wiklund, 2019; Wolfe, Hall, Edwards, & Johnston, 2012). The recent approval and onset of construction of the Site C hydroelectric dam on the Peace River, as well as water withdrawals from the Athabasca River to support the oil sands industry, have heightened concerns about declining freshwater availability as expressed in a petition by the Mikisew Cree First Nation to place WBNP on UNESCO's List of World Heritage in Danger (MCFN, 2014). The resulting UNESCO report identified several

recommendations including to “expand the scope of monitoring and project assessments to encompass possible individual and cumulative impacts on the Outstanding Universal Value of the property and in particular the PAD” (WHC/IUCN, 2017, p. 4).

Recently, Remmer, Klemt, Wolfe and Hall (2018) used an array of datasets, including measurements of water isotope composition and water chemistry collected one year after a major ice-jam flood event in 2014, as well as paleohydrological records, to assess the effects of flooding on lake conditions in the PAD. They found that the 2014 flood event had short-lived, mostly within-year effects on water balance of the flooded lakes, which they attributed to a diminishing influence of river floodwaters as a consequence of cumulative and unrelenting effects of climate change. Given the importance of spring ice-jam floods and their declining influence during recent decades, tracking the occurrence and characterizing the effects of flood events that do occur is crucial to monitoring efforts and design of potential mitigation strategies. The extent of prior flood events in the PAD has typically been estimated from aerial surveys (Straka & Gray, 2014) and, on occasion, satellite imagery (e.g., Pavelsky & Smith, 2008; Toyra & Pietroniro, 2005). But, because of the dynamic and somewhat unpredictable nature of ice-jam flood events, delineation of flood extent from aerial observations is highly dependent on the timing and location of flight paths and absence of obstructions that impair detection of river floodwaters into lakes and vegetated terrain (e.g., cloud cover). Neither of these approaches can readily be used to distinguish magnitude of flooding across a landscape nor distinguish different sources of water that may have entered lakes such as river floodwaters versus snowmelt or rainfall. There remains a clear need for a systematic, measurable, and in situ approach to track spatial extent, as well as magnitude, of river flood events on lakes of the PAD and their effect on lake water balances.

Landscape-scale monitoring and assessment of lake hydrological conditions using water isotope tracers has proven to be an effective approach in many remote, northern, water-rich locations (e.g., Brock, Wolfe, & Edwards, 2007; Gibson & Edwards, 2002; MacDonald et al., 2017). In northern floodplains, this approach is particularly well-suited to partition the relative roles of important hydrological processes on lake water balances because of the strong sensitivity of lake water isotope compositions to influence of isotopically-depleted river water versus isotopic enrichment caused by evaporation. For example, water isotope data have been used to estimate the spatial extent of flood events in the PAD (Wolfe et al., 2008) as well as the Slave River Delta located farther downstream within the Mackenzie River Basin (Brock, Wolfe, & Edwards, 2008). In these studies, spring river floodwater dilution to lakes deemed to have flooded was estimated from the difference between the spring and previous fall measurements of water isotope composition. The modelling approach assumed that the spring isotopic depletion was entirely due to the influence of river floodwaters even though there were also likely contributions from snowmelt and/or rainfall. Nonetheless, the flood extent maps utilizing water isotope tracers aligned well with other evidence and demonstrated the usefulness of collection of lake water samples across these landscapes to obtain this information.

Here, our objective is to delineate the extent and magnitude of a spring ice-jam flood event in the PAD that occurred in late April and early May 2018 using water isotope tracers, supplemented by measurements of specific conductivity and field observations. Improving upon previous approaches utilized in the PAD (Wolfe et al., 2008) and Slave River Delta (Brock et al., 2008), which did not account for influence of precipitation, we set the water isotope data against an isotope framework established from 16 years of meteorological conditions and on-line resources, and then develop a set of landscape-specific binary mixing models that allow

estimation of the proportion of input to flooded lakes attributable to river floodwater and precipitation (snow or rain). These results demonstrate the value of systematic water sampling and isotope analysis for monitoring and assessment of lake hydrological conditions in dynamic floodplain landscapes such as the PAD.

3.2 Methods

3.2.1 Study area

The Peace-Athabasca Delta is episodically fed in the north by the Peace River and more frequently in the south by the Athabasca River (Figure 3.1). This results in distinct sectors with lakes possessing wide-ranging water balances largely depending on the relative influence of river water. The northern Peace sector (to the north of PAD 37 (Jemis Lake)) is a relic delta that receives floodwater only during infrequent high-elevation spring ice-jam flood events. Consequently, lakes are typically isolated or perched (i.e., closed-drainage) and strongly influenced by evaporation (PADPG, 1973; Pietroniro et al., 1999; Wolfe et al., 2007). Lakes in the southern Athabasca sector (PAD 37 and areas to the south) span a broad gradient of hydrological conditions from those that frequently receive river water in the active delta regions (i.e., restricted-drainage) during both the spring ice-jam and open-water seasons to those that are more substantially influenced by evaporation (i.e., closed-drainage). Broad shallow lakes in the central, low-lying portion of the delta receive continuous river inflow (i.e., open-drainage). Groundwater is considered to be a negligible component of lake water balances in the PAD due to discontinuous permafrost, low hydraulic conductivity of flood-deposited fine-grained sediment (clay and fine silt) that line basins, and low horizontal gradients between lakes (Nielsen, 1972; Prowse et al., 1996; Wolfe et al., 2007).

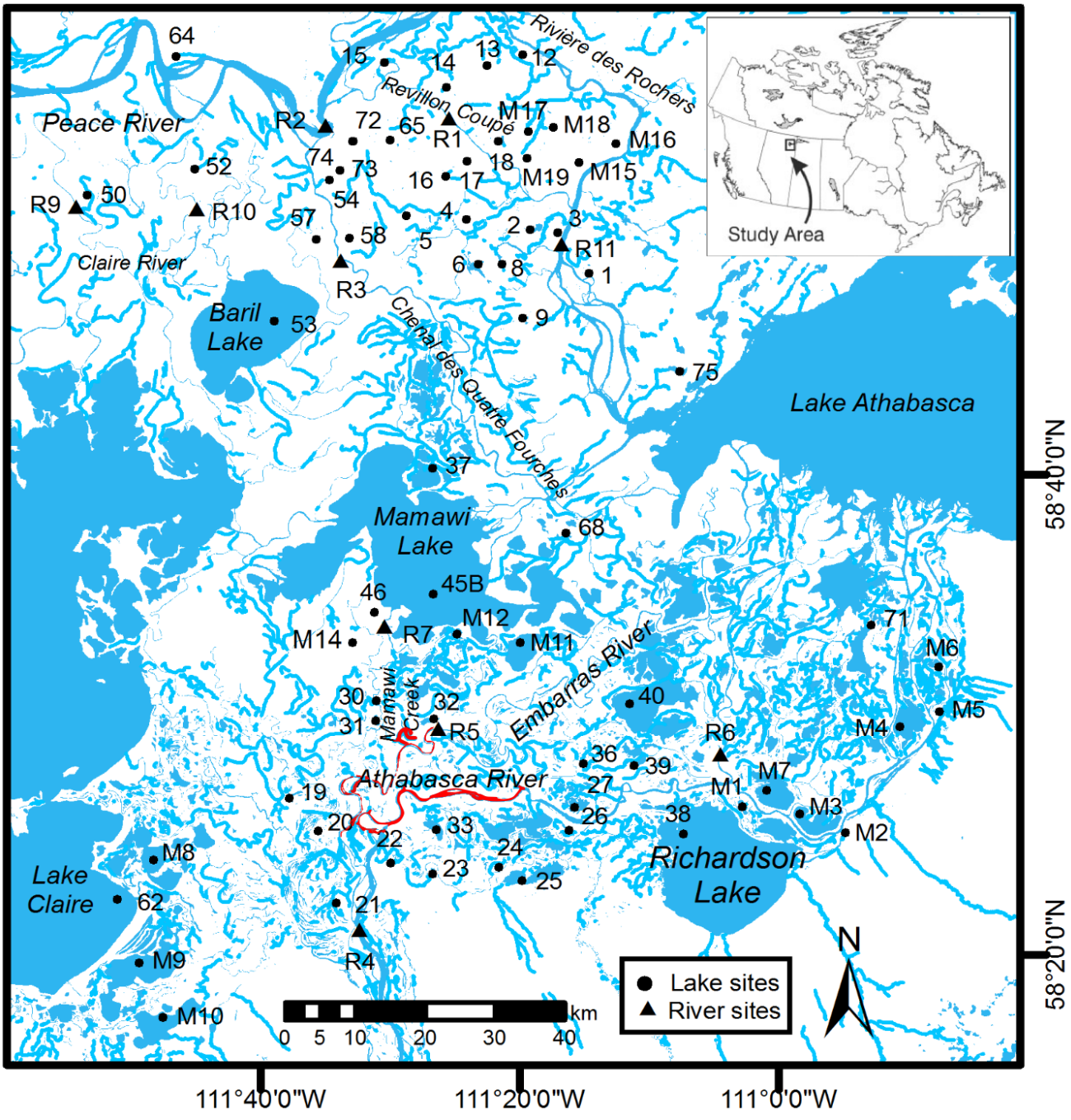

Figure 3.1. Map showing locations of the Peace-Athabasca Delta, Alberta, and the 68 lake (black circles) and 9 river (black triangles) sites sampled during May 15-17, 2018. Approximate locations of river ice-jams are indicated as red areas, as provided by Kevin Timoney (Treeline Ecological Research) based on photos taken during aerial surveys.

3.2.2 Conditions during and preceding the 2018 flood event

Ice-jam flooding occurred along stretches of the Athabasca, Peace, and Slave rivers in late April through early May 2018. For the Peace River, extensive ice-jams developed ≥ ~500 km upstream of the PAD (e.g., Town of Peace River, Sunny Valley, Vermilion Rapids) during April 26-29, 2018, as well as in the Slave River during May 2-4, 2018 at a location ~36-82 km downstream of the northeastern edge of the PAD (Jasek, 2019). Prior to and during this period, ice cover on the Peace River thermally degraded along the reach adjacent to the PAD and was too weak to generate dynamic breakup and substantial overland flooding in the northern Peace sector. However, backwaters from the downstream ice-jam on the Slave River, combined with arrival of a 'jave' (ice-jam-release waves; Beltaos, 2008) from release of an upstream ice-jam at Vermilion Rapids, raised river levels at the northern edge of the PAD by 3-4 m and caused flow reversals into the main PAD channels (Rivière des Rochers, Revillon Coupé, Chenal des Quatres Fourches) during May 3-6, 2018 (Jasek, 2019). Extensive ice-jams formed in the Athabasca River and distributaries (Embarras River, Mamawi Creek; Figure 3.1) within the southern Athabasca sector between at least May 1-3, 2018 when observations were made during aerial surveys by Kevin Timoney (Treeline Ecological Research) and Queenie Gray (Wood Buffalo National Park). The flooding had begun before the first flight on May 1st and had not ended by the last flight on May 3rd (K. Timoney, Q. Gray, pers. comm.). Maps of the spatial extent of the floodwaters have not yet been produced from the aerial surveys. However, observations and photos suggest overland flooding was extensive in the southern Athabasca sector of the PAD, but limited to a few low-lying basins adjacent to the main channels in the northern Peace sector (K. Timoney, pers. comm.).

Snow cover had melted in the PAD about two weeks before the spring floods of 2018 and almost one month before our lake and river sampling (May 15-17), as a consequence of consistent above freezing temperatures that occurred after April 19, 2018 (Alberta Climate Information Service https://agriculture.alberta.ca/acis/alberta-weather-data-viewer.jsp, accessed May 15, 2019). Aerial photos provided by K. Timoney identify that most of the sampled lakes became ice free just before the spring flooding, because they show shallow lakes were ice free but deeper lakes (>2 m) still had some remnant ice cover on May 1, 2018 at the time of flooding. A total of 4.1 mm of precipitation (rain) was recorded at Fort Chipewyan (58.7196° N, 111.1407° W) between April 19 and May 17, 2018, a period that precedes river flooding and extends until the end of our lake and river sampling (Alberta Climate Information Service https://agriculture.alberta.ca/acis/alberta-weather-data-viewer.jsp, accessed May 15, 2019).

3.2.3 Data collection

During May 15-17th, 2018 a set of 68 lakes and 9 river sites spanning the range of hydrological conditions across the PAD were sampled with the aid of a helicopter (Figure 3.1). Water samples and in-situ measurements were collected from a depth of ~10 cm in a mid-lake location (or mid-channel for the river sites). Samples for oxygen and hydrogen isotope analysis were stored in sealed 30 ml high-density polyethylene bottles, and in-situ measurements of specific conductivity were obtained using a YSI ProDSS sonde. Due to the shallow depth of lakes in the PAD, the lake volumes are generally well-mixed at the time of sampling. Thus, the sampling approach provides measurements representative of the total lake storage. Water isotope compositions of the lake and river samples were measured by Off-Axis Integrated Cavity Output Spectroscopy (O-AICOS) at the University of Waterloo – Environmental Isotope Laboratory (UW-EIL). Isotope compositions are expressed as δ-values, which represent deviations in per mil

(‰) from Vienna Standard Mean Ocean Water (VSMOW) such that δ_{sample} = (Rsample/R_{VSMOW}) - 1] x 10^3. 'R' is the ratio of $^{18}O/^{16}O$ or $^{2}H/^{1}H$ in the sample and VSMOW. Values are normalized to -55.5‰ and -428‰ for $\delta^{18}O$ and $\delta^{2}H$, respectively, for Standard Light Antarctic Precipitation (Coplen, 1996). Analytical uncertainties are ±0.09‰ for $\delta^{18}O$ and ±0.4‰ for $\delta^{2}H$. Field observations (described below) were recorded at the time of sampling for each lake.

3.2.4 Data analysis

To determine the flood status for each sampled lake, water isotope compositions were compared to river water isotope compositions, considering simultaneously values of specific conductivity and field observations. Lakes were designated as flooded if 1) water isotope values were close to or overlapping with the isotopically-depleted river water isotope compositions, 2) specific conductivity values were close to the range of the river water values (Peace sector: 164.5 to 176.5 μS cm^{-1}; Athabasca sector: 179.5 to 188.5 μS cm^{-1}), and 3) there was visible evidence of flooding, such as water colour and turbidity (assessed in situ) similar to the closest river or channel, and flooded lake margins and debris (i.e., logs) that appeared to have been carried in by the recent floodwaters. In the few instances where flood status was less obvious, hydrological conditions of nearby lakes were considered in combination with field observations. These cases are detailed in the Results section.

A previously developed isotope framework representing average conditions during 2000-2015 (Remmer et al., 2018) and a coupled-isotope tracer approach (Yi et al., 2008) were used to calculate the isotope composition of input water (δ_I) for each flooded lake (Figure 3.2; Appendix 1). As prescribed by the coupled-isotope tracer approach (Yi et al., 2008), all lake water isotope compositions experiencing the same atmospheric conditions will fall on lake-specific evaporation lines terminating at δ* (i.e., the limiting non-steady-state isotope composition of a

lake approaching desiccation), and their intersection with the Local Meteoric Water Line (LMWL) provides an estimate of δ_I for each lake. In this way, we were able to estimate the isotope composition of the input water entering lakes from our measurement of the isotope composition of lake water. For flooded lakes, we assume that δ_I consists primarily of floodwater supplied during the flood event and, to a lesser degree, precipitation received during the same period. We recognize that the δ_I values may also reflect some signal of input water during prior years, although this is likely to be minimal because of the tendency for large volumes of river water to enter the very shallow lakes of the PAD (typically <1 m maximum depth) when they flood.

A set of four Meteoric Water Line Segments (MWLS) were developed capturing the range of lake input water isotope compositions that result from mixing of either rain or snow with floodwater from the Peace or Athabasca river. Rainfall and snowmelt input includes both precipitation falling directly on the lake surface and runoff from the lake catchment that entered the lake during the period captured by our water isotope samples. Estimates of average ice-free season (May-September) rain isotope composition ($\delta^{18}O$ = -14.22‰, $\delta^{2}H$ = -112.2‰) and average ice-cover season (November-March; note April and October were not used because they typically include both rain and snow) snow isotope composition ($\delta^{18}O$ = -26.02‰, $\delta^{2}H$ = -199.0‰) were obtained from the Online Isotopes in Precipitation Calculator (Bowen, 2016; Bowen & Revenaugh, 2003; IAEA/WMO, 2015), while the isotope composition of the Peace ($\delta^{18}O$ = -21.11‰, $\delta^{2}H$ = -162.6‰) and Athabasca ($\delta^{18}O$ = -18.98‰, $\delta^{2}H$ = -149.9‰) rivers were determined from sampling in May 2018. Calculations of δ_I for the flooded lakes were, thus, constrained to one of the four MWLS, depending on the latitude of the lake (i.e., areas to the north of PAD 37 = influenced by floodwater from the Peace River; PAD 37 and areas to the

south = influenced by floodwater from the Athabasca River - see Figure 3.1) and whether the δ_I value was higher (i.e., more enriched; influenced by rainfall) or lower (i.e., more depleted; influenced by snowmelt) than the respective river isotope composition (Figure 3.2). PAD 37 was chosen to distinguish source of river floodwaters because lakes to the north tend to be flooded by the Peace River, while PAD 37 and lakes to the south are flooded by the Athabasca River. To determine the proportion of input water attributed to river floodwater, four binary mixing models were established. Linear positioning of rain, snow, and river isotope compositions in $\delta^{18}O$-$\delta^{2}H$ space preclude the use of a three-component mixing model. The four binary mixing models are:

For Peace sector lakes containing a mixture of floodwater and rainfall,

$$\%\ Peace\ River\ water = \frac{(\delta_I - \delta_{rain})}{(\delta_{Peace\ River} - \delta_{rain})} \quad \text{Eq.1}$$

for Peace sector lakes containing a mixture of floodwater and snowmelt,

$$\%\ Peace\ River\ water = \frac{(\delta_I - \delta_{snow})}{(\delta_{Peace\ River} - \delta_{snow})} \quad \text{Eq.2}$$

for Athabasca sector lakes containing a mixture of floodwater and rainfall,

$$\%\ Athabasca\ River\ water = \frac{(\delta_I - \delta_{rain})}{(\delta_{Athabasca\ River} - \delta_{rain})} \quad \text{Eq.3}$$

and, for Athabasca sector lakes containing a mixture of floodwater and snowmelt,

$$\%\ Athabasca\ River\ water = \frac{(\delta_I - \delta_{snow})}{(\delta_{Athabasca\ River} - \delta_{snow})} \quad \text{Eq.4}$$

Values generated by equations 1-4 represent estimates of the proportion of input water attributable to river floodwaters and do not necessarily represent the total amount of river floodwater in the lake at the time of sampling because nearly all lakes contained pre-existing water. The one exception is PAD 20, which had desiccated prior to the flood event.

Because the rain and snow end-member isotope compositions are not based on local measurements, but rather derived from a global model, and the values can certainly vary, we consider these end-member values to be the largest uncertainty in our modelling approach. Thus, a sensitivity analysis that incorporated uncertainty in the precipitation end-member isotope compositions was performed to evaluate their influence on flood magnitude estimates. We adjusted rain and snow end-member $\delta^{18}O$ values by ±1.08‰ and ±1.88‰, respectively, based on 1 standard deviation (SD) of the monthly values. The 'OIPC minus' scenario represents application of SD values subtracted from the rain and snow end-member isotope compositions, whereas the 'OPIC plus' scenario represents application of SD values added to the rain and snow end-member isotope compositions. The sensitivity analysis was performed using $\delta^{18}O$ values, since a binary mixing model would produce the same result using $\delta^{2}H$ values. To visualize flood magnitude and explore spatial patterns, the proportion of input water attributed to river floodwater was interpolated between lakes across the surface of the delta. Spatial autocorrelation was assessed using Moran's I (Anselin, 1995). Interpolation was generated using a multiquadratic radial basis function, a deterministic interpolation technique suitable for environmental monitoring (Rusu & Rusu, 2006), with the function and optimal parameters determined through cross-validation. Analyses were performed using ArcMap 10.6 software.

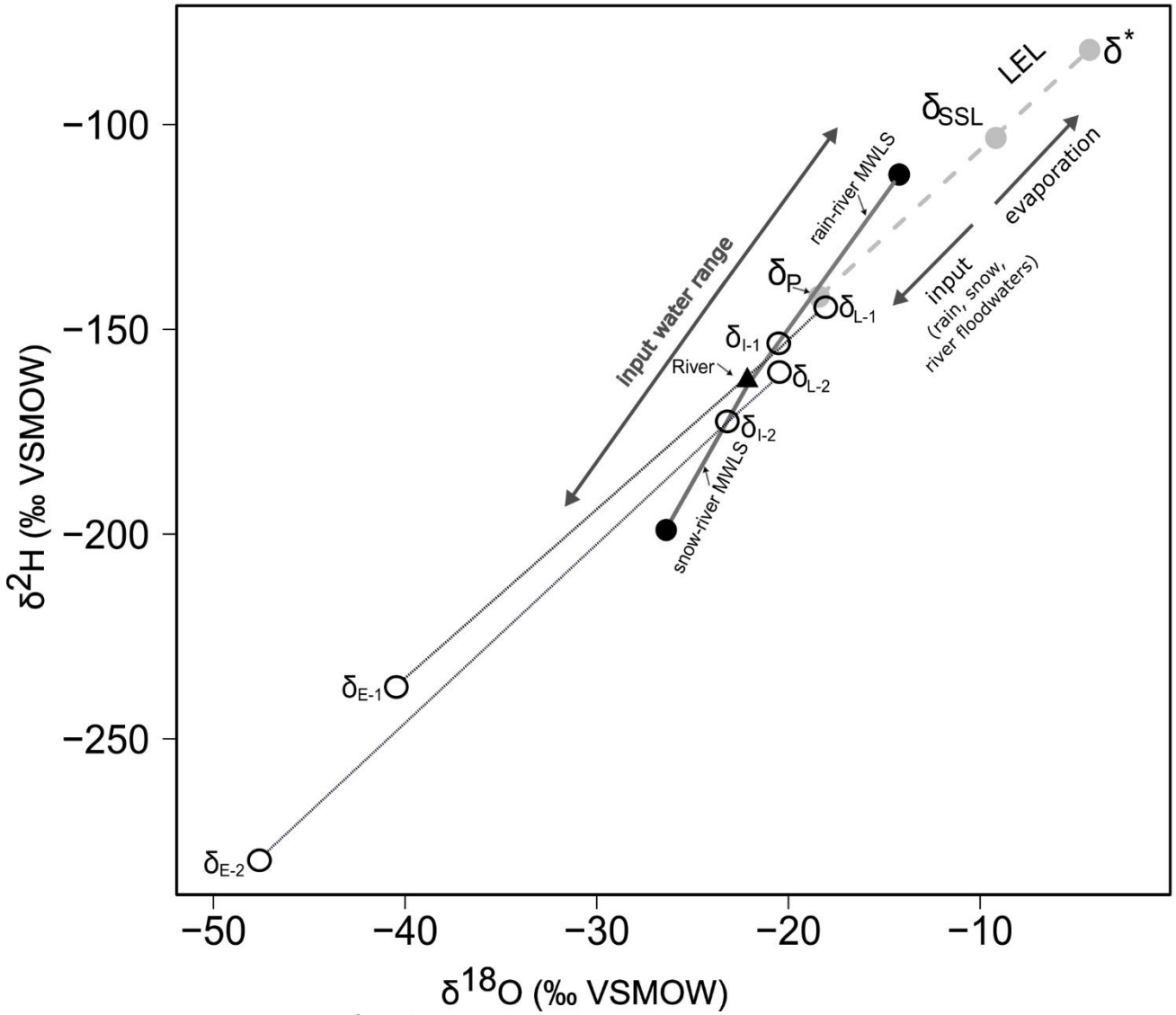

Figure 3.2. Schematic $\delta^{18}O$-$\delta^{2}H$ diagram illustrating water isotope compositions of two hypothetical lakes, one that has received input water consisting mainly of river floodwater and rain (δ_{L-1}) and one that has received input water consisting mainly of river floodwater and snowmelt (δ_{L-2}). Each lake plots along a lake-specific evaporation line. The intersection of lake-specific evaporation lines with Meteoric Water Line Segments (snow-to-river [blue] or river-to-rain [red]) provides an estimate of input water isotope composition (δ_I). Important features of the LEL include the steady-state isotope composition for a terminal basin (δ_{SSL}), which represents the special case of a lake at hydrological and isotopic steady state in which evaporation exactly equals inflow, and the limiting non-steady-state isotope composition (δ^*), which indicates the maximum potential isotopic enrichment of a lake as it approaches complete desiccation. The LEL is anchored at the mean annual isotope composition of precipitation (δ_P). Parameters used in the isotope mass-balance model to derive δ_I include the lake water isotope composition (δ_L) and the isotope composition of evaporated vapor from the lake (δ_E). See Appendix 1 for further details.

3.3 Results

3.3.1 Flood status of lakes

Several lake-water isotope compositions cluster around the river isotope compositions when plotted in $\delta^{18}O$-$\delta^{2}H$ space, which we interpret to reflect substantial influence of river floodwaters (Figure 3.3a). In contrast, many lake water isotope compositions also plot along the LEL between δ_P (isotope composition of weighted mean annual precipitation) and δ_{SSL} (isotope composition of a terminal lake at hydrological and isotopic steady state) indicating evaporative enrichment, which may have occurred during the spring and previous ice-free seasons in the absence of flooding (Figure 3.3b). The isotope compositions of non-flooded Peace and Athabasca sector lakes overlap, suggesting the influence of evaporative isotopic enrichment in the absence of flooding was comparable across the delta (Figure 3.3b). There are a few exceptions (8 of 68 lakes) to our strictly isotope-based interpretation of flood status (described further below). These include some lakes that are positioned along the LEL (PAD 27, 14, 58, 50; Figure 3.3a), but other data and observations indicate that they received some river floodwaters in 2018. Other exceptions include lakes that are positioned close to the MWLS (PAD 9, M2, M10, M5; Figure 3.3b), but measurements of conductivity and field observations led to interpretation that they did not receive river floodwaters in 2018.

Four of the lakes that were offset from the MWLS were considered flooded based on measurements of specific conductivity and visual observations (Figure 3.3a, Table 3.1). Three lakes are in the Peace sector (PAD 14, 50, 58) and one lake is in the Athabasca sector (PAD 27). PAD 50 was highly turbid and field observations noted the water colour matched the nearby Claire River, which was observed to be receiving water from the Peace River. We suspect this lake, which had been experiencing water-level drawdown during recent open-water seasons

(personal observation), received some river water but the isotopically-depleted input water was insufficient to offset the prior evaporative enrichment. Similarly, flooding of PAD 58 and PAD 14 was determined by observation of high turbidity and light brown water colour comparable to the Peace River. Turbid water, high water level, and a flooded lake margin was observed at PAD 27.

Four lakes (Athabasca sector: M2, M5, M10; Peace sector: PAD 9) that plot along the MWLS were classified as not flooded based on measurements of specific conductivity and visual observations (Figure 3.3b, Table 3.1). Lakes M2 and M5 had very low turbidity and specific conductivity was lower than expected if river water had entered the basins. We suspect these lakes may be influenced by isotopically-depleted snowmelt draining through elevated sand dunes located in their catchments. Lake water at PAD 9 was very shallow and clear, which we attribute to a strong influence of isotopically-depleted snowmelt. At M10, turbidity of the water was observed to be low, water levels appeared normal, and lake water colour was comparable to nearby lakes (M8, M9) that we confidently ascertained did not receive river floodwater.

In total, 44% (30/68) of sampled lakes received river floodwaters based on consideration of the water isotope compositions, specific conductivity, and field observations (Table 3.1). Nine of 32 (28%) sampled lakes in the Peace sector were classified as flooded, and 21 of 36 (58%) lakes in the Athabasca sector were classified as flooded.

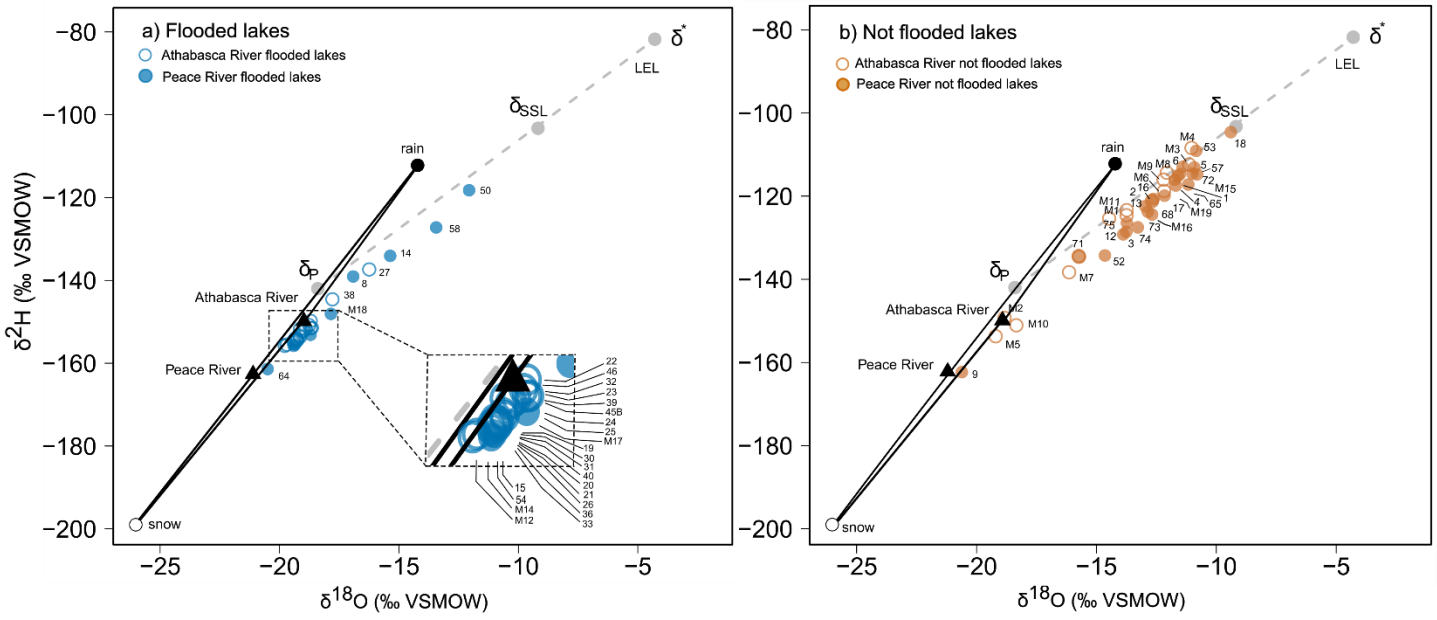

Figure 3.3. $\delta^{18}O$-$\delta^{2}H$ graphs showing the water isotope compositions of a) flooded lakes and b) not flooded lakes sampled in May 2018. Isotope compositions of rain, snow and the Peace and Athabasca rivers are also shown.

3.3.2 Calculation of proportion of input to lakes attributable to river floodwater

Based on calculation of δ_I values, the input water to each flooded lake was determined to consist mainly of a mixture of either Peace (north of PAD 37) or Athabasca (PAD 37 and to the south) river floodwater and rainfall or snowmelt (Figure 3.4; Table 3.2). Lakes were then assigned to one of four MWLS. Input water for 5 of the 9 flooded lakes in the Peace sector consisted mainly of a mixture of river floodwater and rainfall (Figure 3.4a). Input water for the other 4 flooded Peace sector lakes consisted of mainly a mixture of river floodwater and snowmelt (Figure 3.4b). In the Athabasca sector, 2 of the 21 flooded lakes received input water mainly comprised of river floodwater and rainfall (Figure 3.4c), while the other 19 flooded lakes received input water mainly comprised of river floodwater and snowmelt (Figure 3.4d).

Flooded lakes in the Peace sector contained a mixture of river floodwater and rain or snowmelt, while flooded lakes in the Athabasca sector were dominated primarily by a mixture of river floodwater and snowmelt. Based on equations 1 and 2, respectively, the proportion of input water attributable to river floodwater in Peace sector lakes dominated by precipitation in the form of rain ranged from 69% to 98% with an average of 81.8%, while the proportion of input water attributable to river water in lakes dominated by precipitation in the form of snow ranged from 90% to 97% with an average of 93.9% (Table 3.2). Based on equations 3 and 4, respectively, the proportion of input water attributable to river floodwater in Athabasca sector lakes dominated by precipitation in the form of rain ranged from 93% to 98% with an average of 95.5%, while the proportion of input water attributable to river floodwater in lakes dominated by precipitation in the form of snow ranged from 82% to 94% with an average of 86.3% (Table 3.2). The average proportion of input water attributable to river floodwater in the flooded lakes was 87.2% (n = 30), with comparable ranges and averages in the Peace (69-98%, avg = 86.9%, n = 9) and Athabasca sector (82-98%, avg = 87.2%, n = 21; Table 3.2).

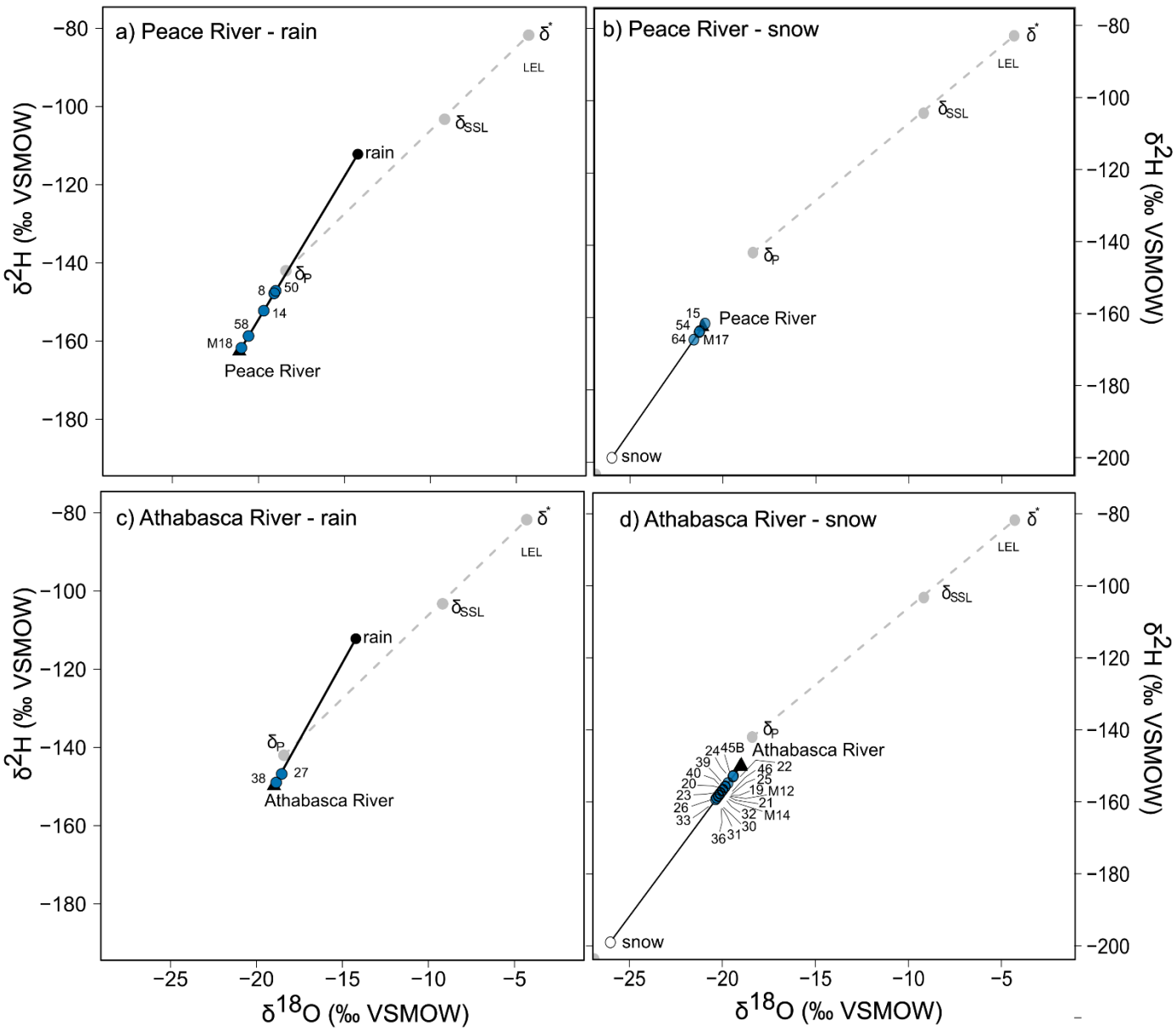

Figure 3.4. Isotope composition of input water (δ_I) for lakes flooded in May 2018 assigned to one of four Meteoric Water Line Segments: a) Peace River – rain, b) Peace River – snow, c) Athabasca River – rain and d) Athabasca River – snow.

3.3.3 Delineation of flood extent and magnitude

Calculations of the proportion of input to lakes attributable to river floodwater were interpolated across the surface of the PAD using a radial basis function to visualize flood extent and magnitude (Figure 3.5a). Because all flooded lakes had >60% input water attributed to river flooding, only contours of 60% river floodwater input and greater are displayed to highlight the flooded areas. Patterns of flooding differed notably between the Peace and Athabasca sectors. In the Peace sector, river floodwater input was mainly constrained to lakes located along the Chenal des Quatre Fourches (PAD 54, 58) and the northern reaches of the Revillon Coupé (PAD 14, 15). Flooding along the Rivière des Rochers and the Claire River was limited to a few sampled lakes (PAD 8, PAD 50). Lakes M17 and M18, which appear to lie at an interior location, received floodwaters from the Rivière des Rochers via a distributary channel. River floodwater was the dominant input into PAD 64, which is in a flood-prone area adjacent to the north shore of the Peace River. In the Athabasca sector, more extensive flooding occurred. River floodwaters entered lakes along Mamawi Creek and western portions of the Embarras and Athabasca rivers. However, flooding was not evident in lakes at the eastern terminus region of the Athabasca Delta. Note that the mapped flooded regions necessarily incorporate lakes that were not sampled, which is reasonable especially for the low-relief Athabasca sector. A sensitivity analysis incorporating uncertainties in the rain and snow end-member isotope compositions in the binary mixing model equations generated small differences in the flood map magnitude estimates (average absolute difference for the 'OIPC minus' scenario = 2.5% (minimum = -5.1% , maximum = 5.5%), Figure 3.5b; average absolute difference for the 'OIPC plus' scenario = 2.4% (minimum = -4.6, maximum = 2.9%), Figure 3.5c)

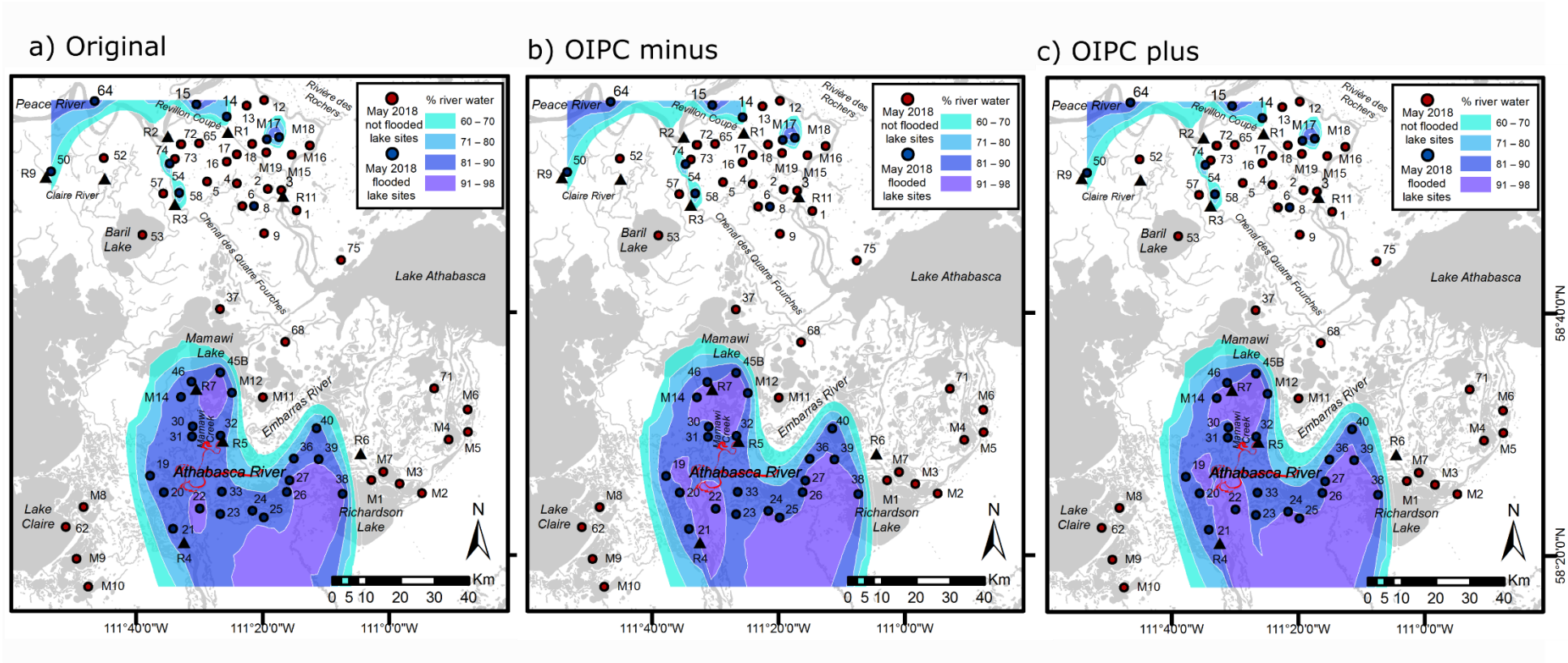

Figure 3.5. a) Map of the Peace-Athabasca Delta showing spatial interpolation (by radial basis function; Moran's I = 0.47) of percent of input water to lakes attributed to river floodwaters in May 2018. Note that the interpolation requires that non-sampled lakes that happen to fall within the >60% to 100% floodwater coloured zones are assumed to have received river floodwaters. Approximate locations of river ice-jams are indicated as red areas, as provided by Kevin Timoney (Treeline Ecological Research) based on photos taken during aerial surveys. b), c) Maps of the Peace-Athabasca Delta showing spatial interpolation of percent of input water to lakes attributed to river floodwaters in May 2018 incorporating sensitivity analyses (Figure 3.5b = rain $\delta^{18}O$ - 1.08‰ and snow $\delta^{18}O$ - 1.88‰, Moran's I = 0.49; Figure 3.5c = rain $\delta^{18}O$ + 1.08‰ and snow $\delta^{18}O$ + 1.88‰, Moran's I = 0.49).

3.4 Discussion

The lateral interaction of rivers and their floodplains is often an important determinant of patterns of biodiversity and species richness (Gregory, Swanson, McKee, & Cummins, 1991; Johnson & Host, 2010; Junk, Bayley, & Sparks, 1989; Ward, 1998; Welcomme, 1979), and monitoring of hydrological connectivity should be considered a vital component of efforts to conserve the ecological integrity of floodplain landscapes. However, measurement of hydrological connectivity can be difficult to obtain in water-rich landscapes, especially during short-lived, episodic flood events (Lindenmayer et al., 2008). Ice-jam floods provide a period of increased hydrological connectivity among rivers, channels, lakes and wetlands of the PAD, and decline in their frequency has remained a prominent concern for decades in recognition that these flood events are critical to maintaining ecological integrity. Thus, it is imperative to track flood events and their influence on hydrological connectivity when they occur, even if some of their effects are short-lived (see Remmer et al., 2018). Historically, this has been done mainly by observation from aircraft, and methods have recently been developed to map flood extent from satellite imagery (Pavelsky & Smith, 2008; Toyra & Pietroniro, 2005). However, neither of these approaches readily allow quantification of flood magnitude, and the mapped flood extents can be strongly influenced by the timing of observations.

Recently, an international organization has identified the need to expand the scope of monitoring in the PAD, among other recommendations, which has translated into an Action Plan for Wood Buffalo National Park (WHC/IUCN, 2017; WBNP, 2019). Here, we demonstrate the utility of systematic sampling of lakes and rivers for analysis of water isotope composition to serve this knowledge requirement, and in particular to quantitatively delineate extent and magnitude of flood events on lakes across the ~6000 km^2 expanse of the delta. This opportunity

arose because, fortuitously, a substantial ice-jam flood event occurred in the midst of our multi-year program of sampling of lakes in the delta, which is designed to generate a monitoring framework to assess changes in hydroecological conditions and sources, distribution and toxicity of contaminants in lakes of the Peace-Athabasca Delta. Had we not been systematically collecting samples prior to and during this time (and engaged in the associated fieldwork planning required to execute the sampling), it would have been substantially more difficult to capture this event in the level of detail presented here, especially if timing and frequency of sampling was sporadic and relied upon by impromptu decision making.

Ice-jams in late April and early May 2018 resulted in flooding of lakes in both sectors of the PAD, although flood extent and magnitude differed between the Peace and Athabasca sectors. High water levels in the Peace River resulted in flow reversals along some river channels, including the Claire River, Chenal des Quatre Fourches, Revillon Coupé and Rivière des Rochers (Jasek, 2019). Results from our study identify that these high river levels led to flooding of several lakes adjacent to these channels (e.g., 96% river floodwater input at PAD 54; Figure 3.4, 3.5, 3.6, Table 3.2), which has long been observed to occur during high water events on the Peace River (e.g., PADPG, 1973; Wolfe et al., 2006). Interpolation indicates that input to lakes in these areas was dominated by river water, and that the proportion of input water attributed to river floodwater decreased with increasing distance from the channels, consistent with independent observations made during aerial surveys indicating there was minimal overland flooding in the Peace sector due to absence of ice-jams in the stretch of the Peace River adjacent to the PAD (Jasek, 2019).

Our isotope-based methods identify considerably greater spatial extent of floodwaters in the Athabasca sector than the Peace sector, consistent with independent observations made during

aerial surveys (Figure 3.5, K. Timoney, pers. comm.). And, results of our methods were supported by photographic evidence and field notes compiled by K. Timoney (Treeline Ecological Research) showing that Blanche Lake (PAD 25), Dagmar Lake (PAD 33), Mamawi Creek Pond (PAD 30), Johnny Cabin Pond (PAD 31), Richardson Lake (PAD 38), Grey Wavy Lake (PAD 40) and Otter Lake (PAD 46) were all flooded by May 1, 2018 (K. Timoney, pers. comm.). In the Athabasca sector, river floodwaters were conveyed primarily by the Athabasca River and Embarras River and entered lakes along the western portion of these rivers. Flooding along the Embarras River and downstream along Mamawi Creek towards Mamawi Lake aligns with paleolimnological evidence and field observations that river floodwaters have been diverted northward along this flow path due to the Embarras Breakthrough in 1982, a natural river avulsion that has since redirected substantial and increasing volumes of Athabasca River flow (via the Embarras River) along Mamawi Creek (Kay et al.,2020; Timoney, 2013; Wolfe et al., 2008). Lack of observed flooding at the eastern terminus region of the Athabasca Delta also aligns with paleolimnological records that indicate less frequent lake flooding in this area since the Embarras Breakthrough (Kay et al., 2019). Given the importance of the Athabasca Delta terminus region to land users, and their concerns about decreasing water levels (IEC, 2018; MCFN, 2014), confirmation that floodwater is not reaching this area, even during the large ice-jam flood of 2018, is an important contribution to conservation dialogues.

Some lakes in the central area of the Athabasca sector received enough river water input to drastically change their lake water balance (PAD 19-21; Figure 3.6). For example, PAD 20, a lake located along the western edge of the flood extent, had desiccated by fall 2017 following a multi-year trend of declining water levels. This provided opportunity to evaluate our flood magnitude estimates because there was no water balance memory at PAD 20, which can

potentially confound interpretation of δ_I values. When sampled in May 2018, this lake contained 2.4 m of water, of which we attribute 85% to river floodwater input and 15% to snowmelt (Figure 3.5, Table 2). This suggests that 0.36 m of the 2.4 m of new water was contributed by snowmelt. Based on records at the Fort Chipewyan meteorological station (Ft. Chipewyan RC, obtained from https://agriculture.alberta.ca/acis/alberta-weather-data-viewer.jsp for the period October 1, 2018 through April 18, 2019 (the snowfall period), only 78 mm (0.078 m) of precipitation fell during the snowfall period. But, the land surrounding the lake has extensive tree and shrub cover, which entraps wind-redistributed snow from adjacent treeless areas. To further evaluate this estimate, we compiled lake depth changes between September 2017 (our prior sampling trip) and May 2018 in Athabasca sector lakes that did not flood. Assuming we sampled lakes in the same locations on both field visits, as intended, lake depth changes ranged from -0.04 m (i.e., a drawdown of 4 cm) to +0.59 m. Thus, our estimate of 0.36 m of snowmelt water contribution to PAD 20 is possible as it falls within this range.

Our sensitivity analysis has demonstrated that incorporating reasonable uncertainty of both the snow and rain end-member isotope compositions does little to change the outcome at the scale presented in Figure 3.5, which is most appropriate for ecosystem management purposes. Indeed, the most important delineation in our approach is simply whether the lake flooded or not, which water isotope tracers, supplemented by measurements of specific conductivity and field observations, effectively identify. Nonetheless, surveys of rain and snow isotope compositions could better constrain these end-members and be used to assess for spatial heterogeneity, thereby enhancing the accuracy of the model and estimates of flood magnitude.

We acknowledge other uncertainties in this modelling approach. For example, flooded lakes likely contain a mixture of river floodwater, plus rain *and* snow, and this may have led to over-

estimating river floodwater contributions because the linear positioning of these end-members in $\delta^{18}O$-$\delta^{2}H$ space precludes the use of a three-component mixing model. We contend that our approach, which considers the two dominant inputs to each lake, provides a reasonable estimation to track the extent and magnitude of river flood events. Indeed, presentation of Figure 3.5 to WBNP staff indicated that our results largely aligned with observations made during their flyovers (Q. Gray, pers. comm.), and flooding was observed at several lakes along the northern and eastern peripheral flood margins based on our approach (i.e., PAD 30, 31, 38, 40, 46; K. Timoney, pers. comm.), as stated above. However, none of the lakes identified as flooded by our approach were estimated to have less than 60% of their input attributed to river floodwaters, even those at the outer margin of the flooded area. There are at least two possible explanations for this outcome. One is that our methods are not sufficiently sensitive to detect flooding when this value is less than 60% due to insufficient change in water isotope values, specific conductivity, and other sources of information. The second is that flooding to these shallow, small volume lakes rarely ever results in less than 60% of the input attributable to river floodwater because once rivers overbank, they supply so much water to the flat terrain that more than half of the lake input is due to this hydrological process. Clearly, this suggests a need for further refinement and testing of our methods and more data acquisition to distinguish these possibilities. Also, interpolation of the calculated proportion of input water attributable to river floodwater is limited in some areas of the delta (e.g., Claire River and the northeastern area of the Athabasca sector) by a low density of sampled lakes. While more lake sampling sites could be added, the set of 68 sampled lakes provides considerable coverage for tracking the main patterns of flooding and hydrological connectivity across the landscape. Despite these uncertainties, the flood map generated by our approach represents a marked improvement over other approaches because it is

less prone to logistical limitations (i.e., sampling can occur after a flood occurs, not at the exact moment of flooding) and can quantify spatial variation in the magnitude of flood influence.

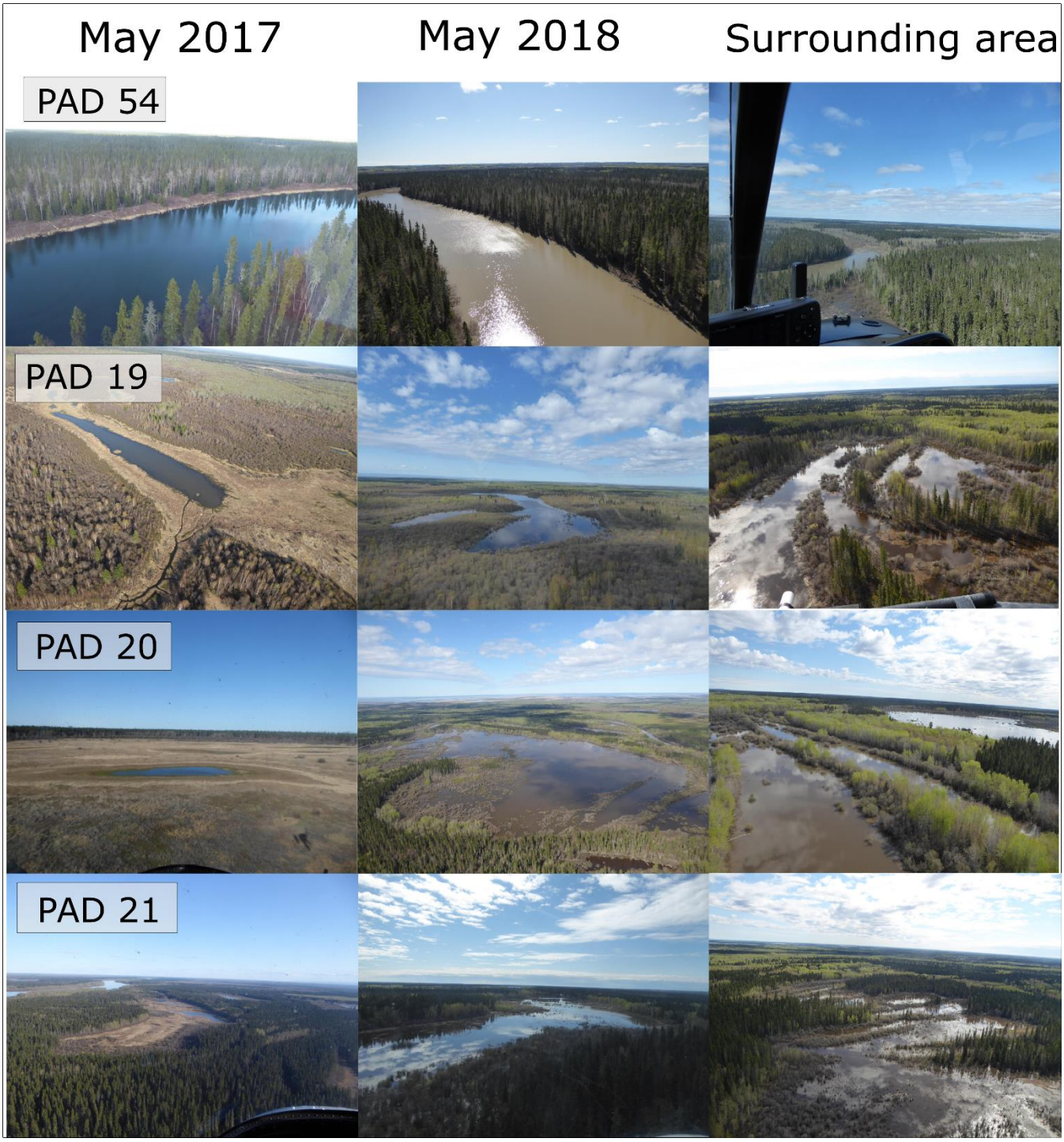

Figure 3.6. Images of selected flooded lakes and surrounding areas in May 2017 (left; no flooding) and May 2018 (middle, right; substantial flooding).

3. 5 Conclusions and recommendations

River water entered lakes in the PAD during an ice-jam flood event in late April to early May 2018. Here we used water isotope tracers, supplemented by measurements of specific conductivity, and field observations, to delineate the extent and magnitude of flooding. We present an isotope-based approach, incorporating landscape-specific set of binary mixing models that allow estimation of the proportion of input water to lakes attributable to river floodwater and rainfall or snowmelt. Nearly half of the 68 lakes we have sampled since 2015 as part of developing the foundation of a monitoring program received river floodwaters in spring 2018, and the estimated proportion of lake input provided by river floodwater to the flooded lakes averaged 87.2%. We found that flooding in the northern Peace sector was primarily limited to lakes along the Chenal des Quatre Fourches and the northern reaches of the Revillon Coupé. Flooding in the Athabasca sector was much more extensive, but did not reach the eastern terminus of the Athabasca Delta as floodwater was conveyed northwards through the Embarras River and into Mamawi Creek, a continuing legacy of the Embarras Breakthrough that occurred in 1982 (Kay et al., 2020; Timoney, 2013; Wolfe et al., 2008).

Monitoring data are an essential component of science-based policy, and long-term records are the most likely to contribute to policy (Hughes, Beas, Barner, & Brewitt, 2017). However, obtaining resources to support continuous long-term monitoring remains a challenge (Lovett et al., 2007). Cost-effective measurements of important variables can increase the likelihood of the long-term sustainability of a monitoring program, allowing them to survive during times of lean budgets and, thus, increase the probability that the data will contribute to policy and decision making. This is particularly true in remote northern landscapes, which present additional logistical and financial challenges (Mallory et al., 2018). For example, conventional water

gauges are expensive to install and maintain at a landscape scale and are frequently damaged or lost during the flood event they aim to capture (e.g., Jasek, 2019). Aerial surveys of flood extent can be informative, but are limited by the timing of the flights. In complex and dynamic floodplain landscapes such as the PAD, hydrological monitoring approaches must be sensitive, timely, flexible and cost-effective. Use of water isotope tracers meets these requirements and, thus, provides an alternative and complementary approach capable of capturing an integrated signal of recent hydrological events and processes. Water isotope tracers have a high level of dexterity, sample collection is straightforward and fast (the 77 sites used in this study were sampled over 2 days) and analytical costs are low. Indeed, senior authors of this paper have long utilized water isotope tracers and other approaches in partnership with other northern National Parks in Canada to assist with meeting their aquatic ecosystem monitoring and reporting obligations. Here we propose water isotope tracers along with measurements of specific conductivity as practical, affordable long-term lake hydrological monitoring tool capable of generating informative results for the PAD, and other remote lake-rich landscapes.

3.6 References

Anselin, L. (1995). Local indicators of spatial association – LISA. *Geographical Analysis*, 27, 93–115.

Barnett, T. P., Pierce, D. W., Hidalgo, H. G., Bonfils, C., Santer, B. D., Das, T., … Dettinger, M. D. (2008). Human-induced changes in the hydrology of the western United States. *Science*, 319, 1080–1083.

Beltaos, S. (Ed.). (2008). River Ice Breakup. Water Resource Publications, LLC., Highlands Ranch, Colorado, USA, 462 pp.

Beltaos, S. (2014). Comparing the impacts of regulation and climate on ice-jam flooding of the Peace-Athabasca Delta. *Cold Regions Science and Technology*, 108, 49–58.

Bowen, G. J. (2016). The Online Isotopes in Precipitation Calculator, version 2.2. Accessible at http://www.waterisotopes.org.

Bowen, G. J., & Revenaugh, J. (2003). Interpolating the isotopic composition of modern meteoric precipitation. *Water Resources Research,* 39, 1299.

Brock, B. E., Wolfe, B. B., & Edwards, T. W. D. (2007). Characterizing the hydrology of shallow floodplain lakes in the Slave River Delta, NWT, Canada, using water isotope tracers. *Arctic, Antarctic, and Alpine Research*, 39, 388-401.

Brock, B. E., Wolfe, B. B., & Edwards, T. W. D. (2008). Spatial and temporal perspectives on spring break-up flooding in the Slave River Delta, NWT. *Hydrological Processes*, 22, 4058–4072.

Coplen, T. B. (1996). New guidelines for reporting stable hydrogen, carbon, and oxygen isotope-ratio data. *Geochimica et Cosmochimica Acta,* 60, 3359–3360.

Dudgeon, D., Arthington, A. H., Gessner, M. O., Kawabata, Z., Knowler, D. J., Lévêque, C., … Sullivan, C. A. (2006). Freshwater biodiversity: importance, threats, status and conservation challenges. *Biological Reviews of the Cambridge Philosophical Society*, 81, 163-82.

Fausch, K. D., Torgersen, C. E., Baxter, C. V., & Li, H. W. (2002). Landscapes to riverscapes: bridging the gap between research and conservation of stream fishes. *Bioscience,* 52, 483–498.

Gibson, J. J. & Edwards, T. W. D. (2002). Regional water balance trends and evaporative transpiration partitioning from a stable isotope survey of lakes in northern Canada. *Global Biogeochemical Cycles*, 16, 1–9.

Gleick, P. (2003). Global freshwater resources: soft-path solutions for the 21st century. *Science,* 302, 1524–1528.

Gregory, S. V., Swanson, F. J., McKee, W. A., & Cummins, K. W. (1991). An ecosystem perspective of riparian zones. *BioScience,* 41, 540–551.

Hall, R. I., Wolfe, B. B., & Wiklund, J. A. (2019). Discussion of "Frequency of ice-jam flooding of Peace-Athabasca Delta". *Canadian Journal of Civil Engineering*, 46, 236–238.

Hughes, B. B., Beas, R., Barner, A., & Brewitt, K. (2017). Long-term studies contribute disproportionately to ecology and policy. *BioScience*, 67, 271–281.

IAEA/WMO. (2015). Global Network of Isotopes in Precipitation. The GNIP Database. Accessible at: https://nucleus.iaea.org/wiser.

Independent Environment Consultants (IEC). (2018). Strategic environmental assessment of Wood Buffalo National Park World Heritage Site. Volume 1, Milestone 3 – Final SEA Report. Independent Environment Consultants (IEC), Markham, Ontario.

Jasek, M. (2019). An emerging picture of Peace River break-up types that influence ice jam flooding of the Peace-Athabasca Delta Part 1: The 2018 Peace River break-up. Canadian Geophysical Union Hydrology Section Committee on River Ice Processes and the Environment. 20th Workshop on the Hydraulics of Ice Covered Rivers. Ottawa, Canada, May 14-16, 2019. Accessible at: http://www.cripe.ca/publications/proceedings/20.

Johnson, L. B., & Host, G. E. (2010). Recent developments in landscape approaches for the study of aquatic ecosystems. *BioOne,* 29, 41–66.

Junk, W. J., Bayley, P. B., & Sparks, R. E. (1989). The flood pulse concept in river–floodplain systems. *Canadian Journal of Fisheries and Aquatic Sciences*, 106, 110–127.

Kay, M. L., Wiklund, J. A., Remmer, C. R., Neary, L. K., Brown, K., Ghosh, A. … Wolfe, B. B. 2020. Bi-directional hydrological changes in perched basins of the Athabasca Delta (Canada) in recent decades caused by natural processes. *Environmental Research Communications*. 1 081001. https://doi.org/10.1088/2515-7620/ab37e7

Lindenmayer, D., Richard, J., Montague-Drake, R., Alexandra, J., Bennett, A., Cale, P., & Fischer, J. (2008). A checklist for ecological management of landscapes for conservation. *Ecology Letters*, 11, 78–91.

Lovett, G. M., Burns, D. A., Driscoll, C. T., Jenkins, J. C., Mitchell, M. J., Rustad, L., … Haeuber, R. (2007). Who needs environmental monitoring? *Frontiers of Ecology and Environment*, 5, 253–260.

MacDonald, L. A., Wolfe, B. B., Turner, K. W., Anderson, L., Arp, C. D., Birks, S. J., … White, H. (2017). A synthesis of thermokarst lake water balance in high-latitude regions of North America from isotope tracers. *Arctic Science*, 149, 118–149.

Mallory, M. L., Gilchrist, H. G., Janssen, M., Major, H. L., Merkel, F., Provencher, J. F., & Strøm, H. (2018). Financial costs of conducting science in the Arctic: examples from seabird research. *Arctic Science*, 4, 624–633.

MCFN. (2014). Petition to The World Heritage Committee Requesting Inclusion of Wood Buffalo National Park on the List of World Heritage in Danger. Mikisew Cree First Nation.

Monk, W. A., Peters, D.L., & Baird, D.J. (2012). Assessment of ecologically relevant hydrological variables influencing a cold-region river and its delta: The Athabasca River and the Peace-Athabasca Delta, northwestern Canada. *Hydrological Processes*, 26, 1828–1840.

Nielsen, G. (1972). Groundwater investigation, Peace-Athabasca Delta, section J. In Peace-Athabasca Delta Project, Technical Report and Appendices: Volume 1, Hydrological Investigations, 36 pp.

PADPG. (1973). Peace–Athabasca Delta Project, technical report and appendices, Volume 1: Hydrological Investigations, Volume 2: Ecological investigations. Peace–Athabasca Delta Project Group, Delta Implementation Committee, Governments of Alberta, Saskatchewan and Canada.

Pavelsky, T. M., & Smith, L.C. (2008). Remote sensing of hydrologic recharge in the Peace-Athabasca Delta, Canada. *Geophysical Research Letters*, 35, L08403, doi:10.1029/2008GL033268.

Pietroniro, A., Prowse, T. D., & Peters, D. L. (1999). Hydrologic assessment of an inland freshwater delta using multi-temporal satellite remote sensing. *Hydrological Processes*, 13, 2483–2498.

Prowse, T. D., & Conly, F. M. (2002). A review of hydroecological results of the Northern River Basins Study, Canada. Part 2. Peace – Athabasca Delta. *River Research and Applications*, 18, 447–460.

Prowse, T. D., Peters, D.L., & Marsh, P. (1996). Modelling the water balance of Peace–Athabasca Delta perched basins. Peace–Athabasca Delta Technical Studies, National Hydrology Research Institute.

Prowse, T. D., Beltaos, S., Gardner, J. T., Gibson, J. J., Granger, R. J., & Leconte, R. (2006). Climate change, flow regulation and land-use effects on the hydrology of the Peace-Athabasca-Slave system: findings from the Northern Rivers Ecosystem Initiative. *Environmental Monitoring and Assessment*, 113, 167–197.

Remmer, C. R., Klemt, W. H., Wolfe, B. B., & Hall, R. I. (2018). Inconsequential effects of flooding in 2014 on lakes in the Peace-Athabasca Delta. *Limnology and Oceanography*, 63, 1502–1518.

Rusu C., & Rusu V. (2006). Radial Basis Functions Versus Geostatistics in Spatial Interpolations. In: Bramer M. (Eds.) Artificial Intelligence in Theory and Practice. IFIP AI

2006. IFIP International Federation for Information Processing, vol 217. Springer, Boston, MA.

Sauchyn, D. J., St-Jacques, J., & Luckman, B. H. (2015). Long-term reliability of the Athabasca River (Alberta, Canada) as the water source for oil sands mining. *Proceedings of the National Academy of Sciences of the United States of America*, 112, 12621–12626.

Schindler, D. W., & Smol, J. P. (2006). Cumulative effects of climate warming and other human activities on freshwaters of arctic and subarctic North America. *Ambio*, 35, 160–168.

Schindler, D. W. & Donahue, W. F. (2006). An impending water crisis in Canada's western prairie provinces. *Proceedings of the National Academy of Sciences of the United States of America*, 103, 7210–7216.

Smol, J. P., Wolfe, A. P., Birks, H. J. B., Douglas, M. S. V, Jones, V. J., Korhola, A., … Weckström, J. (2005). Climate-driven regime shifts in the biological communities of arctic lakes. *Proceedings of the National Academy of Sciences of the United States of America*, 102, 4397–4402.

Straka, J, & Gray, Q. (2014). Wood Buffalo National Park Flood Report, Spring 2014. Parks Canada.

Timoney, K. P. (2013). The Peace-Athabasca Delta – portrait of a dynamic ecosystem. The University of Alberta Press.

Töyrä, J., & Pietroniro. A. (2005). Towards operational monitoring of a northern wetland using geomatics-based techniques. *Remote Sensing of the Environment*, 97, 174–191.

Ward, J. V. (1998). Riverine landscapes: biodiversity patterns, disturbance regimes, and aquatic conservation. *Biological Conservation*, 83, 269–278.

Welcomme, R. L. (1979). Fisheries ecology of floodplain rivers. Longman Publishing, New York.

WHC/IUCN. (2017). Reactive monitoring mission to Wood Buffalo National Park, Canada; mission report, March 2017. United Nations Educational, Scientific and Cultural Organization. Accessible at http://whc.unesco.org/en/documents/156893.

Wiklund, J. A., Hall, R. I., & Wolfe, B. B. (2012). Timescales of hydrolimnological change in floodplain lakes of the Peace–Athabasca Delta, northern Alberta, Canada. *Ecohydrology*, 5, 351–367.

Wolfe, B. B., Karst-Riddoch, T. L., Hall, R. I., Edwards, T. W. D., English, M. C., Palmini, R., ...Vardy, S. R. (2007). Classification of hydrologic regimes of northern floodplain basins (Peace-Athabasca Delta, Canada) from analysis of stable isotopes ($\delta^{18}O$, $\delta^{2}H$) and water chemistry. *Hydrological Processes*, 21, 151–168.

Wolfe, B. B., Hall, R. I., Edwards, T. W. D., Vardy, S. R., Falcone, M. D., Sjunneskog, C., … van Driel, P. (2008). Hydroecological responses of the Athabasca Delta, Canada, to changes in river flow and climate during the 20th century. *Ecohydrology*, 1, 131–148.

Wolfe, B. B., Hall, R. I., Last, W. M., Edwards, T. W. D., English, M. C., Karst-Riddoch, T. L., … Palmini, R. (2006). Reconstruction of multi-century flood histories from oxbow lake sediments, Peace-Athabasca Delta, Canada. *Hydrological Processes*, 20, 4131–4153.

Wolfe, B. B., Hall, R. I., Edwards, T. W. D., & Johnston, J. W. (2012). Developing temporal hydroecological perspectives to inform stewardship of a northern floodplain landscape subject to multiple stressors: Paleolimnological investigations of the Peace-Athabasca Delta. *Environmental Reviews*, 20: 191–210.

Wood Buffalo National Park (WBNP, 2019). World Heritage Site Action Plan. Parks Canada. Accessible at: https://www.pc.gc.ca/en/pn-np/nt/woodbuffalo/info/action.

Woodward, G., Perkins, D., & Brown, L. (2010). Climate change and freshwater ecosystems: Impacts across multiple levels of organization. *Philosophical Transactions of the Royal Society B: Biological Sciences*, 365, 2093–2106.

Yi, Y., Brock, B. E., Falcone, M. D., Wolfe, B. B., & Edwards, T. W. D. (2008). A coupled isotope tracer method to characterize input water to lakes. *Journal of Hydrology*, 350, 1–13.

Tables

Table 3.1. Water isotope compositions, field observations and specific conductivity from 68 lakes and 9 river sites in the Peace-Athabasca Delta sampled in May 2018 and used to categorize the lakes as either flooded or not flooded by the Peace or Athabasca rivers during the spring of 2018.

Lake ID	Water isotope composition		Field notes	Conductivity	Flooded in
	$\delta^{18}O$ (‰ VSMOW)	$\delta^{2}H$ (‰ VSMOW)	Observations	(µS/cm)	spring 2018?
Peace Sector					
R1	-21.24	-162.94	Very turbid, light brown	176.5	Revillon Coupé
R2	-21.11	-162.64	Light brown, very turbid - thick with mud	173.4	Peace River
R3	-21.20	-163.88	Light brown, very turbid, thick with sediment	175.4	Chenal des Quatre Fourches
R9	-20.88	-163.35	Light brown, very turbid, no visible macrophytes	304.4	Claire River
R11	-20.12	-157.90	Light brown, very turbid	164.9	Rivière des Rochers
PAD 1	-11.60	-115.17	Brown water, turbid	329.5	No
PAD 2	-12.66	-121.08	Brown water, turbid, water lilies emerging	264.6	No
PAD 3	-13.88	-129.19	Dark brown water, turbid, water in lake margins	304.6	No
PAD 4	-11.73	-116.03	Greenish brown water, some turbidity	440.6	No
PAD 5	-10.92	-113.10	Greenish brown water, clear (low turbidity)	274.6	No
PAD 6	-11.40	-112.96	Greenish brown water, turbid	280.9	No
PAD 8	-16.92	-139.06	Water colour like river channel (red-brown), high water level	150.5	Yes
PAD 9	-20.61	-162.32	Clear (low turbidity), very shallow	56.0	No
PAD 12	-13.75	-128.58	Dark brown water, clear (low turbidity)	297.9	No
PAD 13	-12.96	-122.41	Dark brown water, clear (low turbidity)	99.5	No
PAD 14	-15.37	-134.08	Light brown, highly turbid water	218.1	Yes

PAD 15	-19.35	-155.46	Light brown, highly turbid water	241.2	Yes
PAD 16	-12.62	-120.65	Greenish brown, turbid	446.4	No
PAD 17	-12.16	-119.88	Brown water, very clear (low turbidity)	184.5	No
PAD 18	-9.39	-104.59	Greenish blue water, very clear (low turbidity)	167.6	No
PAD 50	-12.06	-118.23	Light brown water, high turbidity, silty	324.8	Yes
PAD 52	-14.65	-134.26	Greenish brown water, low turbidity	420.3	No
PAD 53	-10.84	-109.09	Brown water, low turbidity	242.3	No
PAD 54	-19.41	-155.82	Light brown water, high turbidity, flooding obvious	227.2	Yes
PAD 57	-10.99	-114.59	Greenish brown water, fairly turbid, no signs of flooding	381.9	No
PAD 58	-13.44	-127.21	Light brown water, high turbidity	250.4	Yes
PAD 64	-20.50	-161.40	Light brown, very turbid, appears flooded, drowned vegetation, water looks to have come from the west end, no visible macrophytes	254.6	Yes
PAD 65	-11.17	-117.20	Moderate turbidity, flooding not evident	316.9	No
PAD 72	-10.80	-114.74	Water level below high-water mark visible on rocks. No signs of flooding noted	N/A	No
PAD 73	-12.68	-124.42	Water clear, visible to lake bottom	N/A	No
PAD 74	-13.28	-127.51	Water clear, visible to lake bottom	N/A	No
PAD 75	-13.73	-126.41	Water is very clear	N/A	No
M15	-11.52	-114.68	Brown water, low turbidity	201.8	No
M16	-12.86	-123.74	Brown water, low turbidity	120.1	No
M17	-18.70	-153.14	High turbidity, water in lake margins, water levels high	219.3	Yes
M18	-17.85	-148.08	High turbidity, water in lake margins, water levels high	226.7	Yes
M19	-11.69	-117.43	Brown water, low turbidity	189.7	No

Athabasca Sector					
R4	-18.98	-149.85	Medium brown, very turbid	179.7	Athabasca River
R5	-19.12	-151.60	Medium brown, fast flowing, high turbidity, bank erosion (to the North)	188.5	Embarras River
R6	-19.16	-151.69	Medium brown, turbid	181.3	Fletcher Channel
R7	-19.25	-152.30	Turbid, brown	185.1	Mamawi Creek
PAD 19	-19.17	-153.33	High turbidity, high water levels	199.2	Yes
PAD 20	-19.40	-154.51	Obvious flooding, high water level, high turbidity	203.9	Yes
PAD 21	-19.30	-154.14	High turbidity, water throughout lake margins, high water level	211.7	Yes
PAD 22	-18.70	-149.79	Fairly turbid, water throughout lake margins	209.0	Yes
PAD 23	-18.65	-151.48	Fairly turbid, water throughout lake margins	191.0	Yes
PAD 24	-18.98	-152.12	Fairly turbid, water throughout lake margins	189.5	Yes
PAD 25	-19.04	-152.33	Fairly turbid	180.5	Yes
PAD 26	-19.25	-154.32	High turbidity, logs in lake on river side	217.2	Yes
PAD 27	-16.25	-137.35	Fairly turbid, water throughout lake margins, high water level	227.5	Yes
PAD 30	-19.14	-153.63	High turbidity, drowned macrophytes, obvious flooding	217.7	Yes
PAD 31	-19.27	-154.25	High turbidity, drowned macrophytes, obvious flooding	211.4	Yes
PAD 32	-18.70	-151.52	High turbidity, water throughout lake margins and surrounding landscape	244.8	Yes
PAD 33	-19.40	-155.02	High turbidity, water throughout lake margins, high water level	242.4	Yes
PAD 36	-19.29	-154.65	Fairly turbid	225.2	Yes
PAD 37	-13.62	-129.40	Clear water, benthic algal growth	430.7	No
PAD 38	-17.79	-144.57	High turbidity, water throughout lake margins, high water level	175.1	Yes
PAD 39	-18.90	-151.79	Dark tea brown, water in lake margins	223.7	Yes

PAD 40	-19.33	-153.98	High turbidity, no macrophytes visible	222.4	Yes
PAD 45B	-19.14	-151.73	High turbidity, high water levels	211.7	Yes
PAD 46	-18.76	-150.79	Light brown water, low turbidity	239.4	Yes
PAD 62	-14.47	-125.39	Clear water (low turbidity)	531.0	No
PAD 68	-12.68	-121.17	No signs of flooding	N/A	No
PAD 71	-15.74	-134.40	Very low turbidity, dark tea colour	269.7	No
M1	-13.74	-124.59	Greenish brown water, low turbidity, benthic vegetation visible	309.9	No
M2	-18.83	-149.29	Dark brown water, very clear (no turbidity)	47.8	No
M3	-11.14	-112.38	Greenish water, low turbidity	359.0	No
M4	-11.04	-108.39	Greenish brown water, fairly turbid	311.7	No
M5	-19.20	-153.70	Dark brown water, low turbidity	49.2	No
M6	-12.18	-118.75	Greenish brown water, clear (low turbidity)	304.3	No
M7	-16.14	-138.30	Dark tea brown, clear (low turbidity), water in lake margins	270.6	No
M8	-12.07	-114.34	Brown water, clear (no turbidity)	569.0	No
M9	-12.20	-116.02	Red-brown water, low turbidity	777.0	No
M10	-18.34	-151.06	Red-brown water, low turbidity	193.9	No
M11	-13.74	-123.36	Dark brown water, low turbidity	290.7	No
M12	-19.78	-155.82	High turbidity, water in lake margins, water levels high	214.5	Yes
M14	-19.70	-155.50	Silty, some turbidity	217.1	Yes

Table 3.2. Isotope composition of input water, percent river input, percent precipitation input, precipitation type and source of floodwaters for 30 lakes in the Peace-Athabasca Delta that flooded in spring of 2018.

Lake ID	$\delta^{18}O_I$ (‰ VSMOW)	$\delta^{2}H_I$ (‰ VSMOW)	% river input	% precipitation input
Peace sector				
Rain-Peace River water				
PAD 8	-19.05	-147.53	70	30
PAD 14	-19.58	-151.14	78	22
PAD 50	-18.87	-146.25	68	32
PAD 58	-20.30	-156.69	88	12
M18	-20.87	-160.90	97	3
Snow-Peace River water				
PAD 15	-21.20	-163.30	98	2
PAD 54	-21.24	-163.59	97	3
PAD 64	-21.55	-165.89	91	9
M17	-21.38	-164.58	95	5
Athabasca sector				
Rain-Athabasca River water				
PAD 27	-18.62	-146.97	92	8
PAD 38	-18.87	-148.95	98	2
Snow-Athabasca River water				
PAD 19	-19.93	-156.47	87	13
PAD 20	-20.01	-157.08	85	15
PAD 21	-20.03	-157.21	85	15
PAD 22	-19.36	-152.51	95	5
PAD 23	-20.07	-157.46	85	15
PAD 24	-19.78	-155.44	89	11
PAD 25	-19.77	-155.34	89	11
PAD 26	-20.18	-158.25	83	17
PAD 30	-20.09	-157.63	87	13
PAD 31	-20.12	-157.79	85	15
PAD 32	-20.01	-157.04	85	15
PAD 33	-20.20	-158.35	83	17
PAD 36	-20.24	-158.66	82	18
PAD 39	-19.78	-155.43	89	11
PAD 40	-19.92	-156.42	87	13
PAD 45B	-19.40	-152.77	94	6
PAD 46	-19.63	-154.37	91	9
M12	-19.91	-156.34	87	13
M14	-19.92	-156.44	86	14

Chapter 4. Multi-year isoscapes of lake water balances across a dynamic northern freshwater delta

Citation: Remmer CR, Neary, LK, Kay, ML, Wolfe, B, Hall, RI. 2020. Multi-year isoscapes of lake water balances across a dynamic northern freshwater delta. *Environmental Research Letters* 15: 104066. DOI:10.1088/1748-9326/abb267

4.1. Introduction

Security of water supply is essential to sustain vitality of ecosystems, abundance of traditional food sources and responsible development of natural resources. Yet, inland freshwater ecosystems are amongst the most threatened, due to their vulnerability to climate change and human development (e.g., Hassan *et al* 2005, Dudgeon *et al* 2006, Woodward *et al* 2010). In northwestern North America, rapid warming continues to alter seasonal distribution of snow and rain, shorten duration of seasonal ice-cover, and increase rates of evaporation and permafrost thaw (Schindler and Smol 2006). Shrinking snowpack and glacier volumes at mountainous headwater regions have reduced river flows at a time when population growth and industrial development have increased demand for water (Schindler and Donahue 2006, Wolfe *et al* 2008a, Sauchyn *et al* 2015). Altered river flows and sediment regimes are affecting the structure, function and water quality of rivers and floodplains, including key waterways used for hydropower, natural resource extraction, water supply, and transportation (Prowse *et al* 2006, Schindler and Donahue 2006). Drying up of lakes, conversion of wetlands to shrublands, reduced navigability of water routes, and deterioration of wildlife habitat are among the many changes that natural resource agencies and stakeholders are increasingly challenged to mitigate and adapt to (Schindler and Smol 2006, Carroll *et al* 2011, Chavez-Ramirez and Wehtje 2011, Smith *et al* 2015, Huot *et al* 2019).

Despite the above outcomes, it remains challenging to identify the relative importance of multiple potential anthropogenic stressors and natural processes on freshwater resources, because

they typically operate over broad spatial and temporal scales that are inadequately captured by existing monitoring records (Wilkinson *et al* 2020). Yet, accurate identification of the cause(s) of change is required to develop effective policies and actions aimed at protecting water-rich northern landscapes. Thus, government agencies, Indigenous communities, and multi-stakeholder boards urgently require innovative collection and analysis of environmental data, integrated over a broad range of spatial and temporal scales, to inform decisions aimed at ensuring water-rich landscapes remain abundant, clean and productive for future generations.

This is the context for stewardship challenges at the Peace-Athabasca Delta (PAD) in northern Alberta, Canada, where declining lake levels have been a focal concern for decades (e.g., PADPG 1973, MCFN 2014). A large body of literature on potential causes has variably attributed lake-level drawdown to climate change, upstream regulation of Peace River flows since construction of the WAC Bennett Dam in 1968, consumptive water use by upstream oil sands development on the Athabasca River, and natural deltaic processes (e.g., Prowse and Conly 2002, Schindler and Donahue 2006, Wolfe *et al* 2012, 2020, Beltaos 2014, 2018, Kay *et al* 2019). Regardless of cause, reduction in freshwater abundance has had consequences for wildlife (Straka *et al* 2018, Ward *et al* 2018, 2019) and access to traditional territory (MCFN 2014, Vaninni and Vaninni 2019). The PAD is a large (6000 km^2), remote, lake-rich floodplain landscape recognized as a Ramsar Wetland of International Importance and contributed to the listing of Wood Buffalo National Park (WBNP) as a UNESCO World Heritage Site. Given the critical role of water in this landscape, improved characterization of hydrological processes and their influence on lakes is essential to inform ecosystem stewardship decisions and is recognized as a priority recommendation and action by federal and international agencies (WHC/IUCN 2017, WBNP 2019). However, the complexity of the PAD and its numerous lakes, whose water balances are varyingly controlled by river

floodwater, snowmelt, rainfall and evaporation over a range of temporal and spatial scales (Prowse and Conly 2002, Wolfe *et al* 2007), present significant challenges to design effective hydrological monitoring approaches.

Prior water isotope tracer studies in the PAD have demonstrated their value for capturing snapshots of water balance for a season or year (Wolfe *et al* 2007, 2008b, Wiklund *et al* 2012, Remmer *et al* 2018) and the extent and magnitude of ice-jam floods (Remmer *et al* 2020), but the range and variability of contemporary lake hydrological conditions during recent time and over the ~6000 km^2 expanse of the delta has not been adequately characterized. Here we use meteorological data, river water level records and water isotope compositions measured at ~60 lakes and 9 river sites during spring, summer and fall of a 5-year period (2015-2019) to assess the influence of hydrological processes on landscape-scale spatial variation of lake water balances over seasonal to multi-annual time scales. This is needed to evaluate their sensitivity and applicability as a lake hydrological monitoring approach for the delta and to serve as a foundation for water quality and contaminant assessment (Wolfe *et al* 2012). The need for these approaches was identified in a Federal Action Plan, which recommended the development and implementation of an aquatic ecosystem monitoring program for the PAD capable of tracking changes in water supply, water levels and water quality, and the processes driving changes (Wood Buffalo National Park 2019). Integration of an isotope-mass balance model and geospatial analysis allowed development of 'isoscapes' (*sensu* Bowen and Revenaugh 2003) for effective visualization of areas where lakes are most influenced by evaporative water loss and replenishment by river floodwaters and, respectively, identification of portions of the delta vulnerable and resilient to factors driving lake-level drawdown.

4.2 Methods

4.2.1 Study area

Lakes of the PAD are situated mainly within two distinct sectors, which differ in the relative roles of hydrological processes that influence lake water balances (Figure 4.1; Wolfe *et al* 2007). The northern Peace sector is a relic delta where lake water balance is strongly influenced by precipitation and evaporation, except during infrequent, widespread flooding caused by ice-jam events on the Peace River. The southern Athabasca sector, fed continuously by the Athabasca River, contains more active deltaic environments. Here, lake water balance spans a broader gradient of influence from river floodwaters during both spring ice-jam and summer open-water seasons, while lake water balance in slightly more elevated areas is dominated by precipitation and evaporation. Three large lakes (Claire, Mamawi, Richardson) occupy central and southern locations of the PAD and receive continuous river through-flow. The ice-free season typically starts in May and extends until at least late September, whereas lakes are ice covered from October through April.

4.2.2 Water isotope composition and designation of flood status

Surface water samples were collected from 57-60 lakes and 9 river sites spanning the two main sectors of the PAD three times per year during the ice-free seasons of five consecutive years, 2015-2019 (Figure 4.1; Appendix 2). To capture and compare the effects of hydrological processes (i.e., snowmelt, rainfall, spring ice-jam flooding, open-water flooding and evaporation), samples were consistently collected during two to three-week intervals in the spring (May), summer (July) and fall (September) of each year. An exception occurred in 2016 when the Fort McMurray regional wildfire delayed our spring sample collection by three weeks (June). Well-mixed water samples were collected mid-lake (or mid-channel) from a depth of ~10 cm and stored in sealed 30 ml high-

density polyethylene bottles. Lake and river water isotope compositions were measured by Off-Axis Integrated Cavity Output Spectroscopy (O-AICOS) at the University of Waterloo – Environmental Isotope Laboratory (UW-EIL). Isotope compositions are expressed as δ-values, representing deviations in per mil (‰) from Vienna Standard Mean Ocean Water (VSMOW) such that δ-sample = $[(R_{sample}/R_{VSMOW}) - 1] \times 10^3$, where R is the $^{18}O/^{16}O$ or $^{2}H/^{1}H$ ratio in the sample and VSMOW. Results of $\delta^{18}O$ and $\delta^{2}H$ analyses are normalized to -55.5‰ and -428‰, respectively, for Standard Light Antarctic Precipitation (Coplen 1996). Analytical uncertainties are ±0.2‰ for $\delta^{18}O$ and ±0.8‰ for $\delta^{2}H$. In-situ measurements of specific conductivity were obtained using a YSI ProDSS sonde.

Lakes that received river floodwaters during the spring (assumed to result from ice-jams, as in 2018; Remmer *et al* 2020) and open-water season were identified using mainly lake and river water isotope compositions, supported by measurements of specific conductivity and field observations. Following Remmer *et al* (2020), lakes were designated as flooded if 1) lake water isotope values were close to or overlapping with water isotope compositions of flowing rivers, 2) lake specific conductivity values were close to the range of the river water values, and/or 3) there was visible evidence of flooding, such as water colour and turbidity (assessed in situ) similar to the closest river or channel, and flooded lake margins and debris (i.e., logs) that appeared to have been carried in by the recent floodwaters (Supplementary Information 1, Tables S1.2-S1.5).

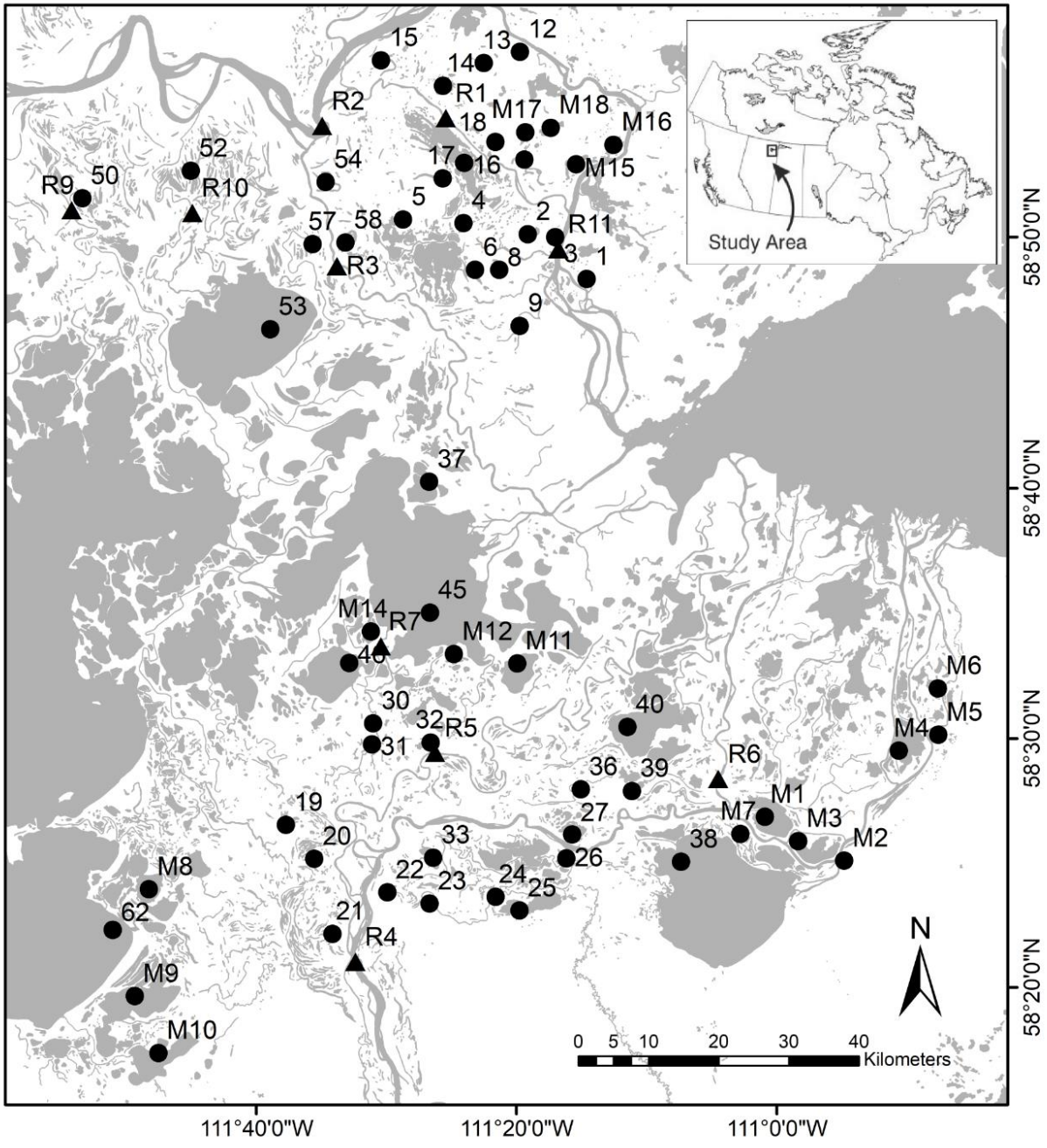

Figure 4.1. Map of the Peace-Athabasca Delta showing locations of the lake (circles) and river (triangles) sampling sites and other landmarks mentioned in the text. EB refers to the Embarras Breakthrough.

4.2.3 Water balance derivation and analysis

Evaporation-to-inflow (E/I) ratios, an informative water-balance metric, were calculated from lake water isotope compositions using a coupled-isotope tracer method (Yi *et al* 2008) and an isotope framework representing average meteorological conditions during 2015-2019 (Supplementary Information 2). This approach to isotope-mass balance modelling systematically accounts for varying input water isotope compositions in the calculation of E/I ratios, which are evident in the scatter of lake water isotope compositions about the predicted Local Evaporation Line (LEL; see Figure 4.3 below). Consistent with other studies (MacDonald *et al* 2017, Remmer *et al* 2018), we set E/I ratios to 1.5 for lakes experiencing strong non-steady-state conditions. Temporal trends of E/I ratios were visualized as generalized additive models (GAMs) for each sector and year using RStudio v1.2.5001 (Rstudio Team 2019), and the ggplot2 v.3.2.1 (Wickham 2016) and mgcv v.1.8.28 (Wood 2017) packages. Spatial interpolations of E/I ratios were presented as 'isoscapes' for all 15 sampling campaigns by ordinary kriging using ArcMap 10.7.1 software because Moran's I was significant ($p < 0.05$; Appendix 2). The extent of river floodwaters across the landscape and areas of lakes with $E/I > 1.0$ (signifying net evaporative drawdown) were delineated on the isoscapes by inverse distance weighting using ArcMap 10.7.1 software.

4.3 Results

4. 3.1 Meteorological conditions and river water levels

Monthly mean air temperature varied seasonally, but did not differ substantially among years or from the 1981-2010 climate normal, except 2016 which was cooler in the spring and warmer in summer through fall (Figure 4.2a). Seasonal and annual precipitation, however, did vary notably among years and relative to the climate normal. Snowfall (precipitation during November to March) was below normal during all five years. Rainfall (precipitation during May to September)

was below normal in the spring (April, May) and early to mid-summer (June, July) of each year, except for July 2015 and June 2018. Late summer and early fall (August, September) rainfall was below normal in 2015 and 2018, and above normal in 2016 and 2019. An unusually large rainfall event occurred on August 16th, 2019, which contributed 44.31 mm of the total monthly precipitation.

Peace and Athabasca river water levels varied seasonally and between years (Figure 4.2b). For both rivers, water levels were typically higher during the spring melt and lower in summer and fall, but there are exceptions. For example, Athabasca River water levels in summer 2019 exceeded those of spring. Marked increases of water level of the Peace River occurred in June and September 2016, August 2018 and July 2019. For the Athabasca River, substantial peak water levels occurred in late April and early May 2018. Summers of 2018 and 2019 were characterized by markedly higher water levels on the Athabasca River than the other years. In contrast, low water levels and low variability for the Athabasca River occurred in 2015 and spring of 2019.

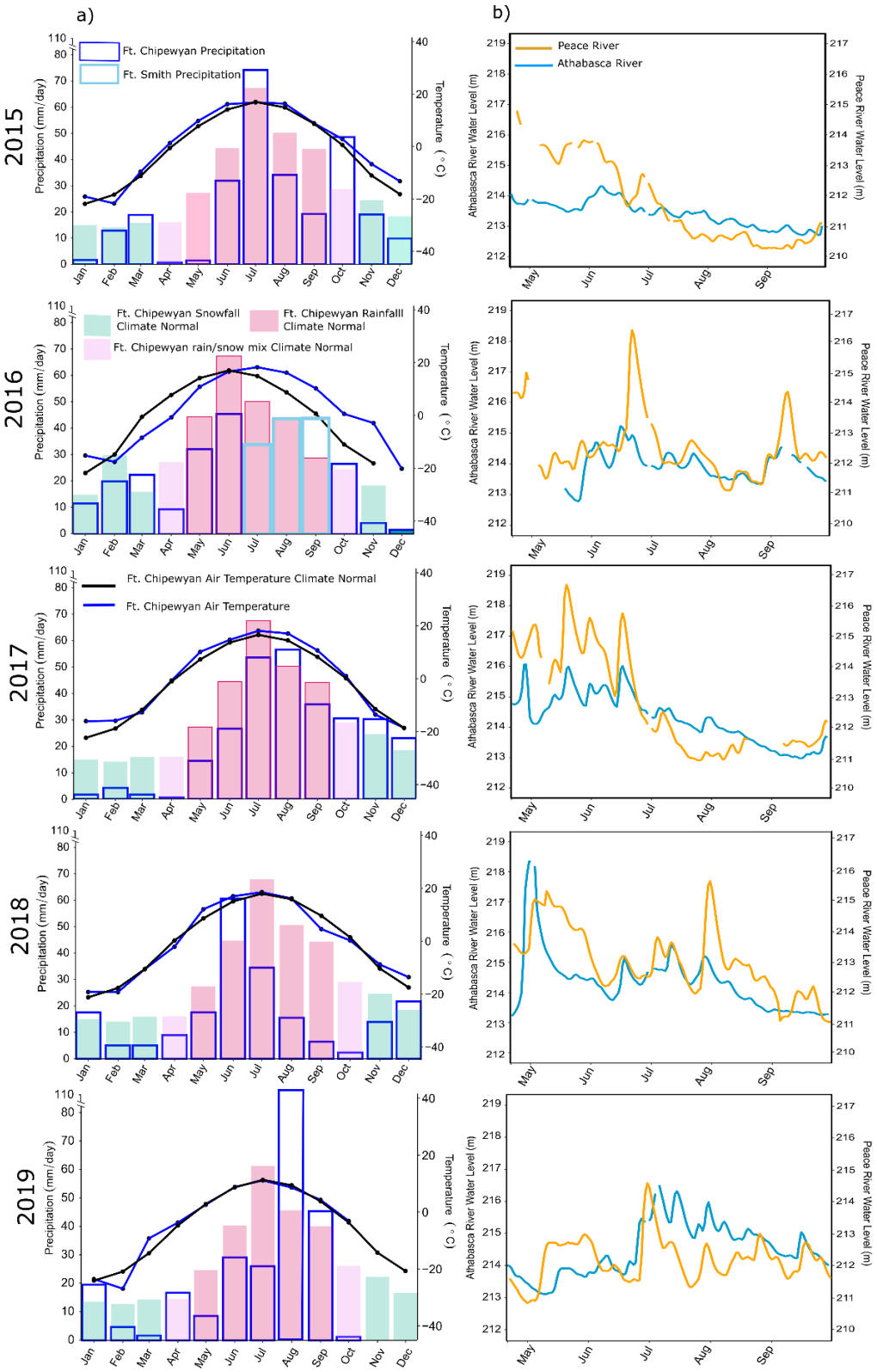

Figure 4.2. (a) Monthly precipitation and monthly mean air temperature for Fort Chipewyan, Alberta (and Fort Smith, NWT—see 2016 precipitation) during 2015–2019 and 30 year (1981–2010) climate normals (https://climate.weather.gc.ca/climate_normals/). (b) River water levels for the Peace River at Peace Point (~80 km upstream of the PAD) and Athabasca River at Embarras Airport (~20 km upstream of the PAD) stations for April 20 to September 30, 2015–2019 (https://wateroffice.ec.gc.ca/ and https://rivers.alberta.ca/). Note that there are gaps in the water-level records.

4.3.2 Lake and river water isotope compositions

River water isotope compositions fall close to the Local Meteoric Water Line (LMWL) as the rivers convey considerable glacier- and snow-melt, which undergo minimal subsequent evaporation (Figure 4.3). In contrast, lake water isotope compositions span the spectrum of the LEL, reflecting a gradient of isotopically-depleted lakes strongly influenced by river floodwaters to isotopically-enriched lakes strongly influenced by evaporation. Varying numbers of lakes that received river floodwaters during spring ice-jam flooding were identified in 2017, 2018 and 2019 (Figure 4.3). The largest spring ice-jam flood event was in May 2018 (27 lakes flooded), with smaller extent of flooding occurring in 2017 (11 lakes) and 2019 (9 lakes). Open-water flooding occurred during summers of 2017-2019 (5, 7 and 13 lakes flooded, respectively), and in fall of 2018 (8 lakes) and 2019 (14 lakes).

We note that the Claire River (R9; Figure 4.3) plots along the LEL and separate from the other rivers during most sampling periods. This site is a relic river channel in the Peace sector that has become disconnected from the Peace River and undergoes evaporative enrichment similar to a disconnected lake. Exception to this was in the spring and fall of 2018 when this site is isotopically depleted and plots close to the flowing river sites as a result of re-connection with the Peace River during high water events. Thus, the Claire River acts as a useful indicator for flooding along the Peace River and its distributary channels.

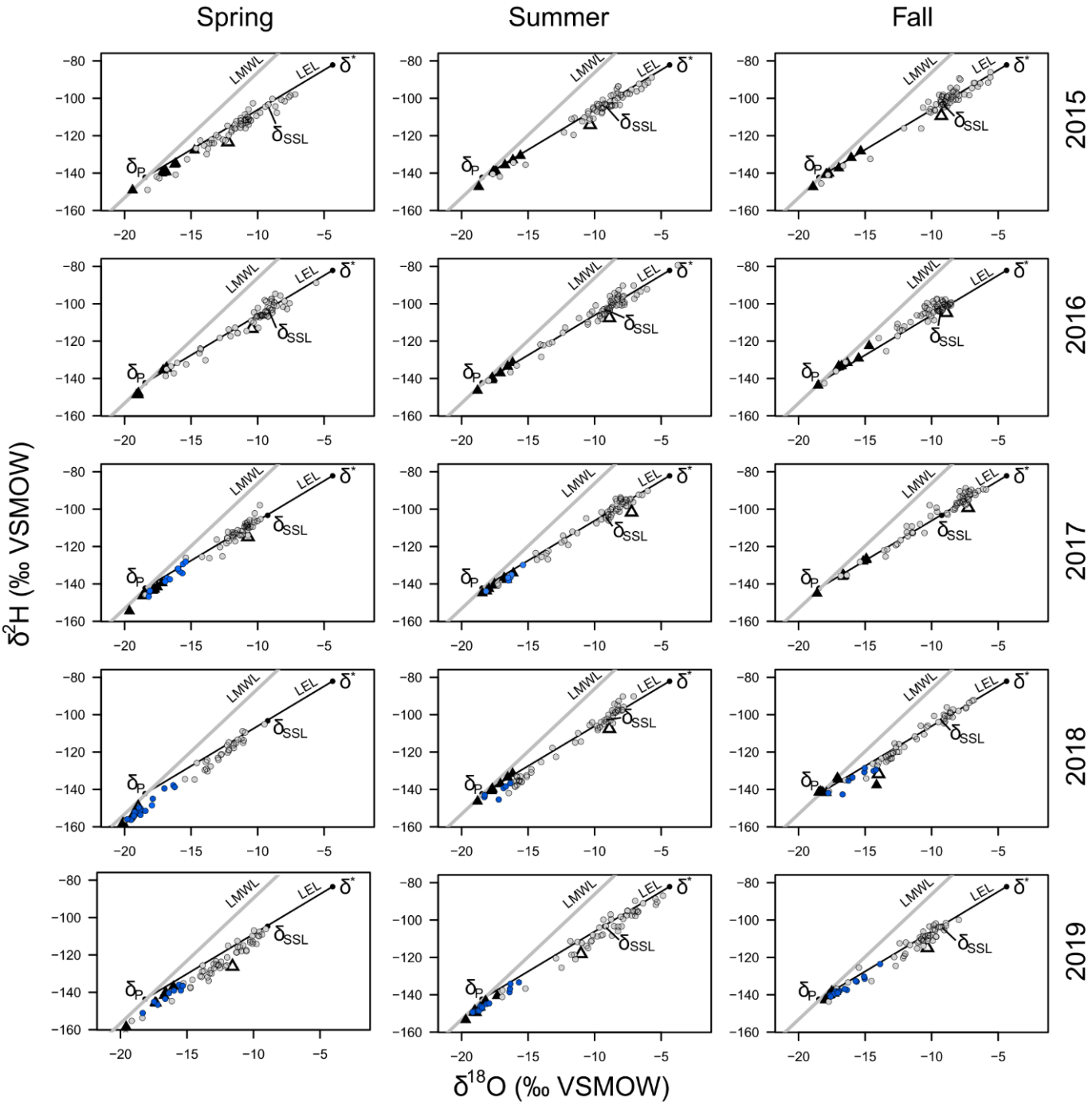

Figure 4.3. Water isotope compositions for 57–60 lake (circles) and 9 river (triangles) sites during the spring, summer and fall of 2015–2019 displayed on $\delta^{18}O$–$\delta^{2}H$ graphs. Solid blue circles are lakes that received river floodwaters while grey circles are lakes that did not receive river floodwaters prior to sampling. Open triangle is the Claire River (R9), which serves to identify flooding along the Peace River and its distributary channels. LMWL refers to the Local Meteoric Water Line ($\delta^{2}H = 6.7\ \delta^{18}O–19.2$; Wolfe *et al* 2007) and the LEL is the predicted LEL ($\delta^{2}H = 4.3\ \delta^{18}O–63.5$) constrained by the mean annual isotope composition of precipitation (δ_P), the terminal basin steady-state isotope composition (δ_{SSL}) and the limiting non-steady-state isotope composition of a water body approaching complete desiccation (δ*; see supplementary information 2).

4.3.3 Trends in lake evaporation-to-inflow ratios

E/I ratios for the lakes vary substantially across the sampling periods and sectors, ranging from near 0 to greater than 1.0 (i.e., net evaporative drawdown; Figure 4.4a). GAM-defined trendlines in E/I ratios display patterns reflecting broad similarities and differences in hydrological processes influencing lake water balance in the Peace and Athabasca sectors of the delta. During each year, trendlines indicate higher E/I ratios (i.e., more intense evaporation) in lakes of the Peace sector than the Athabasca sector, consistent with the relic deltaic environment of the former. For three of the five years (2015, 2016, 2019), Peace and Athabasca E/I trendlines are similar, but offset, rising from spring to summer then declining in the fall. The increase in E/I ratios from spring to summer is generally steeper in the Peace sector than the Athabasca sector and can be attributed to strong influence of evaporation and absence of open-water flooding in the Peace sector. We note that the E/I trendline exceeds 1.0 in the Peace sector during all years signifying net evaporative water loss (except 2018), whereas the E/I trendline remains well below 1.0 for lakes in the Athabasca sector. Parallel declines in the trendline from the summer to fall during 2016 and 2019 in both sectors are due to rainfall, with additional contributions from open-water flooding in the Athabasca sector in 2019 (also see below and Figure 4.4b).

Distinct differences in seasonal E/I trendlines for lakes in the Peace and Athabasca sectors occur during 2017 and 2018. In 2017, the E/I trendline rises rapidly in the Peace sector during the open-water season to values >1.0 and remains high in the fall. In the Athabasca sector, the trendline rises less rapidly between spring and summer and continues to rise steadily in the fall. In 2018, E/I trendlines are also not parallel. E/I ratios rise in lakes of the Peace sector for the entire open-water season, whereas the E/I trendline for the Athabasca sector lakes shows a small initial rise and then a decline from summer to fall. Differences in the spring-to-summer E/I trendlines during these two

years are due to spring ice-jam flooding in the Athabasca sector, which was extensive in 2018 (Remmer *et al* 2020). High E/I ratios in the Athabasca sector during summer and fall of 2017 reflect the evaporative response of lakes during a year without open-water flooding (also see below and Figure 4.4b). This is in contrast to 2018 and 2019, when E/I ratios decline in lakes of the Athabasca sector during the fall due to open-water flooding (also see below and Figure 4.4b).

4. 3.4 Isoscapes of lake evaporation-to-inflow ratios

Additional insight into spatial variation and influence of key hydrological processes on lake water balance, including evaporation and river flooding, can be gleaned from E/I isoscapes for the 15 sampling periods (Figure 4.4b). Regions where E/I ratios exceed 1.0 are noteworthy as they indicate lake-level drawdown by net evaporation. These regions tend to include the central and northwestern Peace sector and the southwestern Athabasca sector (summer and fall 2015, 2017, 2019, spring and summer 2016). Although the meteorological data captured in Fort Chipewyan does not indicate particularly low rainfall in 2016, high E/I ratios in the northwestern portion of the Peace sector in 2016 are consistent with locally arid conditions that promoted wildfires in this area in June through July. Massive wildfires also occurred at the upstream town of Fort McMurray during this period, indicating regionally dry conditions. During the subsequent summer and fall of 2017, high E/I ratios across much of the Peace sector and the southwestern Athabasca sector align with field observations of lake desiccation (also see Remmer *et al* 2020).

Also delineated on Figure 4.4b is river floodwater extent, an important source of water to lakes which offsets water loss by evaporation and produces low E/I ratios. We identified influence of river floodwaters on lakes during 8 of 15 sampling campaigns (53%) including ice-jam flooding during springs of 2017-2019, and open-water flooding during summers of 2017-2019, which remained detectable during falls of the latter two years. Ice-jam flooding in 2017 and 2019 was

limited to lakes in the central Athabasca sector and along the Athabasca River. In contrast, ice-jam flooding in 2018 was widespread and encompassed most of the Athabasca sector and a few lakes in the north-central Peace sector (Remmer *et al* 2020). Open-water flooding also varied in extent, but was generally restricted to the central Athabasca sector and some lakes farther east near the Athabasca River's terminus. Also, continuous river through-flow at Mamawi Lake is identified as persistent low E/I in a localized central region of the PAD.

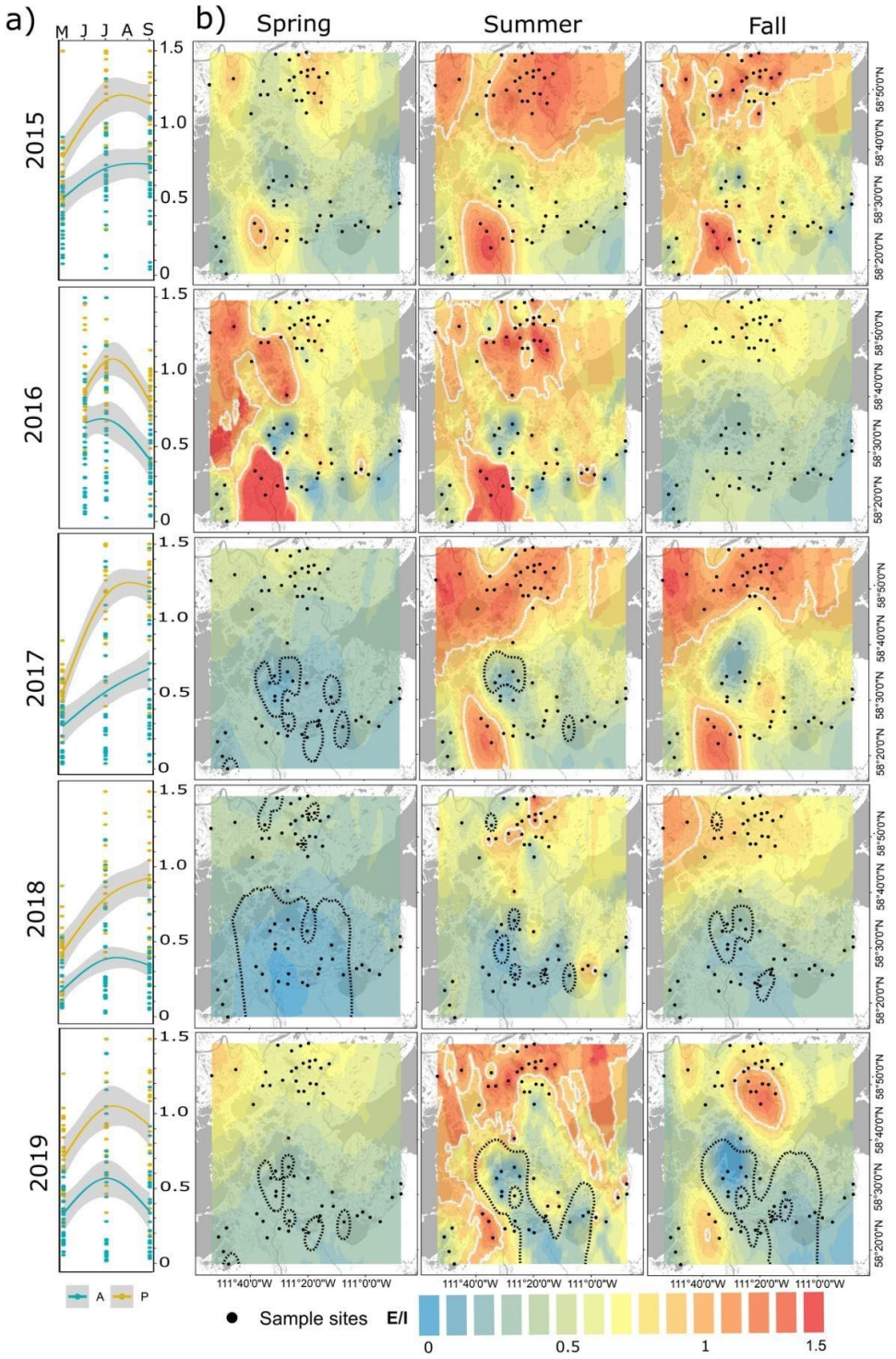

Figure 4.4. (a) Generalized additive models (GAMs) capturing seasonal trends (as lines) in the evaporation-to-inflow (E/I) ratios of lakes (circles) in the Peace (yellow) and Athabasca (blue) sectors of the Peace-Athabasca Delta. Shaded areas represent the 95% confidence interval of the trendline. The data are binned by month of sample collection. (b) 'Isoscapes' displaying spatial interpolation of lake evaporation-to-inflow (E/I) ratios across the Peace-Athabasca Delta during spring, summer and fall of the five-year period 2015–2019. Black dashed lines represent flood extent while white dashed lines represent areas with E/I > 1.0 (i.e. net evaporative drawdown). Warmer colours represent higher E/I ratios and colder colours represent lower E/I ratios, ranging from zero to ⩾1.5, as indicated in the scale. Data are contoured at 0.1 intervals encompassing reasonable levels of uncertainty in model output. Individual lake sites are indicated as black circles.

4.4 Discussion

Analysis of >1000 samples for water isotope composition collected during 15 sampling campaigns over 5 years (2015-2019) in the Peace-Athabasca Delta provides exceptional insight into hydrological processes influencing lake water balances across this dynamic, remote floodplain landscape. Quantification of evaporation-to-inflow (E/I) ratios, summarized using generalized additive models (GAMs) and depicted as isoscapes, provide an effective approach to delineate patterns of lake water balance over time and space and their underlying causes. Our study captured two years with no river flooding (2015, 2016), three years with river flooding (2017-2019), and marked responses of lake water balance to absence and occurrence of this key hydrological process. The data reveal distinctive hydrological differences between Peace and Athabasca sectors of the delta and that substantial seasonal and multi-annual oscillation in lake water balance are an inherent feature of this complex northern freshwater landscape, scales of variability necessary to document and appreciate as a basis for informed conservation and management (Wilkinson *et al* 2020).

A key outcome is identification of spatial and temporal 'hotspots' of lake drying. Results show that evaporative water loss is greatest during summer and persists in the north-central and northwestern Peace and southwestern Athabasca portions of the PAD (Figure 4.4ab), consistent with recent observations and concerns of aquatic habitat deterioration (MCFN 2014, IEC 2018). Marked evaporative water loss during portions of 2015-2017 correspond to years of low water level on the Athabasca River (Figures 4.2b, 4.4b). Occasional high-water peaks on the Peace River during the open-water season had little effect on the lake water balances across the Peace sector, as expected (Prowse and Lalonde 1996). This highlights the vulnerability of lakes in the relic Peace sector and an elevated portion of the Athabasca sector to drawdown and desiccation, especially

with anticipated further declines in the frequency of ice-jam flooding, longer ice-free seasons leading to increased evaporation, and reduced snowmelt runoff (Schindler and Smol 2006, Wolfe *et al* 2008a). Indeed, all five years of our study were characterized by below normal snowfall, perhaps signifying a shift to reduction in supply of this source of water to lakes in the PAD, although influence of rainfall lowered E/I ratios during the fall of some years (2016, 2019). These findings align with a long-term trend of increasing evaporative influence on lakes in the Peace sector evident in sediment records (Wolfe *et al* 2008a, 2020, Remmer *et al* 2018) and identify regions of the delta where water security is most threatened.

A main source of lake water replenishment is river floodwaters, as revealed by low E/I ratios in lakes within flooded areas delineated in the isoscapes (Figure 4.4b). The approach used in this study identified a major ice-jam flood event (spring 2018), as well as more localized spring ice-jam flooding (2017, 2019) and open-water flooding (2017-2019). Both ice-jam and open-water flooding occurred almost exclusively in the Athabasca sector and preferentially along the Athabasca-Embarras-Mamawi river corridor owing to the Embarras Breakthrough (Figure 4.1), a natural river avulsion that occurred in 1982 and has had profound influence on hydrological trajectories of lakes across the Athabasca sector (Kay *et al* 2019). Evidence of flooding in the Athabasca sector during intervals of 2017-2019 correspond to high water recorded on the Athabasca River (Figures 4.2b, 4.4b). Documentation of frequent river floodwater inundation reveals that lakes along preferential flow pathways in the Athabasca sector are most resilient to factors that cause drawdown, substantiating earlier claims (Wolfe *et al* 2008b, Kay *et al* 2019). While spring ice-jam flooding is long known to be an important hydrological process for replenishing slightly more elevated (perched) lakes (Prowse and Lalonde 1996), open-water flooding in the Athabasca sector evidently is also a major contributor to maintaining lake water

balances in this part of the PAD, despite not being widely recognized (IEC 2018). Results further demonstrate that the two sectors of the delta largely function as distinctly different landscapes. The Peace River lies at lower elevation than the delta, thus it bypasses the Peace sector except during episodic ice-jam flood events. In contrast, the Athabasca River flows continuously into and through the Athabasca sector, branching into several distributaries which supply water to low-lying lakes during both the spring (ice-jam) and open-water seasons.

A novel outcome of our 5-year study is that the water balances of lakes in the PAD are markedly dynamic over time and space, as visualized by the isoscapes (Figure 4.4b). Influence of river floodwaters on lake water balances was detected in more than half (8 of 15) of our sampling campaigns demonstrating the value of systematic water isotope sampling and analysis to capture the effects of this important hydrological process, which may otherwise occur undocumented. Further demarcation of 1) portions of the Peace and Athabasca sectors most vulnerable to lake-level drawdown and 2) portions of the Athabasca sector most resilient to lake-level drawdown requires that effective hydrological monitoring programs and stewardship practices need to consider and incorporate these distinct features of the landscape (see also Wolfe *et al* 2012). Water isotope tracers provide a sensitive and efficient approach to address this need. Although regional and national lake water balance syntheses are increasingly using water isotope tracers (e.g., Brooks *et al* 2014, Gibson *et al* 2017, MacDonald *et al* 2017), we advocate that sustained and long-term sampling and analysis is required for highly dynamic freshwater landscapes such as deltas and floodplains to capture the range and variability of contemporary hydrological conditions and to detect potentially shifting relative influence of important drivers.

Opportunities exist to incorporate other methods and approaches to complement use of water isotope tracers, which provide a snapshot of lake water balance integrating the preceding days to

weeks but may not accurately capture hydrological processes occurring at shorter or longer frequencies. For example, water level loggers quantify lake water level rises and declines at short time-steps (Neary *et al* 2019), and likely would have detected the influence of the large rainfall event in August 2019 that was not well captured by the water isotope data collected a month later. Remote sensing has also been used to identify changes in surface water area in the PAD (Töyrä and Pietroniro 2005, Montgomery *et al* 2019), and water isotope tracers may help refine understanding of the hydrological processes responsible. Additional meteorological stations across the 6000 km^2 area of the PAD would likely reveal more localized weather patterns and improve the interpretation of water isotope records. Increased lake sampling density could improve spatial interpolations in sparsely sampled areas, such as the central portion of the delta. Nonetheless, patterns observed in water isotope metrics largely align with available records of hydrological processes, suggesting our approach provides knowledge at spatial and temporal scales relevant to conservation goals, and can serve for systematic and sustained long-term monitoring as needed to detect and document aquatic ecosystem change (Xenopoulos 2019).

4.5 Conclusions

Here, five consecutive years of systematic seasonal sampling of water isotope composition from ~60 lakes and 9 river sites across the remote, expansive Peace-Athabasca Delta identify the key roles of evaporation and river flooding on the water balance of its abundant, shallow lakes. An important feature is the marked seasonal to multi-annual and spatial variability of lake water balance and the hydrological processes driving the variation. Temporal and spatial patterns of isotope-based E/I ratios emerged and provide a basis to forecast change in this dynamic freshwater landscape, given that evaporation and floodwaters directly influence vulnerability and resilience of lakes to drawdown. We identify hotspots of strong evaporative influence in the north-central

and northwestern Peace and southwestern Athabasca portions of the PAD. We also discern the influence of river floodwaters during 8 of 15 sampling periods, and identify the flood-prone central Athabasca sector as an area of low E/I ratios where lakes are less vulnerable to evaporative water loss. We envision that our five-year isotope-based hydrological study provides the foundation of a comprehensive aquatic ecosystem monitoring program for lakes of the PAD, offers a pivotal and timely contribution to execution of the Canadian federal government's Action Plan for Wood Buffalo National Park, and demonstrates the value of the approach for other dynamic, difficult-to-access floodplain and lake-rich landscapes.

4.6 References

Beltaos S 2014 Comparing the impacts of regulation and climate on ice-jam flooding of the Peace-Athabasca Delta *Cold Reg. Sci. Technol.* **108** 49–58

Beltaos S 2018 Frequency of ice-jam flooding of Peace-Athabasca Delta *Can. J. Civ. Eng.* **45** 71–75

Bowen G J and Revenaugh J 2003 Interpolating the isotopic composition of modern meteoric precipitation *Water Resour. Res.* **39** 1299

Bowen G J 2016 The Online Isotopes in Precipitation Calculator version 2.2 Accessible at http://www.waterisotopes.org

Brooks J R, Gibson J J, Birks S J, Weber M H, Rodecap K D and Stoddard J L 2014 Stable isotope estimates of evaporation: inflow and water residence time for lakes across the United States as a tool for national lake water quality assessments *Limnol. Oceanogr.* **59** 2150–2165

Carroll M L, Townshend J R G, DiMiceli C M, Loboda T and Sohlberg R A 2011 Shrinking lakes of the Arctic: Spatial relationships and trajectory of change *Geophys. Res. Lett.* **38** L20406.

Chavez-Ramirez F and Wehtje W 2011 Potential impact of climate change scenarios on Whooping Crane life history *Wetlands* **32** 11–20

Coplen T B 1996 New guidelines for reporting stable hydrogen, carbon, and oxygen isotope-ratio data *Geochim. Cosmochim. Acta* **60** 3359–3360

Craig H and Gordon L I 1965 Deuterium and oxygen 18 variations in the ocean and the marine atmosphere *Stable Isotopes in Oceanographic Studies and Paleotemperatures* ed E Tongiorgi (Pisa, Italy: Laboratorio di Geologia Nucleare) p 9–130

Dudgeon D, *et al.* 2006 Freshwater Biodiversity: Importance, Threats, Status and Conservation Challenges. *Biol. Rev. Camb. Philos. Soc.* **81** 163-82

Edwards T W D, Wolfe B B, Gibson J J and Hammarlund D 2004 Use of water isotope tracers in high latitude hydrology and paleolimnology *Long-Term Environmental Change in Arctic and Antarctic Lakes* ed R Pienitz et al (Dordrecht, Netherlands: Springer) p 187–207

Gibson J J and Edwards T W D 2002 Regional water balance trends and evaporation-transpiration partitioning from a stable isotope survey of lakes in northern Canada *Global Biogeochem. Cy.* **16** 1–9

Gibson J J, Edwards T W D and Prowse T D 1999 Pan-derived isotopic composition of atmospheric water vapour and its variability in northern Canada *J. Hydrol.* **217** 55–74

Gibson J J, Birks S J, Jeffries D and Yi Y 2017 Regional trends in evaporation loss and water yield based on stable isotope mass balance of lakes: The Ontario Precambrian Shield surveys *J. Hydrol.* **544** 500–510

Gonfiantini R 1986 Environmental isotopes in lake studies *Handbook of Environmental Isotope Geochemistry* vol 2 ed P Fritz et al (New York: Elsevier) p 113–168.

Hassan R, Scholes R and Ash N 2005 *Millenium Ecosystem Assessment. Ecosystems and Human Well-being: Current State and Trends*, vol. 1. (Washington, DC: Island Press)

Horita J and Wesolowski D 1994 Liquid-vapour fractionation of oxygen and hydrogen isotopes of water from the freezing to the critical temperature *Geochim. Cosmochim. Acta* **58** 3425–3497

Huot Y, *et al.* 2019 The NSERC Canadian Lake Pulse Network: A national assessment of lake health providing science for water management in a changing climate *Sci. Tot. Environ.* **695** 133668

IAEA/WMO 2015 Global Network of Isotopes in Precipitation *The GNIP Database* Accessible at: https://nucleus.iaea.org/wiser

Independent Environment Consultants (IEC) 2018 *Strategic environmental assessment of Wood Buffalo National Park World Heritage Site* Vol 1 Milestone 3 – Final SEA Report (Markham, Ontario: Independent Environment Consultants)

Kay M L, *et al.* 2019 Bi-directional hydrological changes in perched basins of the Athabasca Delta (Canada) in recent decades caused by natural processes *Environ. Res. Commun.* **1** 081001

MacDonald L A, *et al.* 2017 A synthesis of thermokarst lake water balance in high-latitude regions of North America from isotope tracers *Arctic Sci.* **3** 118-149

Mikisew Cree First Nation (MCFN) 2014 Petition to The World Heritage Committee Requesting Inclusion of Wood Buffalo National Park on the List of World Heritage in Danger

Montgomery J, Brisco B, Chasmer L, Devito K, Cobbaert D and Hopkinson C 2019 SAR and Lidar temporal data fusion approaches to Boreal wetland ecosystem monitoring. *Remote Sens.* **11** 161 doi:10.3390/rs11020161

Neary L, Remmer C, Owca T, Krist J, Wolfe B B and Hall R I 2019 Use of continuous lake level measurements for hydrological monitoring of a complex northern freshwater landscape. ArcticNet Annual Scientific Meeting, Halifax.

PADPG 1973 Peace-Athabasca Delta Project technical report and appendices *Vol 1 Hydrological Investigations and Vol 2 Ecological investigations* (Peace-Athabasca Delta Project Group, Delta Implementation Committee, Governments of Alberta, Saskatchewan and Canada)

Pietroniro A, Prowse T D and Peters D L 1999 Hydrologic assessment of an inland freshwater delta using multi-temporal satellite remote sensing *Hydrol. Process.* **13** 2483–2498

Prowse T D and Lalonde V 1996 Open-water and ice-jam flooding of a northern delta *J. Hydrol.* **27** 85–100

Prowse T D and Conly F M 2002 A review of hydroecological results of the Northern River Basins Study, Canada Part 2 Peace-Athabasca Delta *River Res. Appl.* **18** 447–460

Prowse T D, Beltaos S, Gardner J T, Gibson J J, Granger R J and Leconte R 2006 Climate change, flow regulation and land-use effects on the hydrology of the Peace-Athabasca-Slave system: findings from the Northern Rivers Ecosystem Initiative *Environ. Monit. Assess.* **113** 167–197

R Core Team 2019 R: A language and environment for statistical computing R

Remmer C R**,** Owca T, Neary L, Wiklund J A, Kay M, Wolfe B B and Hall R I 2020 Delineating extent and magnitude of river flooding to lakes across a northern delta using water isotope tracers *Hydrol. Process.* **34** 303-320

Remmer C R, Klemt W H Wolfe B B and Hall R I 2018 Inconsequential effects of flooding in 2014 on lakes in the Peace-Athabasca Delta *Limnol. Oceanogr.* **63** 1502–1518

Sauchyn D J, St-Jacques J and Luckman B H 2015 Long-term reliability of the Athabasca River (Alberta, Canada) as the water source for oil sands mining. *Proc. Natl. Acad. Sci. U S A* **112** 12621-12626

Schindler D W and Smol J P 2006 Cumulative effects of climate warming and other human activities on freshwaters of arctic and subarctic North America *Ambio* **35** 160–168

Schindler D W and Donahue W F 2006 An impending water crisis in Canada's western prairie provinces *Proc. Natl. Acad. Sci. U S A* **103** 7210–7216

Smith L C, Sheng Y, MacDonald G M and Hinzman L D 2005 Disappearing Arctic lakes *Science* **308** 1429

Smol J P, *et al.* 2005 Climate-driven regime shifts in the biological communities of Arctic lakes. *Proc. Natl. Acad. Sci. U S A* **102** 4397–4402.

Straka J, *et al.* 2018 "We Used to Say Rats Fell from the Sky After a Flood:" Temporary Recovery of Muskrat Following Ice Jams in the Peace-Athabasca Delta *Arctic* **71** 218–228

Thornthwaite C W 1948 An approach toward a rational classification of climate *Geogr. Rev.* **38** 55–94

Töyrä J, and Pietroniro A 2005 Towards operational monitoring of a northern wetland using geomatics-based techniques *Remote Sens. Environ.* **97** 174-191

Vannini P and Vannini A 2019 The exhaustion of Wood Buffalo National Park: Mikisew Cree First Nation experiences and perspectives *Interl. Rev. Qual. Res.* **12** 278–303

Ward E M and Gorelick S M 2018 Drying drives decline in muskrat population in the Peace-Athabasca Delta, Canada *Environ. Res. Lett.* **13** 124026

Ward E M, Wysong K and Gorelick S M 2020 Drying landscape and interannual herbivory-driven habitat degradation control semiaquatic mammal population dynamics *Ecohydrology* **13** e2169

WHC/IUCN 2017 Reactive monitoring mission to Wood Buffalo National Park, Canada; mission report, March 2017 *United Nations Educational, Scientific and Cultural Organization* Accessible at http://whc.unesco.org/en/documents/156893

Wickham H 2016 *ggplot2: Elegant Graphics for Data Analysis* (New York: Springer-Verlag)

Wiklund J A, Hall R I and Wolfe B B 2012 Timescales of hydrolimnological change in floodplain lakes of the Peace-Athabasca Delta, northern Alberta, Canada *Ecohydrology* **5** 351–367

Wilkinson G M, Walter J, Fleck R, Pace M L 2020 Beyond the trends: The need to understand multiannual dynamics in aquatic ecosystems *Limnol. Oceanogr. Lett.* (in press) https://doi.org/10.1002/lol2.10153

Wolfe B B, *et al.* 2008a Climate-driven shifts in quantity and seasonality of river discharge over the past 1000 years from the hydrographic apex of North America *Geophys. Res. Lett.* **35** L24402

Wolfe B B, *et al.* 2008b Hydroecological responses of the Athabasca Delta, Canada, to changes in river flow and climate during the 20th century *Ecohydrology* **1** 131–148

Wolfe B B, Hall R I, Edwards T W D and Johnston J W 2012 Developing temporal hydroecological perspectives to inform stewardship of a northern floodplain landscape subject to multiple stressors: Paleolimnological investigations of the Peace-Athabasca Delta *Environ. Rev.* **20** 191–210

Wolfe B B, Hall R I, Wiklund J A and Kay M L 2020 Past variation in Lower Peace River ice-jam flood frequency *Environ. Rev.* (in press) https://doi.org/10.1139/er-2019-0047

Wolfe B B, Karst-Riddoch T L, Hall R I, Edwards T W D, English M C, Palmini R and Vardy S R 2007 Classification of hydrologic regimes of northern floodplain basins (Peace-Athabasca Delta, Canada) from analysis of stable isotopes ($\delta^{18}O$, $\delta^{2}H$) and water chemistry *Hydrol. Process.* **21** 151–168

Wood S N 2017 *Generalized Additive Models: An Introduction with R 2nd edition* (Chapman and Hall/CRC)

Wood Buffalo National Park (WBNP) 2019 *World Heritage Site Action Plan* Parks Canada https://www.pc.gc.ca/en/pn-np/nt/woodbuffalo/info/action

Woodward G, Perkins D and Brown L 2010 Climate change and freshwater ecosystems: Impacts across multiple levels of organization. *Philos. Trans.: Biol. Sci.* **365** 2093-2106

Xenopoulos M A 2019 Editorial: Long-term studies in limnology and oceanography *Limnol. Oceanogr.* **64** S1

Yi Y, Brock B E, Falcone M D, Wolfe B B and Edwards T W D 2008 A coupled isotope tracer method to characterize input water to lakes *J. Hydrol.* **350** 1–13

Chapter 5. Synthesis and Recommendations

5.1 Synthesis

5.1.1. Thesis Overview

The generation of this thesis would not have been possible without an abundance of time spent in the field. Over the course of 5 years, I conducted fieldwork in Fort Chipewyan and the PAD on 17 occasions. During each trip, I was able to observe most or all of the 60-80 lakes and river sites we systematically sampled. This was a unique opportunity, and my time spent flying over the landscape and on the lakes afforded an understanding of their features and characteristics that few others have had the chance to amass. Because of the familiarity I developed with these ecosystems, I was able to identify and pinpoint change where it was not always obvious to fresh eyes. Much literature is written about the PAD, especially as it periodically captures international attention during new cycles around the many controversies and perceived threats. While not without exceptions, it is not unusual for research about the hydrology of the PAD and its river systems to be written by researchers who have had only very limited opportunity to visit the landscape, as expected given the expense and difficulty in reaching this remote place. Having been in the enviable position to witness the progression of seasons over multiple years, each of my data points represents a place that I know, a unique lake with quirks and stories, with its own patterns and way that it fits into the whole. This perspective has allowed me to interpret the results of measurements with nuance, and tell the story of this place with more detail than I could if each sample were just a number. I have observed lakes desiccate and their basins grow over with cattails. I have seen some lakes (though not all) refill during a flood and wondered at the sudden reappearance of a whole aquatic ecosystem. The time spent here was a choice, a recognition during earlier days of graduate school that the

understanding I was seeking would take time to emerge, and that I would need to be willing to stick around and follow the opportunities. We have aimed to address pressing knowledge gaps, and develop methodologies for long-term aquatic ecosystem monitoring that will be able to continue to generate important information about the hydrological processes that influence lake water balances and inform decision making. The large, comprehensive data set used in this thesis is unusual for northern ecosystems, but it has been essential for capturing the spatial and temporal dimensions of lake hydrological change that exist. The hydrological complexity of the PAD cannot be underestimated, and needs to be acknowledged in future efforts to preserve its value.

The research in this Thesis represents a new and novel understanding of the drivers and hydrological processes regulating lake water balance in the PAD. Through our study design and investigations, we developed sustainable and informative methodologies and approaches to capture landscape-scale hydrologic information, and demonstrated the importance and value of systematic, repeated collection of samples for water isotope and water chemistry analyses. In chapter 2, we combined water isotope tracers (2000-2006, 2014, 2015), water chemistry (2015) and ~200-400-year cellulose-inferred lake water $\delta^{18}O$ reconstructions from five representative basins to determine whether there was a legacy effect of a widespread ice-jam flooding event in 2014 and place present hydrological conditions in a long-term temporal perspective. This revealed a multi-decadal trend of increasing evaporative influence across the Peace-Athabasca Delta, unprecedented in the past ~400 years, and unable to be offset by episodic ice-jam flood events. In chapter 3 we used water isotope tracers, supplemented by measurements of specific conductivity and field observations, collected shortly after a rare ice-jam flood event in 2018, to quantify the proportion of input water to the lakes attributable to river input and to determine and

delineate the magnitude and extent of floodwater throughout the delta. Results emphasized the geographically variable role of spring flooding in lake-water recharge, and identified the contributions of summer open-water flooding in the Athabasca sector, important considerations for future interventions aimed at increasing lake water levels. Finally, we generated isoscapes using >1000 lake water isotope compositions collected during 15 sampling campaigns over 5 years (2015–2019) to reveal distinctive hydrological differences between Peace and Athabasca sectors of the delta and document the occurrence of substantial seasonal and multi-annual oscillation in lake water balances. We identified areas of the landscape where lakes are most vulnerable to climate-driven desiccation, as well as those most likely to receive river floodwater. Given the immense importance of water in this landscape, and concurrently the importance of this freshwater ecosystem globally, the new knowledge presented here has the potential to make significant contributions to decision making processes.

5.2 Emergent Properties

5.2.1 Effects of flooding and evaporation are not homogenous across the landscape

Flooding is widely recognized as a dominant driver of lake water balance and aquatic ecosystem conditions of the PAD, and much work has explored shifts in flood frequency and timing (e.g., PADPG 1972, 1973; Prowse and Conly, 1998, 2002; Wolfe et al., 2012, 2020; Beltaos, 2014, 2018) We found that flood events are spatially and temporally variable and their influence on lake conditions is not homogenous across the landscape, and should not be conceptualized as such. We also identified open water flooding as a major recharge mechanism for lakes in the Athabasca sector, a rarely acknowledged and poorly understood process that has stimulated further study (Neary et al., 2021). Both ice-jam and open-water flooding were largely

restricted to the Embarras / Mamawi creek corridor, as the result of the Embarras Breakthrough, a geomorphic change that redirected Athabasca River water in this direction (Kay et al., 2020; Timoney, 2013; Wolfe et al., 2008).

Outside of flooded areas and during non-flood years, lakes experienced strong evaporative drawdown, especially during summer, regardless of whether they were flooded in previous seasons. Hotspots of drying were identified in both the Peace and Athabasca sectors, as well as lakes more resilient to climate effects due to frequent recharge, which occurred predominantly along the Embarras / Mamawi creek corridor. This aligns with paleolimnological records showing a multidecadal trend of increasing importance of evaporative water loss (Remmer et al., 2018 [Chapter 2]; Wolfe et al., 2012). We documented that despite relatively wet conditions and substantial flooding in 2018 and 2019, recharge did not extend to the terminus region of the Athabasca River, which encompasses the traditional territory of the Athabasca Chipewyan First Nation. This observation acknowledges that despite strong influence of hydrological processes that recharge lakes across substantial portions of the delta, the ongoing lake-level drawdown observed by land-users aligns with our results and threatens access to their traditional lands. This fine-scale heterogeneity of discerning influence of floodwater and evaporation on lake balance highlights the need for landscape-scale monitoring and careful selection of study sites to ensure dynamic changes in hydrological conditions are adequately captured.

5.2.2 Novel approaches to lake isotope hydrology

Beyond the landscape-specific application in the PAD, this research has developed and refined novel approaches to lake isotope hydrology in remote regions. Previous work by Brock et

al. (2008) had developed approaches to calculate the spring isotopic depletion of flooded lakes in the Slave River Delta under the assumption that all depletion was attributed to river floodwaters, despite acknowledging that there were also likely contributions from precipitation. A key theoretical advancement was development of the coupled-isotope tracer approach of Yi et al. (2008) that described a methodology for estimating the isotope composition of source waters to lakes (δ_I) while preserving mass conservation and thus ensuring $\delta^{18}O$ and $\delta^{2}H$ derived E/I ratios are equivalent. Building upon these approaches, we constrained the δ_I of lakes flooded in 2018 to one of four landscape specific Meteoric Water Line Segments (MWLS) that result from mixing of either rain or snow with floodwater from the Peace or Athabasca river. This allowed estimation of the proportion of input to flooded lakes attributable to river floodwater or precipitation (rain or snow). As management actions are implemented in the PAD, this approach will be valuable in assessing the success of interventions and tracking changes in hydrological processes over time. Although this represents a significant improvement in delineating flood magnitude, further refinement is possible. Our approach can not simultaneously partition the influence of snowmelt and rainfall due to the linear positioning of these end-members in $\delta^{18}O$-$\delta^{2}H$ space. Current work in the Columbia River Basin is addressing this by using Bayesian mixing models to generate a three-component mixing model incorporating $\delta^{18}O$, $\delta^{2}H$ and specific conductivity. Our approach incorporated simple estimates of uncertainty based on sensitivity to key parameters, but could be improved by incorporating a recently developed mathematical framework for uncertainty estimation of isotopic source waters by Bowen et al. (2018).

The value of combining isotope hydrology with geospatial analysis is an emerging research theme throughout this Thesis. The landscape-specific isoscapes presented here

contribute to a growing trend of using high resolution isoscapes to answer targeted ecological questions (Dixon et al., 2010; Rascher et al., 2012, Bai et al., 2013; Cheesman and Cernusak, 2016). Here we have demonstrated the ability of isoscapes to discern patterns of hydrologic connectivity between rivers and their floodplain lakes, a difficult process to capture despite its importance in determining ecosystem biodiversity and biogeochemical cycling (Junk et al.,1989; Gregory et al., 1991; Ward, 1998; Lindenmayer et al., 2008; Johnson and Host, 2010). We concurrently demonstrate the use of isoscapes in determining the heterogeneous effects of geomorphic change and climate driven water drawdown at the landscape scale, with important implications under predictions of rising temperature and longer ice-free seasons (Schindler and Donahue, 2006). Isoscapes have also proven a useful tool in communicating scientific results to multiple stakeholder and audiences. The results of isotopic analysis can be challenging to convey to non-disciplinary audiences, in their raw form, but we have found great success in using isoscapes to translate our results into a format that appeals to decision makers and conveys the key messages. Our isoscapes figures were influential in securing support for continued partnership with Parks Canada, and their intuitive visual appeal has often opened the door for more detailed conversation with audiences.

5.2.3 *Necessity of systematic sampling*

Many of our findings were the result of systematic seasonal sampling of lake water for isotopes and water chemistry over multiple years, which captured numerous flood events that would have otherwise gone undetected. The sampling in this project represents 5 years of continuous effort to sample 60 – 80 lake and river sites. The large, comprehensive data set used in this thesis is unusual for northern ecosystems, but it has been essential for capturing the spatial and temporal dimensions of lake hydrological change that exist. Importantly, we observed that

hydrological processes are occurring at spatially and temporally varying scales. For example, a flood year in the central Athabasca sector can simultaneously be a dry year in the central Peace sector, and lakes in flood prone areas may be flooded once or multiple times a season, depending on their location. The quantitative information that can be derived from water isotopes, including input water sources, the magnitude of flooding and evaporation-to-inflow ratios, identify important hydrological processes (e.g., ice-jam flooding, open-water flooding, evaporation) that influence the lake water balances over space and time. Water loggers provide highly detailed water level information, but often are not deployed early enough to capture spring flooding and cannot independently determine input water sources. Remote sensing has the ability to capture landscape scale information but does not derive the magnitude of water level changes. For these reasons, water isotopes provide unique value and are an effective and informative tool for monitoring flood-plain landscapes. Research integrating isotopic data with water loggers and remote sensing can draw upon the strength of each approach and provide enhanced understanding. As Parks Canada begins to implement conservation actions, such as building a weir or conducting strategic dam releases from the upstream WAC Bennett Dam, systematic sampling of lake water for measurement of isotope composition can track the success of actions that provide increased water input to lakes and raise lake water levels, and can be used to inform adaptive and mitigative management strategies.

5.3 Contributions and links to on-going work

The research in this thesis formed the foundational hydrologic layer of several other research contributions including to 1) develop complementary approaches to capture fine-scale influences on lake water balance (Neary et al., 2021), 2) assess contemporary enrichment of metal concentrations in lake surface sediments (Owca et al., 2020), 3) understand how

hydrological processes regulate physical, chemical and ecological conditions over a range time and spatial scales (Remmer et al., 2019), and 4) generate baseline information for conventional and novel paleohydrological studies (Kay et al., 2019, 2020, 2021; Savage et al., 2021). Building from the data-sets and analysis presented here, Neary et al. (2021) refined lake categorization based on water level loggers deployed in a subset of ~50 lakes in 2018 and 2019. The lakes were categorized as drawdown (≥15 cm decline), stable (<15 cm decline), gradual rise or sharp rise depending on the relative roles of evaporation, spring and summer flooding, and precipitation on their water level. Metal concentrations in lake surface sediments of seven priority pollutants listed under the US Environmental Protection Agency's Clean Water Act were assessed by Owca et al. (2020), including sediment collected in lakes identified by water isotopes as flooded in 2018 (Chapter 2). Results demonstrated no substantial enrichment of metal concentrations in surface sediments above the baseline concentrations and highlight the value of opportunistic sampling of recently deposited flood sediment to capture river sediment metals concentrations at the time of the spring freshet, when contaminants accumulated in the winter snowpack are discharged to the rivers. Ongoing work aims to identify the primary water-quality gradients, their spatial patterns and their linkages to hydrological processes using the combination of the water isotopes and water chemistry collected from the lakes sampled in chapter 3 (Remmer et al., 2019). Identification of suitable, flood-prone lakes for sediment core reconstructions of flood history (Kay et al., 2019), river metals deposition (Kay et al., 2020), and a novel approach to discriminating lake sediment sources based on elemental composition (Kay et al., 2021), relied on the isotopic compositions of lake water. Collectively, this Thesis, in combination with the above studies, form the research foundation of a monitoring framework for the delta capable of detecting cumulative effects on aquatic ecosystems.

Sampling of the lakes of the PAD has continued beyond the end of my field seasons, with fieldwork performed by the staff at WBNP and Community Based Monitors in 2020 and 2021. ‘In 2019, we were commissioned by Parks Canada to generate a Technical Report that presents our framework for a long-term monitoring program and standard operating procedures for the sample collection and analysis within the hydrology, limnology and contaminants components, as conducted by our research group in the PAD since 2015 (Remmer et al., 2020). The research in the data chapters of this Thesis provided the foundational hydrologic framework that allowed the adoption of ongoing monitoring under the 2019 federal Action Plan. This knowledge transfer is an important achievement, and new insights emerge with the addition of each new season of data.

5.4 Future work and recommendations

We strongly advocate for ongoing monitoring of the lakes in the PAD described here, and anticipate new knowledge will emerge over longer time-scales. The complexity and hydrologically dynamic nature of the PAD necessitate continued sampling of the 60 sites used in Chapter 3, in order to adequately capture the spatial heterogeneity of hydrological processes. This spatially comprehensive set of lakes also allows the use of geostatistical models (e.g., isoscapes), an important consideration for detecting and recognizing hydrological patterns. As data years are added, temporal trend analysis can be incorporated into the data analysis to better understand long-term shifts in lake conditions. This approach has been demonstrated in in the Old Crow Flats, Yukon, where MacDonald et al. (2021) recently compiled 13 years of water isotope data resulting from sustained monitoring of hydrologically representative lakes to identify shifting influence of hydrological processes on water balance of lakes across the landscape. Shifts over time in the percentage of the landscape predicted to fall into each of the

categories identified by Neary et al. (2021) could be used to target remediation action in areas undergoing rapid or sustained change. Future research should also incorporate analysis of biotic communities of lakes, which are expected to be significantly influenced by shifting hydrological conditions (Straka et al., 2018; Ward et al., 2018, 2019, 2021; Wiklund et al., 2010). Periphytic algae, which serve a fundamental role in shallow lake food webs, were collected during each of 2015-2019 field seasons but have yet to be enumerated and analyzed. Based on the hydrological knowledge generated in this Thesis, I predict changes in periphyton community composition resulting from hydrolimnological conditions will be strongly spatially heterogenous, with ramifications for aquatic food webs, biogeochemical cycles and water quality. The methods and approaches presented here have potential in other floodplain and shallow lake systems, such as those throughout the Canadian North and Arctic, as well as the many lakes of the Prairies. As technology advances, the integration of remote sensing with the direct sampling of lake water for measurement of water isotope composition has much potential to improve characterization of flood events and other landscape scale processes in the PAD and other remote, northern floodplains. Shallow lake systems in particular would benefit from the repeated, systematic sampling approaches presented here, as they are sensitive to catchment and climate shifts, acting as bellwethers of ecosystem change.

References

Allen, S. T., Kirchner, J. W., & Goldsmith, G. R. (2018). Predicting spatial patterns in precipitation isotope (δ^2H and $\delta^{18}O$) seasonality using sinusoidal isoscapes. *Geophysical Research Letters*, 45, 4859– 4868. https://doi.org/10.1029/2018GL077458

Bai, E., Boutton, T.W., Liu, F., Wu, X.B., & Archer, S.R. (2013) ^{15}N isoscapes in a subtropical savanna parkland: spatial-temporal perspectives. *Ecosphere*, 4(1), 4. DOI:10.1890/ES12-00187.1

Barnett, T. P., Pierce, D.W., Hidalgo, H.G., Bonfils, C., Santer, B.D., Das, T., Bala, G., Wood, A.W., Nozawa, T., Mirin, A.A., Cayan, D.R., & Dettinger, M.D. (2008). Human-induced changes in the hydrology of the western United States. *Science*, 319, 1080–1083. doi:10.1126/science.1152538

Beltaos, S. (2014). Comparing the impacts of regulation and climate on ice-jam flooding of the Peace-Athabasca Delta. *Cold Regions Science and Technology*, 108, 49-58. doi:10.1016/j.coldregions.2014.08.006

Beltaos, S. (2018). Frequency of ice-jam flooding of Peace-Athabasca Delta. *Canadian Journal of Civil Engineering*, 45(1), 71–75. https://doi.org/10.1139/cjce-2017-0434

Beltaos, S., & Bonsal, B. (2021). Climate change impacts on Peace River ice thickness and implications to ice-jam flooding of the Peace-Athabasca Delta, Canada. *Cold Regions Science and Technology*, 186, 103279. https://doi.org/10.1016/j.coldregions.2021.103279.

Birkel, C., Correa-Barahona, A., Martinez-Martinez, M. (2020). Headwaters drive streamflow and lowland tracer export in a large-scale humid tropical catchment. *Hydrological Processes*, 34, 3824– 3841. https://doi.org/10.1002/hyp.13841

Birkel, C., Helliwell, R., Thornton, B., Gibbs, S., Cooper, P., Soulsby, C., … Midwood, A. J. (2018). Characterization of surface water isotope spatial patterns of Scotland. *Journal of Geochemical Exploration*, 194, 71– 80. https://doi.org/10.1016/j.gexplo.2018.07.011

Bowen, G. J. (2010). Isoscapes: Spatial pattern in isotopic biogeochemistry. *Annual Review of Earth and Planetary Sciences*, 38(1), 161– 187. https://doi.org/10.1146/annurev-earth-040809-152429

Bowen, G.J., Putman, A., Brooks, J.R., Bowling, D.R., Oerter, E.J., & Good, S.P. Inferring the source of evaporated waters using stable H and O isotopes. *Oecologia,* 187, 1025–1039 (2018). https://doi.org/10.1007/s00442-018-4192-5

Bowen, G. J., & Revenaugh, J. (2003). Interpolating the isotopic composition of modern meteoric precipitation. *Water Resources Research*, 39(10), 1– 13. https://doi.org/10.1029/2003WR002086

Brock, B. E., Wolfe, B. B., & Edwards, T. W. D. (2007). Characterizing the hydrology of shallow floodplain lakes in the Slave River Delta, NWT, Canada, using water isotope tracers. *Arctic, Antarctic, and Alpine Research*, 39, 388-401. DOI: 10.1657/1523-0430(06-026)[BROCK]2.0.CO;2

Brock, B. E., Wolfe, B. B., & Edwards, T. W. D. (2008). Spatial and temporal perspectives on spring break-up flooding in the Slave River Delta, NWT. *Hydrological Processes*, 22, 4058–4072. https://doi.org/10.1002/hyp.7008

Brooks, J. R., Wigington, P. J., Phillips, D. L., Comeleo, R., & Coulombe, R. (2012). Willamette River basin surface water isoscape ($\delta^{18}O$ and $\delta^{2}H$): Temporal changes of source water within the river. *Ecosphere*, 3(5), art39. https://doi.org/10.1890/ES11-00338.1

Brooks, J.R., Gibson, J.J., Birks, S.J., & Weber, M.H. (2014). Stable isotope estimates of evaporation: Inflow and water residence time for lakes across the United States as a tool for national lake water quality assessments. *Limnology and Oceanography*, 59, 2150-2165. 10.4319/lo.2014.59.6.2150

Burn D. H., Mohammed, S., & Zhang, K. (2010). Detection of trends in hydrological extremes for Canadian watersheds. *Hydrological Processes*, 24, 1781–1790. doi:10.1002/hyp.7625

Cheesman A.W., & Cernusak, L.A. (2016). Isoscapes: a new dimension in community ecology. *Tree Physiology*, 36(12), 1456–1459. https://doi.org/10.1093/treephys/tpw099

Craig, H, & Gordon, L. I. (1965). Deuterium and oxygen 18 variations in the ocean and the marine atmosphere, p. 9–130. In E. Tongiorgi [Ed.], Stable Isotopes in Oceanographic Studies and Paleotemperatures. Laboratorio di Geologia Nucleare, Pisa: Italy.

Cui, J., Tian, L., Biggs, T.W., & Wen, R. (2017). Deuterium-excess determination of evaporation to inflow ratios of an alpine lake: Implications for water balance and modeling. *Hydrological Processes*, 31(5), 1034-1046. 10.1002/hyp.11085

Dansgaard, W. (1964) Stable isotopes in precipitation. *Tellus*, 16(4), 436-468. DOI: 10.3402/tellusa.v16i4.8993

Davidson, N.C. (2014). How much wetland has the world lost? Long-term and recent trends in global wetland area. *Marine and Freshwater Research,* 65(10), 934-941. https://doi.org/10.1071/MF14173

Dery, S.J., & Wood, E. F. (2005). Decreasing river discharge in northern Canada. *Geophysical Research Letters*, 32 (10), 10401. doi:10.1029/2005GL022845

Díaz, S., Settele, J., Brondízio, E., Ngo, H.T., Guèze, M., & Agard, J. (2019). Summary for policymakers of the global assessment report on biodiversity and ecosystem services of the Intergovernmental Science-Policy Platform on Biodiversity and Ecosystem Services. *Plenary of the Intergovernmental Science-Policy Platform on Biodiversity and Ecosystem Services,* Seventh session, Paris, 29 April–4 May 2019. 39 p.

Dixon, E.R., Blackwell, M.S.A., Dhanoa, M.S., Berryman, Z., Martinez, N.d.l.F., Junquera, D., Martinez, A., Murray, P.J., Kemp, H.F., Meier-Augenstein, W., Duffy, A., & Bol, R. (2010). Measurement at the field scale of soil $\delta^{13}C$ and $\delta^{15}N$ under improved grassland. *Rapid Communications in Mass Spectrometry*, 24(5), 511–518. https://doi.org/10.1002/rcm.4345

Dudgeon, D., Arthington, A.H., Gessner, M.O., Kawabata, Z.-I., Knowler, D.J., Lévêque, C., Naiman, R.J., Prieur-Richard, A.-H., Soto, D., Stiassny, M.L.J., & Sullivan, C.A. (2006). Freshwater biodiversity: importance, threats, status and conservation challenges. *Biological Reviews*, 81(2), 163-182. https://doi.org/10.1017/S1464793105006950

Fausch, K.D., Torgersen, C.E., Baxter, C.V., & Li, H.W. (2002). Landscapes to riverscapes: bridging the gap between research and conservation of stream fishes. *Bioscience*, 52 (6), 483–498. doi:10.1641/0006-3568(2002)052[0483:LTRBTG]2.0.CO;2

Gat, J. (2003). Oxygen and hydrogen isotopes in the hydrologic cycle. *Annual Review of Earth and Planetary Sciences*, 24(1), 225-262. 10.1146/annurev.earth.24.1.225

Gibson, J.J. (2001). Forest-tundra water balance signals traced by isotopic enrichment in lakes. *Journal of Hydrology*, 251(1-2), 1-13. https://doi.org/10.1016/S0022-1694(01)00428-0.

Gibson, J.J. (2002). Short-term evaporation and water budget comparisons in shallow Arctic lakes using non-steady isotope mass balance. *Journal of Hydrology*, 264 (1-4), 242-261. https://doi.org/10.1016/S0022-1694(02)00091-4

Gibson, J.J., & Edwards, T.W.D. (2002). Regional water balance trends and evaporative transpiration partitioning from a stable isotope survey of lakes in northern Canada. *Global Biogeochemical Cycles*, 16(2), 1–9. doi:10.1029/2001GB001839

Gibson, J.J., Birks, S.J., Jeffries, D., & Yi, Y. (2017). Regional trends in evaporation loss and water yield based on isotope mass balance of lakes: the Ontario Precambrian Shield surveys. *Journal of Hydrology*, 544, 500–510. https://doi.org/10.1016/j.jhydrol.2016.11.016

Gibson, J.J., Birks, S.J., Yi, Y., Moncur, M.C., & McEachern, P.M. (2016). Stable isotope mass balance of fifty lakes in central Alberta: assessing the role of water balance and climate in determining trophic status and lake level. *Journal of Hydrology: Regional Studies*, 6, 13–25. https://doi.org/10.1016/j.ejrh.2016.01.034.

Gibson, J.J., Edwards, T.W.D., Birks, S.J., St Amour, N.A., Buhay, W.M., McEachern, P., Wolfe, B.B. & Peters, D.L. (2005). Progress in isotope tracer hydrology in Canada. *Hydrological Processes*, 19(1), 303-327. https://doi.org/10.1002/hyp.5766

Gibson, J.J., Prepas, E.E., McEachern, P. (2002). Quantitative comparison of lake throughflow, residency, and catchment runoff using stable isotopes: Modelling and results from a regional survey of Boreal lakes. *Journal of Hydrology*, 262(1-4), 128-144. 10.1016/S0022-1694(02)00022-7

Gleick, P. (2003). Global freshwater resources: soft-path solutions for the 21st century. *Science*, 302 (5650), 1524–1528. doi:10.1126/science.1089967

Gonfiantini R. (1986). Environmental isotopes in lake studies, p. 113-168. In Fritz, P., & Fontes, J. C. [Eds.], Handbook of Environmental Isotope Geochemistry, Volume 2. New York: Elsevier.

Gregory, S.V., Swanson, F.J., McKee, W.A., & Cummins, K.W. (1991). An ecosystem perspective of riparian zones. *BioScience*, 41(8), 540–551. https://doi.org/10.2307/1311607

Hassan, R., Scholes, R., & Ash,N. (2005). Millenium Ecosystem Assessment. Ecosystems and human well-being: Current state and trends, vol. 1. Washington, DC: Island Press.

Hatvani, I.G., Erdélyi, D., Vreča, P., & Kern, Z. (2020). Analysis of the spatial distribution of stable oxygen and hydrogen isotopes in precipitation across the Iberian peninsula. *Water*, 12(2), 481. https://doi.org/10.3390/w12020481

Johnson, L.B., & Host, G.E. (2010). Recent developments in landscape approaches for the study of aquatic ecosystems. *BioOne*, 29(1), 41–66. https://doi.org/10.1899/09-030.1

Juffe-Bignoli D., Brooks, T.M., Butchart, S.H.M., Jenkins, R.B., Boe, K., & Hoffmann, M. (2016). Assessing the cost of global biodiversity and conservation knowledge. *PLoS ONE*, 11(8), e0160640. https://doi.org/10.1371/journal.pone.0160640

Junk, W.J., Bayley, P.B., & Sparks, R.E. (1989). The flood pulse concept in river–floodplain systems. *Canadian Journal of Fisheries and Aquatic Sciences*, 106, 110–127.

Kang, S., Yi, Y., Xu, Y., Xu, B., & Zhang, Y. (2017). Water isotope framework for lake water balance monitoring and modelling in the Nam Co Basin, Tibetan Plateau. *Journal of Hydrology: Regional Studies*, 12, 289-302. 10.1016/j.ejrh.2017.05.007

Kay, M.L., Swanson, H.K., Burbank, J., Owca, T.J., MacDonald, L.A., Savage, C.A.M., Remmer, C.R., Neary, L.K., Wiklund, J.A., Wolfe, B.B. & Hall, R.I. (2021). A Bayesian mixing model framework for quantifying temporal variation in source of sediment to lakes across broad hydrological gradients of floodplains. *Limnology and Oceanography Methods*, 19(8), 540-551. https://doi.org/10.1002/lom3.10443

Kay, M.L., Wiklund, J.A., Neary, L.K., Brown, K., Ghosh, A., MacDonald, E., Thomson, K., Vucic, J.M., Wesenberg, K, Hall, R.I., & Wolfe, B.B. (2019). Bi-directional hydrological changes in perched basins of the Athabasca Delta (Canada) in recent decades caused y natural processes. *Environmental Research Communications*, 1, 0881001. https://doi.org/10.1088/2515-7620/ab37e7

Kay, M.L., Wiklund, J.A., Remmer, C.R., Owca, T.J., Klemt, W.H., Neary, L.K., Brown, K., MacDonald, E., Thomson, K., Vucic, J.M., Wesenberg, K., Hall, R.I., & Wolfe, B.B. (2020). Evaluating temporal patterns of metals concentrations in floodplain lakes of the Athabasca Delta (Canada) relative to pre-industrial baselines. Science of the Total Environment, 20(704), 135309. doi:10.1016/j.scitotenv.2019.135309

Kendall. C., & Coplen, T.B. (2001). Distribution of oxygen-18 and deuterium in river waters across the United States. *Hydrological Processes*, 15(7), 1363-1393. DOI:10.1002/hyp.217

Lamontagne, J.R., Jasek, M., & Smith, J.D. (2021). Coupling physical understanding and statistical modeling to estimate ice jam flood frequency in the northern Peace-Athabasca Delta under climate change. *Cold Regions Science and Technology*, 192, 103383. https://doi.org/10.1016/j.coldregions.2021.103383

Lindenmayer, D., Richard, J., Montague-Drake, R., Alexandra, J., Bennett, A., Cale, P., & Fischer, J. (2008). A checklist for ecological management of landscapes for conservation. *Ecology Letters*, 11, 78–91. doi:10.1111/j.1461-0248.2007.01114.x

MacDonald, L. A., Balasubramaniam, A. M., Hall, R. I., Wolfe, B. B., Sweetman, J. N. (2012). Developing biomonitoring protocols for shallow Arctic lakes using diatoms and artificial substrate samplers. *Hydrobiologia*, 683, 231–248. doi: 10.1007/s10750-011-0960-5.

MacDonald, L.A., Wolfe, B.B., Turner, K.W., Anderson, L., Arp, C.D., Birks, S.J., Bouchard, F., Edwards, T.W.D., Farquharson, N., Hall, R.I., McDonald, I., Narancic, B., Ouimet, C., Pienitz, R., Tondu, J., & White, H. (2017). A synthesis of thermokarst lake water balance in high-latitude regions of North America from isotope tracers. *Arctic Science*, 3, 118-149. doi:10.1139/as-2016-0019

MacDonald, L.A., Turner, K.W., McDonald, I., Kay, M.L., Hall, R.I., & Wolfe, B.B. (2021). Isotopic evidence of increasing water abundance and lake hydrological change in Old Crow Flats, Yukon, Canada. *Environmental Research Letters*, 16: 124024.

MacKinnon, B.D., Sagin, J., Baulch, H.M., Lindenschmidt, K.-E., & Jardine, T.D. (2016). Influence of hydrological connectivity on winter limnology in floodplain lakes of the Saskatchewan River Delta, Saskatchewan. Canadian Journal of Fisheries and Aquatic Sciences, 73(1), 140-152. 10.1139/cjfas-2015-0210

MCFN. (2014). Petition to The World Heritage Committee Requesting Inclusion of Wood Buffalo National Park on the List of World Heritage in Danger. Mikisew Cree First Nation.

Mountain, N., James, A., & Chutko, K. (2015). Groundwater and surface water influences on streamflow in a mesoscale Precambrian Shield catchment. *Hydrological Processes*, 29(18), 3941-3953. 10.1002/hyp.10590

Narancic, B., Wolfe, B.B., Pienitz, R., Meyer, H., & Lamhonwah, D. (2017). Landscape-gradient assessment of thermokarst lake hydrology using water isotope tracers. *Journal of Hydrology*, 545, 327-338, 10.1016/j.jhydrol.2016.11.028

Neary L.K., Remmer C.R., Krist J., Wolfe B.B., & Hall, R I. (2021). A new lake classification scheme for the Peace-Athabasca Delta (Canada) characterizes hydrological processes that cause lake-level variation. *Journal of Hydrology: Regional Studies*, 38: 100948.

Owca, T.J., Kay, M.L., Faber, J., Remmer, C.R., Zabel, N., Wiklund, J.A., Wolfe, B.B., & Hall, R.I. (2020). Use of pre-industrial baselines to monitor anthropogenic enrichment of metals concentrations in recently deposited sediment of floodplain lakes in the Peace-Athabasca Delta (Alberta, Canada). *Environmental Monitoring and Assessment*, 192, 106. https://doi.org/10.1007/s10661-020-8067-y

PADPG. (1973). Peace–Athabasca Delta Project, technical report and appendices, volume 1: hydrological investigations, volume 2: ecological investigations. Peace–Athabasca Delta Project Group, Delta Implementation Committee, Governments of Alberta, Saskatchewan and Canada.

Peace-Athabasca Delta Implementation Committee (PADIC). (1987). Peace-Athabasca Delta water management works evaluation: a report prepared under the Peace-Athabasca Delta Implementation Agreement. Governments of Alberta, Saskatchewan and Canada.

Peace–Athabasca Delta Technical Studies (PADTS). (1996). Final Report. PADTS Steering Committee, Fort Chipewyan, Alberta; 106 pp

Peters, D.L., Prowse, T.D., Pietroniro, A., & Leconte, R. (2006). Flood hydrology of the PeaceAthabasca Delta, northern Canada. *Hydrological Processes*, 20(19), 4073-4096. https://doi.org/10.1002/hyp.6420.

Peters, D.L., Niemann, K.O., Skelly, R. (2021). Remote sensing of ecosystem structure – Part 2: Initial findings of ecosystem functioning through intra- and inter-annual comparisons with Earth Observation data. *Remote Sensing*, 13, 3219. https://doi.org/10.3390/rs13163219.

Pietroniro, A., Prowse, T.D., & Peters, T.D. (1999). Hydrologic assessment of an inland freshwater delta using multi-temporal satellite remote sensing. *Hydrological Processes*,

13, 2483–2498, doi:10.1002/(SICI)1099-1085(199911)13:16<2483::AID-HYP934>3.0.CO;2-9

Prowse, T.D., & Conly, F.M. (1998). Impacts of climatic variability and flow regulation on ice-jam flooding of a northern delta. *Hydrological Processes*, 12, 1589–1610. doi:10.1002/(SICI)1099-1085(199808/09)12:10/11<1589::AID-HYP683>3.0.CO;2-G

Prowse, T.D., & Conly, F.M. (2002). A review of hydroecological results of the Northern River Basins Study, Canada. Part 2. Peace – Athabasca Delta. *River Research and Applications*, 18(5), 447–460. https://doi.org/10.1002/rra.682

Prowse, T.D., Beltaos, S., Gardner, J.T., Gibson, J.J., Granger, R.J., & Leconte, R. (2006). Climate change, flow regulation and land-use effects on the hydrology of the Peace-Athabasca-Slave system: findings from the Northern Rivers Ecosystem Initiative. *Environmental Monitoring and Assessment*, 113(1-3), 167–197. doi: 10.1007/s10661-005-9080-x

Rascher, K.G., Hellmann, C., Maguas, C., & Werner, C. (2012). Community scale 15N isoscapes: tracing the spatial impact of an exotic N2-fixing invader. *Ecology Letters*, 15(5), 484–491. https://doi.org/10.1111/j.1461-0248.2012.01761.x

Remmer, C.R., Neary, L.K., Wolfe, B.B. & Hall, R.I. (2020). Technical Report for Monitoring Lakes in the Peace-Athabasca Delta, Alberta. Prepared for Wood Buffalo National Park, Parks Canada.

Remmer, C., Neary, L., Owca, T., Wolfe, B.B., & Hall, R.I. (2019). Isoscapes and limnoscapes of the Peace-Athabasca Delta: A foundation for hydrolimnological monitoring. *Society of Canadian Limnologist annual conference*, London, Ontario, Canada.

Rood, S.B., Samuelson, G.M., Weber, J.K., & Wywrot, K.A. (2005). Twentieth-century decline in streamflows from the hydrographic apex of North America. *Journal of Hydrology*, 306(1), 215–233. doi:10.1016/j.jhydrol.2004.09.010

Rozanski, K., Araguás-Araguás, L., & Gonfiantini, R. (1993). Isotopic Patterns in Modern Global Precipitation. In Climate Change in Continental Isotopic Records (eds P.K. Swart, K.C. Lohmann, J. Mckenzie and S. Savin). https://doi.org/10.1029/GM078p0001

Sauchyn, D.J., St-Jacques, J., & Luckman, B. H. (2015). Long-term reliability of the Athabasca River (Alberta, Canada) as the water source for oil sands mining. *Proceedings of the National Academy of Sciences of the United States of America*, 112(41), 12621–12626. https://doi.org/10.1073/pnas.1509726112

Scalzitti, J., Strong, C., & Kochanski, A. (2016). Climate change impact on the roles of temperature and precipitation in western U.S. snowpack variability. *Geophysical Research Letters*, 43(10) 5361–5369. doi:10.1002/2016GL068798

Scheliga, B., Tetzlaff, D., Nuetzmann, G., & Soulsby, C. (2017). Groundwater isoscapes in a montane headwater catchment show dominance of well-mixed storage. *Hydrological Processes*, 31, 3504– 3519. https://doi.org/10.1002/hyp.11271

Schindler, D.W. & Donahue, W.F. (2006). An impending water crisis in Canada's western prairie provinces. *Proceedings of the National Academy of Sciences of the United States of America*, 103(19), 7210–7216. https://doi.org/10.1073/pnas.0601568103

Schindler, D.W., & Smol, J.P. (2006). Cumulative effects of climate warming and other human activities on freshwaters of arctic and subarctic North America. *Ambio*, 35, 160–168. https://doi.org/10.1139/f00-179

Smol, J.P., Wolfe, A.P., Birks, H.J.B., Douglas, M S.V, Jones, V.J., Korhola, A., & Weckström, J. (2005). Climate-driven regime shifts in the biological communities of arctic lakes. Proceedings of the National Academy of Sciences of the United States of America, 102(12), 4397–4402. https://doi.org/10.1073/pnas.0500245102

Sokal M. A., Hall R. I., Wolfe B. B. (2008). Relationships between hydrological and limnological conditions in lakes of the Slave River Delta (NWT, Canada) and quantification of their roles on sedimentary diatom assemblages. *Journal of Paleolimnology*, 39, 533-550. https://doi.org/10.1007/s10933-007-9128-8

Southee, F.M., Edwards, B.A., Chetkiewicz, C-L.B., & O'Connor, C.M. (2021). Freshwater conservation planning in the far north of Ontario, Canada: identifying priority watersheds for the conservation of fish biodiversity in an intact boreal landscape. *FACETS*, 6(1), 90-117. https://doi.org/10.1139/facets-2020-0015

Straka, J.R., Antoine, A., Bruno, R., Campbell, D., Campbell, R., Campbell, R., Cardinal, J., Gibot, G., Gray, Q.Z., Irwin, S., Kindopp, R., Ladouceur, R., Ladouceur, W., Lankshear, J., Maclean, B., Macmillan, S., Marcel, F., Marten, G., Marten, L., McKinnon, J., Patterson, L.D., Voyageur, C., Voyageur, M., Whiteknife, G., & Wiltzen, L.(2018). "We used to say rats fell from the sky after a flood". Temporary recovery of muskrat following ice jams in the Peace-Athabasca Delta. *Arctic*, 71(2), 218-228. https://doi.org/10.14430/arctic4714.

Terzer, S., Wassenaar, L.I., Araguás-Araguás, L.J., & Aggarwal, P.K. (2017). Global isoscapes for $\delta^{18}O$ and $\delta^{2}H$ in precipitation: improved prediction using regionalized climatic regression models. *Hydrology and Earth System Sciences*, 17, 4713–4728, https://doi.org/10.5194/hess-17-4713-2013.

Timoney, K., Peterson, G., Fargey, P., Peterson, M., McCanny, S., & Wein, R. (1997). Spring ice-jam flooding of the Peace– Athabasca Delta: evidence of a climatic oscillation. *Climate Change*, 35(4), 463–483. doi:10.1023/A:1005394031390.

Timoney, K.P. (2013). The Peace-Athabasca Delta – portrait of a dynamic ecosystem. The University of Alberta Press.

Turner, K.W., Wolfe, B.B., Edwards, T.W., Lantz, T.C., Hall, R.I., & Larocque, G., (2014). Controls on water balance of shallow thermokarst lakes and their relations with catchment characteristics: a Multi-year, landscape-scale assessment based on water isotope tracers and remote sensing in Old Crow Flats, Yukon (Canada). *Global Change Biology*, 20(5), 1585–1603. https://doi.org/10.1111/gcb.12465

Vannini, P., & Vannini, A. (2019). The exhaustion of Wood Buffalo National Park: Mikisew Cree First Nation experiences and perspectives. *International Review of Qualitative Research*, 12(3), 278-303. https://doi.org/10.1525/irqr.2019.12.3.278

Ward, E.M., & Gorelick, S.M. (2018). Drying drives decline in muskrat population in the Peace-Athabasca Delta, Canada. *Environmental Research Letters*, 13(12), 124026. https://doi.org/10.1088/1748-9326/aaf0ec

Ward, E.M., Solari, K.A., Varudkar, A., Gorelick, S.M., & Hadly, E.A. (2021). Muskrats as a bellwether of a drying delta. *Communications Biology*, 4, 750. https://doi.org/10.1038/s42003-021-02288-7

Ward, E.M., Wysong, K., & Gorelick, S.M. (2020). Drying landscape and interannual herbivory-driven habitat degradation control semiaquatic mammal population dynamics. *Ecohydrology*, 13, e2169. https://doi.org/10.1002/eco.2169

Ward, J.V. (1998). Riverine landscapes: biodiversity patterns, disturbance regimes, and aquatic conservation. *Biological Conservation*, 83(3), 269–278. https://doi.org/10.1016/S0006-3207(97)00083-9

Wassenaar, L.I., Van Wilgenburg, S.L., Larson, K., & Hobson, K.A. (2009). A groundwater isoscape (δD, δ18O) for Mexico. *Journal of Geochemical Exploration*, 102(3), 123-136. 10.1016/j.gexplo.2009.01.001

WHC/IUCN. (2017). Reactive monitoring mission to Wood Buffalo National Park, Canada; mission report, March 2017. United Nations Educational, Scientific and Cultural Organization. available at http://whc.unesco.org/en/documents/156893.

Wiklund J.A, Bozinovski N., Hall R.I., Wolfe B.B. (2010). Epiphytic diatoms as flood indicators. *Journal of Paleolimnology*, 44, 25-42. https://doi.org/10.1007/s10933-009-9383-y

Wiklund, J.A., Hall, R.I., & Wolfe, B.B. (2012). Timescales of hydrolimnological change in floodplain lakes of the Peace–Athabasca Delta, northern Alberta, Canada. *Ecohydrology*, 5(3), 351–367. doi:10.1002/eco.226

Wolfe, B.B., Falcone, M.D., Clogg-Wright, K.P., Mongeon, C.L., Yi, Y., Brock, B.E., St. Amour, N.A., Mark, W.A., & Edwards, T.W.D. (2007a). Progress in isotope paleohydrology using lake sediment cellulose. Journal of Paleolimnology, 37, 221–231. doi:10.1007/s10933-006-9015-8

Wolfe, B.B., Hall, R.I., Edwards, T.W.D., & Johnston, J.W. (2012). Developing temporal hydroecological perspectives to inform stewardship of a northern floodplain landscape subject to multiple stressors: Paleolimnological investigations of the Peace-Athabasca Delta. *Environmental Reviews*, 20(3), 191–210. https://doi.org/10.1139/a2012-008

Wolfe, B.B., Hall, R.I., Edwards, T.W.D., Vardy, S.R., Falcone, M.D., Sjunneskog, C., & van Driel, P. (2008). Hydroecological responses of the Athabasca Delta, Canada, to changes in river flow and climate during the 20th century. *Ecohydrology*, 1(2), 131–148. https://doi.org/10.1002/eco.13

Wolfe B.B., Hall R.I., Wiklund J.A., & Kay, M.L. (2020). Past variation in Lower Peace River ice-jam flood frequency. *Environmental Reviews*, 28(3), 209–217. https://doi.org/10.1139/er-2019-0047

Wolfe, B.B., Karst-Riddoch, T.L., Hall, R.I., Edwards, T.W.D., English, M.C., Palmini, R., McGowan, S., Leavitt, P.R., & Vardy, S.R. (2007b). Classification of hydrologic regimes of northern floodplain basins (Peace-Athabasca Delta, Canada) from analysis of stable isotopes ($\delta^{18}O$, $\delta^{2}H$) and water chemistry. *Hydrological Processes*, 21(2), 151–168. doi:10.1002/hyp.6229

Wood Buffalo National Park (WBNP). 2019. World Heritage Site Action Plan. Parks Canada. Accessible at: https://www.pc.gc.ca/en/pn-np/nt/woodbuffalo/info/action.

Woodward, G, Perkins, D., & Brown, L. (2010). Climate change and freshwater ecosystems: Impacts across multiple levels of organization. *Philosophical Transactions of the Royal Society: Biological Science*, 365(1549), 2093-2106. doi: 10.1098/rstb.2010.0055

Wright, S.N., Novakowski, K.S. (2020). Hydrogeologic and climate drivers of water isotopes in fractured rock: A word of caution for the use of groundwater isoscapes in humid continental settings. *Journal of Hydrology*, 586, 124857. 10.1016/j.jhydrol.2020.124857

Yi, Y., Brock, B.E., Falcone, M.D., Wolfe, B.B., & Edwards, T.W.D. (2008). A coupled isotope tracer method to characterize input water to lakes. *Journal of Hydrology*, 350(1-2), 1–13, doi:10.1016/j.jhydrol.2007.11.008

Appendices

Appendix 1: Isotope Framework (Chapter 2, 3 & 4)

A.1.1 Meteorological Calculations

Relative humidity (*h*) and temperature (*T*) were calculated as the average evaporation-flux-weighted values during the period of 2000-2015 for Chapter 2 and Chapter 3 and during the period of 2015-2019 for Chapter 4, using climate data from Environment Canada and the National Research Council of Canada. The average ice-free season *h* and *T* were flux-weighted based on potential evapotranspiration determined by Thornthwaite (1948):

(E.1) $$h_{flux} = \sum \frac{(h \times E_t)}{(E_t)}$$

(E.2) $$T_{flux} = \sum \frac{(T_a \times E_t)}{(E_t)}$$

where T_a is the monthly average temperature and E_t is the monthly total evaporation. E_t was calculated using the equation:

(E.3) $$E_t = 1.6 \cdot \frac{L}{12} \cdot \frac{N}{30} \left[\frac{10 \cdot T_a}{I}\right]^a$$

where L is the average day length in hours in a month, N is the number of days in the month, I is the annual heat index and a is a calculated coefficient. I was calculated as the total of each ice-free month using the equation:

(E.4) $$I = \sum I_i$$

and I_i was calculated using the equation:

(E.5) $$I_i = \left(\frac{T_a}{5}\right)^{1.5}$$

and a was calculated using the equation:

(E.6) $$a = 0.49 + 0.0179 \cdot I - 7.71 \cdot 10^{-5} \cdot I^2 + 6.75 \cdot 10^{-7} \cdot I^3$$

A.1.2 Isotopic Framework Calculations

Isotopic framework parameters were calculated using calculations (in decimal notation) and approaches described in detail in Gonfiantini (1986), Gibson and Edwards (2002), Edwards et al. (2004) and Yi et al. (2008), which are based on the linear resistance model of Craig and Gordon (1965).

The LEL for the PAD region was determined using either the 15-year average of environmental conditions (Chapter 2 & 3) or the 5-year average (Chapter 4) described above, as well as pre-existing isotopic data and calculated evaporation- flux-weighted terms. The LEL was determined as a regression of the isotope composition precipitation (δ_P), the isotope composition of a terminal basin at steady state (δ_{SSL}) and the theoretical limiting non-steady-state composition of a water body approaching complete desiccation (δ^*). δ_P was obtained from the Online Isotope

in Precipitation Calculator (Bowen and Revenaugh, 2003; IAEA/WMO, 2015; Bowen, 2016). δ_{SSL} was determined from the average isotope composition of PAD 18, a terminal basin at isotopic and hydrologic steady state located in an elevated portion of the PAD (Yi et al., 2008). δ* was calculated from Gonfiantini (1986):

(E.7) $$\delta^* = \frac{h \cdot \delta_{AS} + \varepsilon_k + \varepsilon^* / \alpha^*}{h - \varepsilon_k - \varepsilon^* / \alpha^*}$$

where *h* is the relative humidity (see A.1.1), δ_{AS} is the isotope composition of atmospheric moisture for the ice-free season, ε_k is the kinetic separation factor between liquid and vapour phases, ε^* is the equilibrium separation factor between liquid and vapour phases and α* is the equilibrium liquid-vapour isotope fractionation factors.

α* for δ^2H and $\delta^{18}O$ were derived from the equations described by Horita and Wesolowski (1994):

(E.8) $$1000\ ln\ ln\ \alpha^* = 1158.8\left(\frac{T^3}{10^9}\right) - 1620.1\left(\frac{T^2}{10^6}\right) + 794.84\left(\frac{T^3}{10^3}\right) + 2.9992\left(\frac{10^9}{T^3}\right) - 161.04$$

for δ^2H and

(E.9) $$1000\ ln\ ln\ \alpha^* = -7.685 + 6.7123\left(\frac{10^3}{T}\right) - 1.6664\left(\frac{10^6}{T^2}\right) + 0.35041\left(\frac{10^9}{T^3}\right)$$

for $\delta^{18}O$, where *T* represents the interface temperature in degrees Kelvin. The equilibrium separation factor between liquid and vapour phases is expressed as:

(E.10) $$\varepsilon^* = \alpha^* - 1$$

and the kinetic separation factor between liquid and vapour phases is expressed as

(E.11) $$\varepsilon_k = 0.0125(1-h)$$

for δ^2H and

(E.12) $$\varepsilon_k = 0.0142(1-h)$$

for δ^{18}O, where *h* is the relative humidity (Gonfiantini, 1986). Isotope composition of atmospheric moisture for the ice-free season (δ_{AS}) was calculated using the equation from Gibson et al. (1999):

(E.13) $$\delta_{AS} = \frac{\left[\frac{(\delta_{SSL}-\varepsilon^*)}{\alpha^*-\varepsilon_k} - \delta_P(1-h+\varepsilon_k)\right]}{h}$$

Results of the isotope framework calculations are reported in Table A1 and A1.2.

A.1.3 Calculation of Evaporation to Inflow Ratios

The PAD isotope frameworks were used to calculate evaporation-to-inflow ratios (E/I), an index of lake-water balance described by Yi et al. (2008) and others:

(E.14) $$\frac{E}{I} = \frac{(\delta_I-\delta_L)}{(\delta_E-\delta_L)}$$

where δ_L is the isotope compositions of lake water, δ_I is the isotope compositions of input water and δ_E is the isotope composition of evaporative flux. δ_I was estimated as the intersection of a regression through δ_E and δ^* and the Local Meteoric Water Line, utilizing the coupled isotope tracer approach (Yi et al., 2008). This approach was used to account for the different potential input water isotope compositions to lakes across this complex landscape. δ_E was calculated using the Craig and Gordon (1965) equation:

(E.15) $$\delta_E = \frac{(\delta_L-\varepsilon^*)/\alpha^* - h\cdot\delta_{AS} - \varepsilon_k}{1-h+\varepsilon_k}$$

Table A1. Values used for calculations of the 15-year isotopic framework, with references and equation numbers where appropriate.

Parameter	Value	Source	Equation
h	66.19	Environment Canada,	E.1
T	14.33 °C	NRCC	E.2
$\alpha^*(^{18}O, ^{2}H)$	1.010, 1.09		E.8, E.9
$\varepsilon^*(^{18}O, ^{2}H)$ (‰)	10.33, 91.26		E.10
$\varepsilon_k(^{18}O, ^{2}H)$ (‰)	4.80, 4.23		E.12
$\delta_{As}(^{18}O, ^{2}H)$ (‰)	-26.90, -203.64		E.13
$\delta_P(^{18}O, ^{2}H)$ (‰)	-18.4, -142	OIPC	
$\delta^*(^{18}O, ^{2}H)$ (‰)	-4.29, -81.76		E.7
$\delta_{SSL}(^{18}O, ^{2}H)$ (‰)	-9.18, -104.26	Reference Lake (PAD 18)	
Slope	4.27		
Intercept	-63.46		

Table A1.2. Values used for calculations of the 5 year isotope framework, with references and equation numbers where appropriate.

Parameter	Value	Source	Equation
h	66.24	Environment Canada,	E.1
T	14.62	NRCC	E.2
$\alpha^*(^{18}O, ^{2}H)$	1.0103, 1.0909		E.8, E.9
$\varepsilon^*(^{18}O, ^{2}H)$ (‰)	10.30, 90.90		E.10
$\varepsilon_k(^{18}O, ^{2}H)$ (‰)	4.79, 4.22		E.12
$\delta_{As}(^{18}O, ^{2}H)$ (‰)	-26.84, -203.18		E.13
$\delta_P(^{18}O, ^{2}H)$ (‰)	-18.4, -142	OIPC	
$\delta^*(^{18}O, ^{2}H)$ (‰)	-4.30, -81.82		E.7
$\delta_{SSL}(^{18}O, ^{2}H)$ (‰)	-9.18, -104.26	Reference Lake (PAD 18)	
Slope	4.3		
Intercept	-63.5		
LMWL Slope	6.7	Wolfe et al (2007)	
LMWL Intercept	-19.2	Wolfe et al (2007)	

Appendix 2: Study Lakes (Chapter 4)

The GPS locations of the 57-60 lakes and 9 river sites sampled during 2015-2019 are contained in Table A2.1.1. Sampling occurred consistently at the same GPS point during each sampling campaign, generally at the center of each lake or river channel. In the spring, samples were collected on May 26-31 2015, June 29-30 2016, May 16-17 2017, May 15-17 2018 and May 13-15 2019. Nearby fires in the Fort McMurray region prevented sampling in May 2016. Summer samples were collected July 27-28 2015, July 27-28 2016, July 11-12 2017, July 10-11 2018 and July 12-14 2019. Fall samples were collected September 15-16 2015, September 28-29 2016, September 12-14 2017, September 11-14 2018 and September 11-14 2019. Water isotope and specific conductivity data are reported in Tables A2.2, A2.3 and A2.4. Flood status is reported in Table A2.5.

Table A2.1.1 Locations of lakes and rivers sampled during spring, summer and fall of 2015-2019 in the Peace-Athabasca Delta, Alberta, Canada.

Lake	Longitude	Latitude
1	-111.24	58.81
2	-111.32	58.84
3	-111.28	58.83
4	-111.40	58.84
5	-111.48	58.84
6	-111.39	58.81
8	-111.36	58.81
9	-111.33	58.77
12	-111.33	58.96
13	-111.38	58.95
14	-111.43	58.93
15	-111.51	58.95
16	-111.40	58.88
17	-111.43	58.87
18	-111.36	58.90
19	-111.63	58.44
20	-111.59	58.42
21	-111.57	58.37
22	-111.50	58.40
23	-111.44	58.39
24	-111.36	58.39
25	-111.33	58.38
26	-111.27	58.42
27	-111.26	58.44
30	-111.52	58.51
31	-111.52	58.50
32	-111.44	58.50
33	-111.44	58.42
36	-111.25	58.47
37	-111.45	58.67
38	-111.12	58.42
39	-111.19	58.46
40	-111.19	58.51
45	-111.44	58.58
46	-111.55	58.55
50	-111.89	58.86
52	-111.75	58.88
53	-111.65	58.77
54	-111.58	58.87

57	-111.59	58.83
58	-111.55	58.83
62	-111.85	58.37
M1	-111.02	58.45
M2	-110.91	58.42
M3	-110.97	58.43
M4	-110.84	58.49
M5	-110.79	58.50
M6	-110.79	58.53
M7	-111.05	58.44
M8	-111.80	58.40
M9	-111.82	58.33
M10	-111.79	58.29
M11	-111.33	58.55
M12	-111.41	58.56
M14	-111.52	58.57
M15	-111.26	58.88
M16	-111.21	58.89
M17	-111.32	58.90
M18	-111.29	58.91
M19	-111.32	58.88
R1	-111.42	58.91
R2	-111.58	58.91
R3	-111.56	58.81
R4	-111.54	58.35
R5	-111.44	58.49
R6	-111.07	58.47
R7	-111.51	58.56
R9	-111.90	58.85
R11	-111.75	58.85

Table A2.1.2 Hydrogen isotope compositions (‰ VSMOW) from 57-60 lakes and 9 river sites in the Peace-Athabasca Delta sampled in spring, summer and fall of 2015-2019.

Lake	15-May	15-Jul	15-Sep	16-Jun	16-Jul	16-Sep	17-May	17-Jul	17-Sep	18-May	18-Jul	18-Sep	19-May	19-Jul	19-Sep
1	-104.1	-98.0	-96.1	-103.6	-99.0	-99.7	-110.7	-99.1	-95.8	-115.2	-103.6	-98.8	-107.9	-95.1	-103.3
2	-111.1	-100.9	-98.6	-103.4	-98.8	-98.9	-108.2	-96.8	-93.4	-121.1	-105.6	-100.3	-110.3	-97.7	-104.6
3	-107.2	-99.1	-96.3	-106.2	-100.1	-101.0	-114.4	-97.9	-94.0	-129.2	-106.9	-100.9	-116.2	-98.9	-110.0
4	-117.5	-107.0	-103.2	-105.7	-100.0	-99.8	-108.1	-94.7	-91.5	-116.0	-97.7	-93.2	-111.5	-88.2	-108.8
5	-112.8	-103.2	-100.1	-105.6	-100.4	-100.4	-108.9	-99.5	-94.1	-113.4	-102.5	-97.5	-107.3	-95.3	-99.4
6	-119.3	-110.3	-105.8	-105.8	-101.5	-100.6	-108.5	-99.8	-93.0	-113.0	-99.6	-96.8	-105.8	-94.8	-101.1
8	-126.4	-111.2	-106.1	-116.8	-109.5	-106.1	-125.0	-117.4	-112.0	-139.1	-128.8	-122.2	-131.5	-118.1	-117.7
9	-113.7	-94.5	-93.3	-115.2	-104.9	-110.4	-133.8			-162.3	-124.9	-112.6	-160.4	-120.0	-132.9
12	-101.1	-92.3	-91.6	-102.8	-93.1	-104.5	-110.5	-89.7	-89.7	-128.6	-104.1	-96.2	-116.2	-89.9	-107.7
13	-111.3	-103.9	-103.8	-115.3	-110.6	-109.1	-116.6	-107.1	-101.7	-122.6	-114.0	-110.1	-116.8	-107.4	-108.4
14	-111.6	-104.4	-103.0	-106.1	-103.5	-103.3	-109.0	-102.1	-98.8	-134.1	-122.1	-116.9	-119.5	-111.1	-110.5
15	-129.4	-119.1	-115.7	-114.2	-108.8	-108.4	-113.5	-118.7	-112.2	-155.5	-141.5	-133.7	-135.9	-125.0	-119.8
16	-113.7	-103.1	-100.6	-105.4	-100.4	-101.4	-111.2	-94.5	-93.0	-120.7	-102.6	-98.6	-123.8	-95.0	-111.6
17	-111.5	-103.7	-100.2	-109.6	-104.8	-103.6	-113.1	-100.6	-97.4	-119.9	-107.8	-103.3	-112.2	-97.4	-104.9
18	-102.9	-102.6	-102.4	-103.7	-102.5	-102.9	-104.9	-102.7	-102.5	-104.7	-104.7	-103.5	-104.3	-102.9	-103.4
19	-98.0	-91.1	-88.2	-101.3	-94.8	-99.7	-116.7	-100.9	-94.5	-153.3	-135.3	-123.9	-128.1	-107.9	-110.5
20	-98.9	-88.4	-85.6	-88.4	-78.9	-98.3	-97.4	-104.4		-154.5	-135.6	-123.0	-125.2	-102.9	-110.4
21	-108.9	-97.1	-94.1	-99.3	-91.7	-100.4	-119.9	-98.5	-89.0	-154.1	-137.8	-122.8	-130.0	-105.4	-113.3
22	-115.5	-103.1	-97.9	-102.3	-96.9	-103.3	-117.8	-103.8	-96.6	-149.8	-137.2	-129.6	-135.4	-120.5	-124.0
23	-111.1	-103.5	-102.7	-106.7	-103.1	-104.3	-115.0	-105.0	-99.7	-151.3	-138.2	-129.0	-129.9	-118.1	
24	-122.1	-111.9	-107.1	-108.7	-105.3	-105.2	-113.3	-121.9	-114.0	-152.1	-134.9	-126.7	-129.5	-138.1	-132.5
25	-132.2	-117.8	-115.5	-126.1	-120.2	-113.5	-132.8	-123.1	-116.1	-152.3	-134.7	-130.4	-137.3	-136.3	-118.8
26	-123.5	-104.8	-98.5	-124.0	-115.0	-109.4	-136.5	-126.6	-112.0	-154.3	-138.8	-125.9	-141.7	-146.8	-137.4
27	-113.6	-102.9	-98.7	-98.7	-96.2	-97.3	-105.4	-94.5	-89.1	-137.3	-130.5	-120.7	-123.0	-111.8	-112.9

30	-123.5	-106.7	-102.7	-131.2	-121.7	-113.8	-145.3	-136.9	-118.8	-153.7	-142.5	-134.8	-151.9	-148.5	-136.3
31	-123.5	-105.9	-97.9	-133.0	-121.4	-111.6	-145.4	-136.1	-118.2	-154.3	-143.7	-133.3	-144.8	-148.9	-137.7
32	-111.0	-101.2	-99.8	-104.2	-99.3	-102.4	-113.6	-101.0	-97.7	-151.5	-132.8	-123.1	-126.3	-113.3	-114.8
33	-97.4	-104.7	-105.1	-132.0	-120.9	-116.8	-137.1	-125.0	-112.4	-155.0	-138.0	-124.9	-137.2	-144.4	-136.9
36	-115.7	-105.0	-102.0	-105.8	-102.3	-103.0	-113.0	-99.6	-95.5	-154.6	-135.3	-124.8	-128.0	-114.6	-131.0
37	-109.7	-99.4	-98.8	-98.2	-95.9	-100.6	-109.6	-91.8	-97.4	-129.9	-98.3	-98.4	-132.0	-94.6	-125.0
38	-126.3	-110.6	-104.5	-113.3	-112.3	-112.2	-131.6	-129.4	-111.9	-144.6	-133.0	-123.1	-138.6	-144.1	-136.4
39	-110.0	-98.0	-93.9	-98.8	-95.5	-98.4	-107.3	-93.8	-90.3	-151.8	-132.0	-120.3	-123.5	-108.3	-110.8
40	-113.3	-93.1	-88.9	-94.2	-95.4	-100.7	-128.9	-123.0	-108.7	-154.0	-134.9	-119.8	-127.1	-107.6	-132.2
45	-141.5	-140.1	-140.5	-134.5	-140.7	-130.8	-144.2	-143.4	-135.2	-151.7	-142.6	-140.5	-143.3	-148.1	-139.7
46	-121.7	-104.4	-97.7	-123.5	-107.2	-101.5	-138.2	-140.2		-150.6	-132.6	-133.1	-133.4	-148.0	-139.1
50	-115.7	-107.5	-101.9	-106.3	-101.8	-100.2	-113.7	-95.8	-90.7	-118.2	-98.5	-91.7	-112.3	-86.5	-111.9
52	-103.9	-95.9	-91.2	-112.5	-107.5	-102.7	-124.8	-105.7	-96.9	-134.3	-114.4	-104.2	-124.4	-103.1	-108.5
53	-116.6	-107.8	-102.8	-102.0	-98.4	-97.5	-112.5	-94.2	-89.9	-109.1	-109.4	-105.4	-113.1	-99.1	-102.4
54	-140.4	-135.1	-132.0	-129.7	-127.9	-124.9	-125.7	-126.4	-124.9	-155.8	-145.0	-142.2	-142.9	-136.2	-132.2
57	-121.7	-110.4	-104.2	-104.4	-100.4	-99.0	-106.5	-91.9	-88.8	-114.6	-96.9	-92.2	-115.7	-94.4	-105.1
58	-115.2	-103.2	-97.4	-106.4	-103.1	-102.2	-114.9	-97.8	-91.9	-127.2	-103.3	-95.5	-123.8	-91.4	-108.4
62	-122.2	-110.0	-101.3	-104.2	-100.4	-117.9	-125.6	-113.7	-108.6	-125.4	-117.3	-114.9	-123.8	-110.8	-111.5
M1	-119.3	-109.8	-106.6	-100.7	-98.5	-101.4	-108.6	-112.3	-107.6	-124.8	-98.5	-111.3	-121.8	-132.8	-129.8
M2	-108.1	-134.0	-135.6	-136.7	-132.6	-135.6	-143.2	-134.6	-127.8	-149.3	-132.6	-134.6	-149.3	-137.1	-140.5
M3	-111.8	-103.7	-101.4	-98.3	-95.4	-98.6	-105.5	-95.3	-92.4	-112.4	-95.4	-99.5	-108.1	-94.7	-104.6
M4	-110.4	-100.4	-98.8	-97.6	-94.5	-99.6	-107.1	-93.2	-89.8	-108.4	-94.5	-95.6	-105.1	-89.3	-102.9
M5	-148.5	-141.4	-145.1	-138.2	-136.2	-142.1	-146.3	-137.7	-134.9	-153.7	-136.2	-141.5	-153.5	-140.7	-143.2
M6	-142.3	-96.9	-100.2	-101.8	-97.3	-102.7	-111.1	-95.1	-90.1	-118.8	-97.3	-100.2	-114.0	-90.6	-109.6
M7	-111.4	-97.7	-95.5	-95.2	-89.8	-102.1	-112.1	-116.3	-103.2	-138.3	-89.8	-115.3	-121.6	-133.7	-123.1
M8	-105.4	-93.1	-89.5	-96.9	-89.8	-99.2	-115.8	-104.4	-98.7	-114.3	-89.8	-105.5	-113.3	-99.3	-105.7
M9	-102.2	-94.5	-94.0	-97.1	-92.3	-97.3	-101.8	-94.0	-88.2	-116.0	-92.3	-100.2	-110.7	-96.5	-101.4
M10	-124.8	-105.1	-98.4	-112.3	-103.6	-105.7	-127.7	-111.6	-100.9	-151.1	-103.6	-117.0	-134.2	-111.3	-119.4

M11	-111.6	-102.4	-101.3	-100.3	-97.1	-104.9	-111.9	-101.1	-96.2	-123.9	-97.1	-106.4	-114.0	-103.6	-108.0
M12	-120.3	-106.6	-100.2	-117.8	-105.2	-106.0	-131.3	-139.3	-121.0	-155.8	-105.2	-128.2	-134.7	-145.7	-137.9
M14	-114.2	-102.5	-97.6	-98.4	-93.8	-96.9	-111.8	-136.1	-121.5	-155.5	-93.8	-121.4	-126.8	-146.3	-138.5
M15	-99.8	-94.9	-91.4	-101.5	-97.1	-99.4	-106.6	-96.0	-95.7	-114.7	-97.1	-100.5	-108.2	-97.0	-103.3
M16	-107.2	-97.1	-98.1	-105.7	-106.3	-103.5	-113.1	-102.6	-99.6	-123.7	-106.3		-116.9	-102.8	-108.1
M17	-109.4	-97.6	-97.4	-106.2	-100.0	-101.4	-109.1	-95.7	-93.3	-153.2	-100.0	-119.4	-125.4	-107.8	-108.0
M18	-112.2	-103.0	-101.1	-106.7	-101.7	-102.1	-109.2	-98.4	-96.5	-148.1	-101.7	-119.5	-123.5	-110.5	-109.3
M19	-100.3	-91.8	-91.2	-102.8	-97.3	-100.7	-105.9	-94.0	-96.3	-117.4	-97.3	-101.6	-111.2	-97.1	-102.5
R1	-135.4	-133.0	-128.3	-148.8	-131.6	-131.6	-139.4	-134.2	-126.5	-162.9	-131.6	-134.7	-135.6	-143.2	-138.3
R2	-149.2	-147.4	-147.4	-147.8	-146.5	-143.7	-154.5	-143.9	-145.1	-162.6	-146.5	-141.1	-157.0	-153.4	-142.8
R3	-127.8	-135.7	-137.4	-148.8	-137.1	-122.6	-143.0	-140.8	-127.9	-163.9	-137.1	-133.8	-140.4	-146.8	-138.1
R4	-140.1	-139.1	-140.2	-134.3	-140.2	-133.8	-144.8	-144.9	-135.1	-149.8	-140.2	-141.6	-144.2	-149.7	-139.9
R5	-139.0	-139.5	-140.9	-134.6	-140.8	-133.3	-142.8	-140.1	-135.5	-151.6	-140.8	-141.5	-144.4	-149.4	-138.9
R6	-139.5	-139.3	-140.8	-134.7	-139.7	-133.5	-143.5	-142.6	-135.6	-151.7	-139.7	-141.7	-144.2	-148.2	-140.0
R7	-139.5	-139.3	-140.6	-134.2	-140.3	-133.5	-146.4	-137.7	-136.1	-152.3	-140.3	-141.8	-144.5	-149.5	-140.3
R9	-123.4	-114.2	-109.3	-113.3	-107.6	-104.8	-114.8	-101.6	-99.3	-163.3	-107.6	-131.8	-124.8	-118.1	-114.9
R11	-134.9	-130.7	-131.8	-135.5	-133.6	-129.2	-141.6	-136.7	-127.1	-157.9	-133.6	-137.7	-138.6	-140.5	-139.2

Table A2.1.3 Oxygen isotope compositions (‰ VSMOW) from 57-60 lakes and 9 river sites in the Peace-Athabasca Delta sampled in spring, summer and fall of 2015-2019.

Lake	15-May	15-Jul	15-Sep	16-Jun	16-Jul	16-Sep	17-May	17-Jul	17-Sep	18-May	18-Jul	18-Sep	19-May	19-Jul	19-Sep
1	-9.3	-7.9	-8.3	-9.3	-7.8	-8.5	-11.4	-8.6	-7.8	-11.7	-9.4	-8.5	-9.9	-6.9	-9.4
2	-10.6	-8.4	-8.7	-9.2	-7.7	-8.4	-10.7	-7.8	-7.6	-12.7	-9.8	-8.7	-10.5	-7.9	-9.7
3	-8.5	-7.8	-8.0	-9.6	-7.7	-8.7	-11.7	-7.5	-7.5	-13.9	-9.7	-8.3	-11.1	-7.8	-10.7
4	-11.9	-9.3	-9.2	-9.5	-8.0	-8.6	-10.6	-7.5	-7.1	-11.7	-8.1	-7.1	-10.5	-5.3	-10.8
5	-10.8	-8.6	-8.1	-9.3	-7.9	-8.5	-10.5	-8.2	-7.2	-10.9	-8.7	-7.9	-9.6	-6.7	-7.9
6	-12.1	-10.3	-9.7	-9.6	-8.7	-8.8	-10.8	-8.7	-7.8	-11.4	-8.9	-8.3	-9.8	-7.0	-8.8
8	-13.6	-10.3	-9.6	-11.9	-10.4	-9.9	-14.1	-12.4	-11.4	-16.9	-14.7	-13.3	-14.8	-11.6	-11.9
9	-10.6	-6.4	-6.4	-11.4	-9.2	-12.5	-15.6			-20.6	-13.9	-11.0	-19.8	-12.8	-16.2
12	-7.9	-6.1	-6.3	-8.8	-6.4	-10.4	-10.7	-5.9	-6.4	-13.8	-8.5	-7.3	-10.8	-5.2	-10.2
13	-10.4	-8.7	-8.7	-11.4	-10.4	-10.2	-12.1	-9.8	-8.8	-12.9	-10.9	-10.5	-11.5	-9.3	-9.6
14	-10.8	-9.2	-9.0	-9.9	-9.3	-9.3	-10.3	-8.9	-8.2	-15.4	-12.8	-12.0	-12.2	-10.2	-10.6
15	-13.7	-11.5	-10.7	-10.7	-9.7	-9.7	-10.6	-11.9	-10.4	-19.4	-16.4	-14.8	-15.0	-12.4	-12.0
16	-11.1	-8.7	-8.3	-9.7	-8.6	-9.5	-11.0	-7.3	-7.2	-12.6	-9.2	-8.5	-12.9	-6.6	-10.9
17	-10.4	-8.6	-7.9	-10.2	-9.2	-9.4	-11.1	-8.3	-7.3	-12.2	-9.7	-8.9	-10.3	-6.8	-9.0
18	-9.1	-9.1	-9.0	-9.3	-9.2	-9.1	-9.7	-8.9	-8.7	-9.4	-9.2	-9.4	-9.3	-9.1	-9.2
19	-7.4	-5.9	-5.5	-8.0	-6.7	-8.9	-11.6	-8.0	-7.1	-19.2	-15.4	-13.2	-13.4	-8.6	-9.8
20	-7.6	-5.6	-5.5	-5.5	-3.7	-9.8	-9.7	-9.1		-19.4	-15.4	-12.9	-12.7	-7.9	-10.2
21	-10.0	-7.3	-6.9	-7.5	-6.0	-8.9	-12.7	-8.0	-5.8	-19.3	-15.9	-12.9	-13.7	-8.1	-10.5
22	-10.8	-8.0	-7.1	-7.7	-6.9	-9.5	-12.2	-8.7	-7.3	-18.7	-15.7	-14.3	-15.0	-11.3	-12.6
23	-10.9	-9.0	-9.0	-9.7	-8.9	-9.8	-12.2	-9.4	-8.3	-18.6	-15.9	-14.1	-14.1	-11.4	
24	-12.3	-10.8	-10.0	-10.4	-9.3	-10.1	-11.8	-13.4	-11.7	-19.0	-15.5	-14.0	-14.2	-16.3	-15.5
25	-15.2	-12.2	-12.0	-14.3	-13.1	-12.1	-15.8	-13.5	-12.2	-19.0	-15.6	-15.0	-16.2	-16.3	-12.0
26	-13.3	-9.3	-8.3	-14.2	-12.3	-11.5	-16.7	-14.2	-11.3	-19.2	-16.8	-14.3	-16.8	-18.4	-16.8
27	-11.6	-9.6	-8.8	-8.6	-8.2	-8.9	-10.5	-7.9	-6.9	-16.2	-14.7	-13.0	-13.2	-10.9	-11.5

30	-13.2	-9.7	-9.1	-16.0	-13.7	-12.3	-18.3	-16.4	-12.6	-19.2	-18.2	-16.2	-18.6	-19.0	-17.0
31	-13.5	-9.9	-8.6	-16.4	-14.0	-12.0	-18.4	-16.2	-12.5	-19.3	-18.2	-15.9	-17.4	-19.1	-17.1
32	-10.8	-8.7	-8.5	-9.2	-8.6	-9.4	-11.8	-8.9	-8.0	-18.7	-15.0	-13.0	-13.4	-10.5	-11.0
33	-7.1	-9.4	-10.0	-15.3	-13.3	-12.5	-16.5	-13.9	-11.3	-19.4	-16.6	-13.9	-15.7	-18.0	-16.3
36	-11.6	-9.3	-8.8	-9.4	-8.9	-9.4	-11.7	-8.3	-7.5	-19.3	-15.6	-13.3	-13.5	-10.4	-14.9
37	-10.6	-8.2	-8.4	-7.9	-7.8	-9.5	-10.6	-6.6	-10.1	-13.7	-8.3	-8.5	-13.6	-7.4	-15.4
38	-14.5	-11.6	-10.5	-12.1	-12.1	-12.5	-15.9	-15.3	-11.8	-17.8	-15.7	-13.7	-16.6	-17.8	-16.4
39	-11.2	-8.7	-8.0	-8.7	-8.1	-9.1	-10.7	-7.9	-7.4	-18.9	-15.0	-12.8	-13.0	-9.7	-10.9
40	-11.2	-8.1	-7.8	-8.6	-8.8	-10.4	-15.5	-14.3	-11.4	-19.3	-15.8	-12.8	-14.1	-10.0	-15.6
45	-17.5	-17.6	-17.7	-16.7	-17.9	-16.4	-18.1	-18.1	-16.7	-19.1	-18.2	-17.6	-17.7	-18.7	-17.5
46	-13.4	-10.0	-9.3	-14.2	-11.1	-10.4	-16.9	-17.1		-18.7	-15.5	-15.9	-15.5	-18.6	-17.3
50	-11.6	-9.4	-8.5	-9.1	-8.8	-8.7	-11.2	-7.0	-6.7	-12.1	-8.4	-6.7	-10.0	-4.8	-12.3
52	-8.6	-6.7	-5.7	-9.8	-9.4	-9.1	-12.6	-8.8	-7.4	-14.6	-11.4	-9.0	-12.3	-8.1	-9.6
53	-11.9	-10.4	-9.6	-9.0	-8.7	-9.2	-11.6	-7.6	-7.1	-10.8	-11.2	-10.2	-11.0	-8.7	-9.7
54	-16.1	-15.1	-14.5	-13.8	-13.9	-13.3	-13.5	-13.4	-13.4	-19.4	-17.1	-16.6	-16.4	-15.1	-14.4
57	-12.5	-10.0	-8.9	-8.8	-8.3	-8.5	-10.7	-6.3	-6.0	-11.0	-7.8	-6.8	-10.8	-6.8	-9.6
58	-11.2	-8.4	-7.4	-9.1	-8.8	-9.1	-12.2	-7.5	-6.6	-13.4	-9.0	-7.3	-12.2	-5.3	-10.3
62	-14.2	-11.4	-10.2	-10.2	-9.8	-13.9	-15.3	-12.3	-11.8	-14.5	-13.1	-12.7	-14.0	-11.7	-11.8
M1	-13.0	-10.7	-10.1	-8.5	-8.5	-9.6	-10.9	-11.2	-10.8	-13.8	-8.5	-11.2	-12.6	-15.6	-15.0
M2	-10.8	-16.0	-16.6	-16.2	-15.8	-17.1	-18.0	-16.1	-15.3	-18.8	-15.8	-16.4	-18.5	-16.8	-17.5
M3	-11.5	-9.7	-9.2	-8.8	-7.7	-9.1	-10.2	-8.3	-7.6	-11.1	-7.7	-9.0	-10.3	-7.4	-9.8
M4	-10.5	-9.3	-9.1	-9.4	-8.2	-9.8	-10.8	-8.0	-7.8	-11.0	-8.2	-8.8	-10.2	-6.9	-10.1
M5	-18.2	-17.0	-18.2	-16.8	-16.2	-18.0	-18.1	-16.4	-16.3	-19.2	-16.2	-17.7	-19.4	-16.9	-17.6
M6	-17.3	-8.2	-9.0	-9.9	-8.6	-10.1	-11.2	-8.0	-7.1	-12.1	-8.6	-8.9	-11.2	-6.3	-10.7
M7	-11.2	-8.5	-8.2	-8.2	-7.0	-10.3	-11.7	-12.2	-10.0	-16.1	-7.0	-12.4	-13.0	-16.2	-13.8
M8	-10.6	-8.1	-7.7	-8.8	-7.8	-10.3	-13.0	-10.5	-9.5	-12.1	-7.8	-10.7	-12.1	-9.2	-10.5
M9	-10.3	-8.2	-8.5	-8.9	-8.1	-9.5	-10.1	-8.3	-7.4	-12.2	-8.1	-9.7	-11.4	-8.7	-9.6
M10	-13.9	-10.0	-9.1	-11.6	-10.1	-11.0	-15.3	-11.6	-9.5	-18.3	-10.1	-12.6	-15.8	-11.2	-12.7

M11	-11.2	-9.2	-9.2	-8.7	-8.2	-10.5	-11.8	-9.4	-8.0	-13.7	-8.2	-10.3	-11.4	-9.5	-10.6
M12	-12.9	-10.4	-9.2	-12.7	-10.3	-10.7	-15.9	-17.2	-13.2	-19.8	-10.3	-14.9	-15.5	-18.5	-16.9
M14	-12.2	-9.7	-9.0	-9.3	-8.4	-9.5	-12.1	-16.4	-13.5	-19.7	-8.4	-13.1	-13.9	-18.4	-17.0
M15	-8.8	-7.1	-6.7	-9.1	-8.2	-8.9	-10.2	-7.6	-7.5	-11.5	-8.2	-8.6	-9.8	-7.5	-9.3
M16	-9.7	-7.5	-7.8	-9.7	-9.5	-9.3	-11.3	-8.7	-8.2	-12.9	-9.5		-11.5	-8.4	-10.2
M17	-10.7	-8.0	-8.0	-9.9	-8.5	-9.0	-10.7	-7.8	-7.3	-18.7	-8.5	-12.4	-13.2	-9.4	-10.0
M18	-10.6	-9.0	-8.9	-10.0	-9.0	-9.3	-10.9	-8.6	-7.9	-17.8	-9.0	-12.5	-12.8	-10.1	-10.1
M19	-8.1	-6.6	-6.7	-8.9	-7.8	-8.7	-9.9	-7.2	-7.8	-11.7	-7.8	-8.9	-10.3	-7.1	-8.8
R1	-16.3	-16.1	-15.3	-19.0	-16.2	-16.3	-17.2	-16.1	-14.9	-21.2	-16.2	-17.0	-16.3	-18.2	-17.2
R2	-19.4	-18.7	-18.9	-19.0	-18.8	-18.5	-19.6	-18.1	-18.6	-21.1	-18.8	-18.4	-19.9	-19.7	-18.0
R3	-14.7	-16.7	-17.0	-19.1	-17.1	-14.7	-17.8	-17.5	-15.1	-21.2	-17.1	-17.1	-17.0	-18.6	-17.5
R4	-17.2	-17.6	-17.7	-16.8	-17.7	-17.0	-18.5	-18.4	-16.7	-19.0	-17.7	-18.5	-17.7	-18.9	-17.6
R5	-16.9	-17.5	-17.9	-16.9	-17.8	-16.8	-17.7	-17.5	-16.6	-19.1	-17.8	-18.2	-17.7	-19.1	-17.4
R6	-17.1	-17.4	-17.9	-16.9	-17.7	-17.0	-17.9	-17.9	-16.6	-19.2	-17.7	-18.2	-17.7	-19.0	-17.6
R7	-16.9	-17.5	-17.9	-16.8	-17.7	-17.0	-18.6	-16.6	-16.7	-19.2	-17.7	-17.9	-17.6	-19.0	-17.7
R9	-12.2	-10.3	-9.3	-10.4	-8.9	-8.9	-10.7	-7.2	-7.3	-20.9	-8.9	-14.0	-11.9	-11.0	-10.3
R11	-16.2	-15.6	-16.0	-17.1	-16.5	-15.5	-17.5	-16.8	-14.9	-20.1	-16.5	-14.1	-16.9	-17.3	-17.3

Table A2.1.4 Specific conductivity (µS/cm) from 57-60 lakes and 9 river sites in the Peace-Athabasca Delta measured in spring, summer and fall of 2015-2019.

Lake	15-May	15-Jul	15-Sep	16-Jun	16-Jul	16-Sep	17-May	17-Jul	17-Sep	18-May	18-Jul	18-Sep	19-May	19-Jul	19-Sep
1	395.6	330.9	357.6	331.3	324.7	339.1	364.2	427.0	337.6	329.5	361.3	261.8	405.5	331.2	335.4
2	350.1	263.0	376.0	248.8	258.0	370.1	314.3	291.3	287.6	264.6	238.4	258.4	386.3	268.3	362.6
3	303.1	321.2	478.9	299.9	307.3	370.4	355.8	359.8	388.8	304.6	300.0	349.2	458.6	347.1	377.6
4	450.9	306.4	441.5	279.7	311.9	457.2	342.5	349.0	366.2	440.6	349.5	354.4	566.0	444.5	813.0
5	330.0	252.4	301.4	233.9	240.2	304.2	284.2	291.0	290.5	274.6	248.5	196.0	322.0	262.8	298.7
6	411.9	314.7	314.4	297.4	245.8	334.4	307.0	336.0	224.9	280.9	314.6	190.1	361.5	293.2	287.5
8	274.6	208.0	286.5	280.5	247.0	260.4	198.1	238.0	231.7	150.5	237.2	172.2	225.3	191.9	203.6
9	583.0	402.4		713.0	674.0	1222.0	566.0			56.0	1084.6		1718.0	1494.0	930.0
12	173.9	246.8	441.2	239.3	244.4	333.5	251.8	285.5	306.5	297.9	236.4	276.1	432.0	361.2	
13	114.3	125.4	124.4	114.2	111.5	109.0	94.1	125.7	96.9	99.5	112.6	76.6	138.7	136.8	127.5
14	243.0	210.2	264.7	209.6	216.4	258.1	231.7	231.0	255.5	218.1	179.3	166.2	287.3	248.0	283.0
15	347.7	216.6	256.8	218.0	208.0	237.8	271.9	237.0	225.5	241.2	227.4	170.3	290.1	192.3	202.1
16	343.7	342.6	463.2	395.7	359.4	462.2	415.0	395.0	422.5	446.4	391.5	338.4	505.0	505.0	571.0
17	186.9	206.8	232.8	186.2	202.8	235.9	186.1	245.0	212.5	184.5	188.7	161.1	200.8	216.4	252.7
18	210.4	224.4	228.7	215.8	218.0	219.8	188.4	255.8	210.1	167.6	216.0	166.6	219.2	222.2	225.3
19	123.0	148.3	183.6	136.5	165.5	208.4	211.2	227.5	301.3	199.2	297.8	219.3	213.8	269.5	240.1
20	179.3	181.5	248.9	195.9			582.0	423.6		203.9	361.5	274.1	213.2	274.1	228.3
21	199.6	211.5	307.7	231.2	204.6	353.9	331.0	307.0	353.8	211.7	357.6	261.5	201.3	272.4	236.3
22	209.8	195.7	246.9	166.4	174.3		185.5	161.6	223.1	209.0	333.4	256.3	273.2	293.8	234.2
23	158.5	460.8	184.3	142.2	138.2		144.1	167.3	133.2	191.0	210.1	150.0	225.1	193.4	216.9
24	215.3	198.5	249.2	174.8	9.7	211.0	195.5	218.4	185.0	189.5	188.2	147.1	265.5	216.8	215.4
25	137.3	116.8	119.0	126.5	114.1	98.4	197.5	177.7	131.6	180.5	181.7	100.8	169.0	141.8	125.5
26	252.9	206.9	244.9	228.2	219.2	98.4	162.8	253.0	170.9	217.2	167.5	114.2	276.4	259.1	303.6
27	289.8	260.9	230.8	257.2	264.9	236.4	287.8	339.0	227.2	227.5	244.7	183.1	317.3	280.2	223.4

30	461.2	439.2	396.3	323.9	279.3	305.6	203.5	433.0	307.6	217.7	232.9	239.5	331.4	247.1	386.2
31	383.1	399.9	409.1	272.1	213.0	207.4	210.8	406.0	254.5	211.4	238.1	220.5	341.6	245.3	321.3
32	249.4	217.7	360.8	172.9	200.4	307.5	232.7	188.7	269.3	244.8	254.3	237.2	344.5	256.6	347.4
33	554.0	547.0	813.0	232.6	204.1	296.2	193.5	405.8	230.1	242.4	228.9	155.6	429.0	256.7	387.5
36	242.2	171.2	248.2	183.0	155.4	237.5	217.3	196.0	218.9	225.2	183.1	152.7	316.0	181.5	274.7
37	360.8	620.0	700.0	683.0	701.0	610.0	480.5	473.0	598.0	430.7	377.6	423.0	214.6		677.0
38	273.4	241.0	230.5	244.2	176.7	231.4	132.8	239.0	201.2	175.1	219.3	138.6	212.0	170.1	193.1
39	170.6	199.3	206.2	225.9	248.0	291.9	254.2	257.0	201.2	223.7	294.2	167.7	316.0	288.0	233.6
40	407.6	306.6	444.6	474.1	353.0	432.0	295.8	418.9	226.1	222.4	302.8	222.3	261.1	241.0	252.0
45	292.4	277.1	319.7	223.6	254.4	260.6	205.1	292.0	280.8	211.7	220.1	214.1	285.0	246.7	265.8
46	386.0	365.7	365.0	347.4	287.0	394.0	281.5	341.0	239.5	239.4	346.2	192.3	309.1	264.1	301.6
50	395.8	260.0	378.7	223.5	249.9	323.1	297.3	318.0	338.3	324.8	346.9	296.1	489.9	388.4	
52	276.5	213.9	325.0	387.5	366.7	455.3	283.2	549.0	443.6	420.3	565.8	390.3	458.2	626.0	567.0
53	409.2	288.0	324.2	251.1	266.3	303.0	326.4	299.0	213.8	242.3	222.5	162.0	354.8	289.9	266.6
54	342.6	268.7	289.8	268.8	234.7	269.8	280.7	306.7	254.4	227.2	255.0	185.4	299.4	229.8	230.9
57	486.2	395.6	405.0	243.2	253.5	384.1	351.2	293.9	356.3	381.9	388.6	309.1	391.6	368.5	415.1
58	421.2	262.5	417.4	209.0	195.6	346.9	281.0	282.0	324.2	250.4	246.6	273.8	406.9	312.1	607.0
62	680.0	741.0	1028.0	932.0	905.0	799.0	462.5	986.0	916.0	531.0	564.0	449.8	464.5	71.1	817.0
M1	160.6	210.9	355.8	230.7	263.5	355.2	298.1	370.0	300.2	309.9	241.8	221.0	380.8	257.1	329.0
M2	66.4	65.5	48.6	44.7	42.3	39.1	24.9	41.2	30.8	47.8	50.2	26.4	38.7	39.9	40.4
M3	457.6	284.5	438.5	13.7	266.6	369.2	342.3	330.0	334.0	359.0	255.3	243.3	348.0	276.9	318.6
M4	205.7	258.4	243.6	333.0	294.4	296.4	295.3	374.0	254.2	311.7	300.6	194.6	373.8	389.9	363.7
M5	55.7	76.0	70.2	76.3	75.9	66.8	45.8	86.4	64.2	49.2	68.9	43.8	54.2	71.7	77.8
M6	294.5	239.2	356.5	245.7	272.7	355.1	273.1	287.0	267.7	304.3	244.1	251.3	333.1	337.2	367.5
M7	323.5	223.1	326.9	229.9	218.5	298.9	248.0	335.0	250.3	270.6	299.1	239.9	366.8	263.9	307.2
M8	569.0	729.0	942.0	881.0	941.0	1007.0	830.0	1045.0	803.0	569.0	653.9	489.9	434.6	735.0	730.0
M9	796.0	854.0	921.0	814.0	935.0	1111.0	630.0	993.0	1035.0	777.0	860.8	691.0	836.0	991.0	1107.0
M10	249.2	336.2	412.8	238.9	246.5	296.2	133.3	250.6	176.7	193.9	224.1	173.6	216.5	187.5	295.5

M11	378.1	444.9	545.0	527.0	559.0	499.9	415.8	535.0	469.8	290.7	409.7	313.5	430.3	430.8	441.9
M12	309.4	232.3	244.1	329.9	341.8	374.1	278.1	304.3	218.5	214.5	216.8	157.1	297.4	250.6	262.1
M14	260.8	246.0	287.2	262.0	334.9	303.3	276.0	304.0	177.4	217.1	216.9	160.1	325.9	286.5	195.8
M15	190.3	186.3	296.4	238.6	255.8	280.6	197.5	293.3	260.7	201.8	250.1	212.5	262.3	271.1	318.3
M16	161.5	169.9	187.2	154.6	171.4	161.4	86.7	170.9	141.1	120.1	150.3		178.7	173.6	176.9
M17	190.9	161.1	225.3	168.0	190.6	247.0	202.5	203.3	152.1	219.3	188.2	184.9	304.6	180.2	255.5
M18	315.4	234.2	266.9	237.9	248.2	270.0	278.8	292.8	197.4	226.7	231.6	181.4	322.3	222.5	293.0
M19	195.9	248.3	287.9	251.8	259.1		179.4	287.0	234.8	189.7	263.1	189.1	252.4	314.4	308.9
R1	214.9	185.0	155.7	251.6	200.2	203.9	146.0	212.0	77.8	176.5	139.2	125.7	134.9	211.3	241.2
R2	214.7	264.5	266.9	233.2	238.1	238.3	200.0	322.6	206.0	173.4	241.9	238.2	269.7	232.4	262.7
R3	488.2	322.9	339.6	246.3	274.0	451.0	223.4	296.9	120.5	175.4	297.3	260.0	324.4	251.9	262.3
R4	293.5	265.0	311.7	221.7	264.8	252.0	194.5	288.5	286.3	179.7	227.3	213.0	291.0	254.8	259.2
R5	298.3	270.5	321.4	233.3	267.1	263.4	200.5	294.5	284.3	188.5	232.0	215.9	290.1	251.6	263.9
R6	289.6	262.7	304.8	226.2	261.8	153.5	189.8	280.0	278.7	181.3	220.2	207.8	283.8	249.6	256.4
R7	299.5	268.6	314.8	227.0		262.8	194.9	288.5	284.1	185.1	229.5	213.5	290.0	238.1	264.1
R9	367.8	211.9	260.1	218.4	209.9	212.0	369.2	269.8	237.5	304.4	254.2	212.0	167.9	327.5	392.5
R11	258.8	149.5	195.6	210.1	216.6	182.4	178.5	224.2	73.2	164.9	147.9	182.3	170.5	218.1	237.2

Table A2.1.5 Flood status of lakes in the Peace-Athabasca Delta sampled during spring, summer and fall of 2015-2019. Flood status was based on water isotope compositions, specific conductivity and field observations; 1 denotes a flooded lake, 0 denotes a non-flooded lake.

Lake	May-17	Jul-17	May-18	Jul-18	Sept-18	May-19	Jul-19	Sep-19
1	0	0	0	0	0	0	0	0
2	0	0	0	0	0	0	0	0
3	0	0	0	0	0	0	0	0
4	0	0	0	0	0	0	0	0
5	0	0	0	0	0	0	0	0
6	0	0	0	0	0	0	0	0
8	0	0	1	0	0	0	0	0
9	0	0	0	0	0	0	0	0
12	0	0	0	0	0	0	0	0
13	0	0	0	0	0	0	0	0
14	0	0	0	0	0	0	0	0
15	0	0	1	0	0	0	0	0
16	0	0	0	0	0	0	0	0
17	0	0	0	0	0	0	0	0
18	0	0	0	0	0	0	0	0
19	0	0	1	0	0	0	0	0
20	0	0	1	0	0	0	0	0
21	0	0	1	0	0	0	0	0
22	0	0	1	0	0	0	0	0
23	0	0	1	0	0	0	0	0
24	0	0	1	0	0	0	1	1
25	1	0	1	0	1	1	1	0
26	1	0	1	1	1	1	1	1
27	0	0	1	0	0	0	0	0
30	1	0	1	1	1	1	1	1
31	1	0	1	1	1	1	1	1
32	0	0	1	0	0	0	0	0
33	1	0	1	1	0	1	1	1
36	0	0	1	0	0	0	0	1
37	0	0	0	0	0	0	0	0
38	1	1	1	1	0	1	1	1
39	0	0	1	0	0	0	0	0
40	1	0	1	0	0	0	0	1
45	1	1	1	1	1	1	1	1
46	1	1	1	0	1	1	1	1
50	0	0	0	0	0	0	0	0

52	0	0	0	0	0	0	0	0
53	0	0	0	0	0	0	0	0
54	0	0	1	1	1	0	0	0
57	0	0	0	0	0	0	0	0
58	0	0	0	0	0	0	0	0
62	0	0	0	0	0	0	0	0
M1	0	0	0	0	0	0	1	1
M2	0	0	0	0	0	0	0	0
M3	0	0	0	0	0	0	0	0
M4	0	0	0	0	0	0	0	0
M5	0	0	0	0	0	0	0	0
M6	0	0	0	0	0	0	0	0
M7	0	0	0	0	0	0	1	1
M8	0	0	0	0	0	0	0	0
M9	0	0	0	0	0	0	0	0
M10	1	0	0	0	0	1	0	0
M11	0	0	0	0	0	0	0	0
M12	1	1	1	0	1	0	1	1
M14	0	1	1	0	0	0	1	1
M15	0	0	0	0	0	0	0	0
M16	0	0	0	0	0	0	0	0
M17	0	0	1	0	0	0	0	0
M18	0	0	1	0	0	0	0	0
M19	0	0	0	0	0	0	0	0

A2.2 Spatial Autocorrelation

For each sampling point Moran's I, a measure of spatial autocorrelation, was calculated to determine whether sufficient spatial autocorrelation exists to allow interpolation. All Moran's I values were significant (P-value < 0.05) during each sampling interval.

Table A2.2.1 Moran's I and associated z-scores for evaporation-to-inflow ratios of lakes in the Peace-Athabasca Delta for spring, summer and fall of 2015-2019.

Sampling Campaign	Moran's I	z-score
15-May	0.33238	4.83283
15-Jul	0.43330	6.14922
15-Sep	0.32749	4.70754
16-Jun	0.22474	4.33363
16-Jul	0.20555	3.36076
16-Sep	0.52759	7.42974
17-May	0.48683	6.81348
17-Jul	0.50941	7.04374
17-Sep	0.40898	5.54293
18-May	0.49198	6.97674
18-Jul	0.57469	8.09639
18-Sep	0.50310	7.00697
19-May	0.43083	6.14071
19-Jul	0.38191	5.42574
19-Sep	0.74392	10.2738